Variable Star and Exoplanet Section of Czech Astronomical Society and Štefánik Observatory

Proceedings of the 48th Conference on Variable Stars Research

Štefánik Observatory, Prague, Czech Republic, EU

11th – 13th November 2016

Editor-in-chief **Radek Kocián**

Participants of the conference

TABLE OF CONTENTS

INTRODUCTION

The Variable Star and Exoplanet Section of the Czech Astronomical Society organized traditional autumn conference on research and news in the field of variable stars. The conference was held at Štefánik observatory in Prague. In addition to many contributions that were presented on site, we had an opportunity to hear lectures given by invited speakers from abroad via Internet. All presented contributions can be viewed on our YouTube channel.

I would like to thank all conference participant and all speakers for their contributions. I also would like to thank the Director of Štefánik Observatory, Mr. Jakub Rozehnal, for providing venues for conference and to Mr. Filip Walter and his colleagues for catering.

Ladislav Šmelcer

president of Variable Star and Exoplanet

Section of Czech Astronomical Society

Valašské Meziříčí, March 2017

NOTES

The scientific content of the proceedings contributions was not reviewed by the OEJV editorial board.

The BVRI photometry of the UZ Equulei system

V. BAHÝL[1,3], M. GAJTANSKA[2], P. HANISKO[1,3]

(1) Júlia Observatory, Zvolenská Slatina, Slovak Republic, basoft@zv.psg.sk

(2) KFEAM, DF TU Zvolen, Masarykova 24, 960 53 Zvolen, Slovak Republic

(3) SZA (Slovak Union of Astronomers), Tomášovská 63, 979 01 Rimavská Sobota, Slovak Republic

Abstract: There are described and analyzed the results of the observations of the UZ Equulei system in the summer of the year 2016. The BVRI photometry had been used and the relevant light curves had been constructed. The classification of the system as the EB had been confirmed from two subsequent light curves.

Abstrakt: V práci sú popisované a analyzované výsledky pozorovania zákrytovej sústavy UZ Equulei v lete roku 2016. Pozorovania boli realizované v sústave BVRI filtrov a pre každý z nich bola konštruovaná odpovedajúca svetelná krivka. Klasifikácia systému ako EB bola potvrdená na základe dvoch po sebe idúcich svetelných kriviek.

Introduction

The UZ Equulei is the Beta Lyrae eclipsing binary system for which there is rather lack of observations even if this system is of short period and enough bright to be easy observed.

Figure 1: The identification map of the UZ Equulei system.

We decided to observe this system in the frame of the tests of our CCD camera MI G2-1600 equipped with the filter wheel and BVRI filters. The fifth position in the filter wheel is empty. The camera is attached to our Celestron 9.25" Schmidt – Cassegrain telescope f/2350.

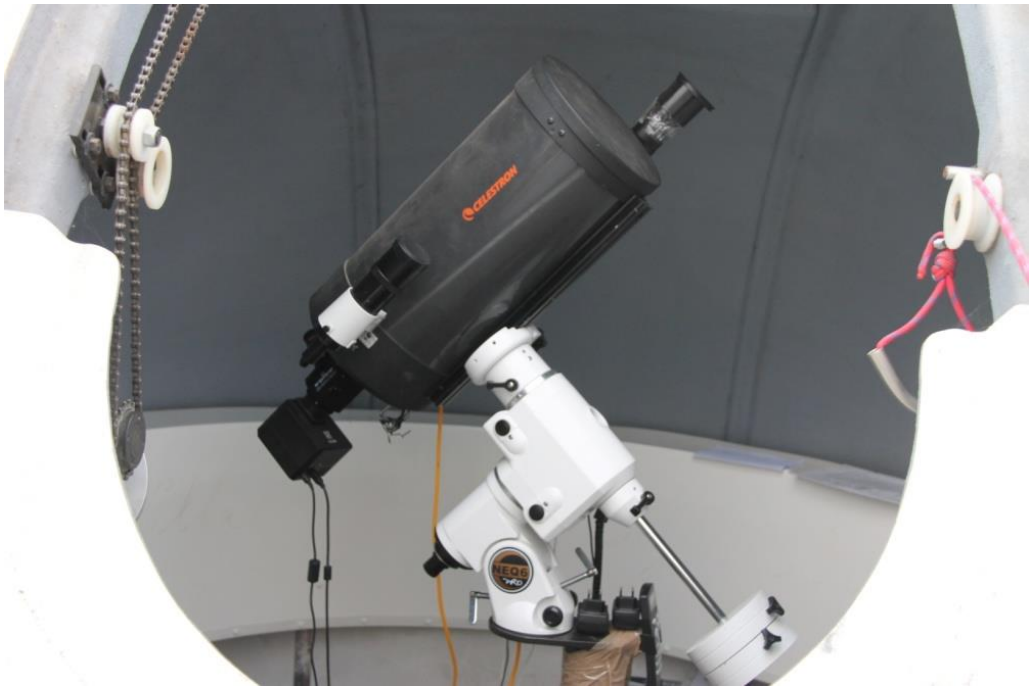

Figure 2: Our telescope and CCD camera.

Observations and analysis

We have realized our observations on July, August and September 2016, especially on July 29th, August 28th and 31st, September 1st, 7th, 8th, 10th, 22nd and 23rd. We feel the sky to be clear in the night of observations.

The determination of our used comparison and check stars and of the variable stars are as follows:

- Variable star m = 9.304; TYC 1113-877 (GSC 01113–00877)
- Comparison star m = 10.074; TYC 1113-951
- Check star m = 10.128; TYC 1113-111

We have used the Muniwin software package to treat the observed subsequently data in any filter.

In the treatment of the measured data we have also used the software package Statistica and the program *vstar.jnpl* which we have freely downloaded from the AAVSO Web page.

In our computations we have used the light curve values given in the *var2.astro.cz* page as follow (according to Dubovsky Pavol):

M_0 = 52816.827 and PER = 0.86707 d

We have constructed the light curves for the measurements without filter and for the BVRI filters too. The usage if the *vstar.jnpl* program allowed us to assembly the color indexes of the star UZ Equulei for the period of our measurements.

The results

Before all, we have checked the integrity of our measurements especially if our results (data) are not shifted in the magnitudes. In accordance with the data presented on the Fig. 3, we can conclude that our data are not shifted or influenced by any systematic error. The abbreviation “nn” and number are representing the individual days (nights) of observations in the Fig. 3.

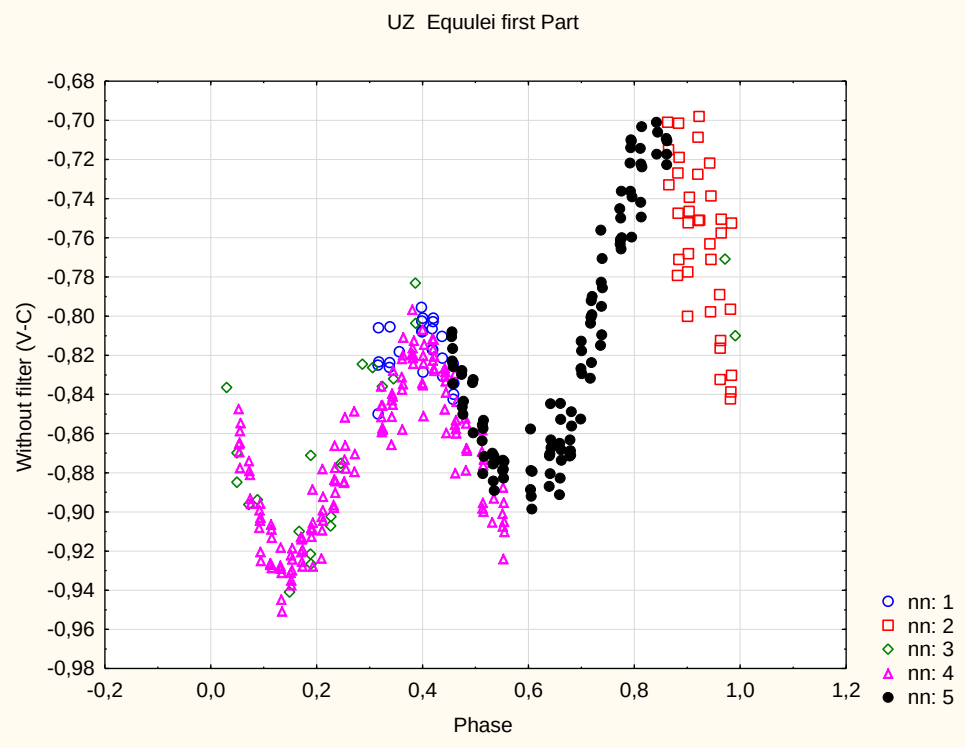

Figure 3: The light curve of the UZ Equulei in the integral light.

We have treated our data in all the filters by the usage of the program *vstar.jnpl* and we have obtained so called means. This data we have included into the analysis further.

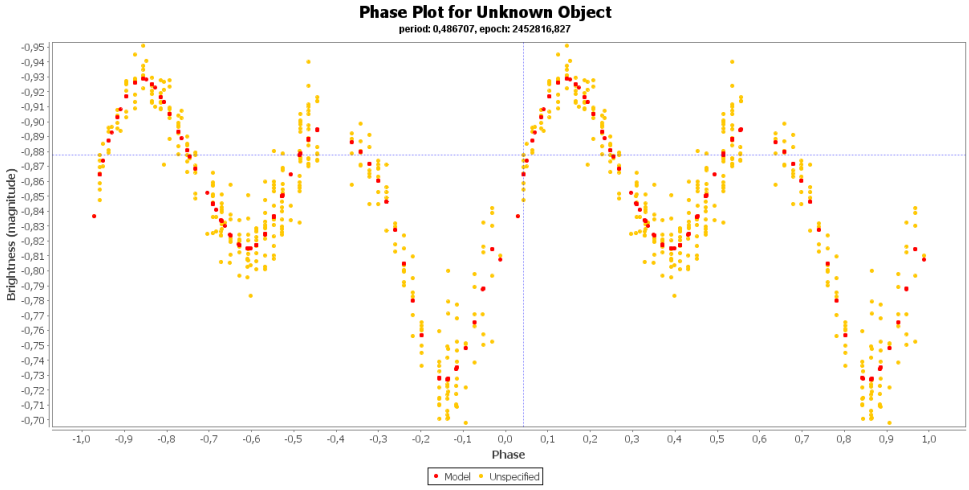

Figure 4: The same data as on the Fig. 3 but with reversed Δm (as it should to be) from the program *vstar.jnpl*. The big red points are the means.

Our basic results are on the Fig. 5. We see that the primary minimum is deeper that the secondary one in the case of the integral light, only – the dashed line. There is to be mention that the primary minimum is almost missing for the infra filter. Next the secondary minima for the integral light and for the infra filter are rather shifted in time in comparison with the minimum event in the B, V and R filters.

We have successfully assembled two successive light curves from our data as there is depicted on the Fig. 6. There seen us that the V-C difference is decreasing in time. I.e. the system is darkening as a whole. Of course to conclude this from two light curves is rather courageous but we have to take notice of the changes between these two light curves. We hope that in the next observational season we will be able to confirm or to refute this thesis. So, there is why we will not begin to speculate about its reason or origin, in this time.

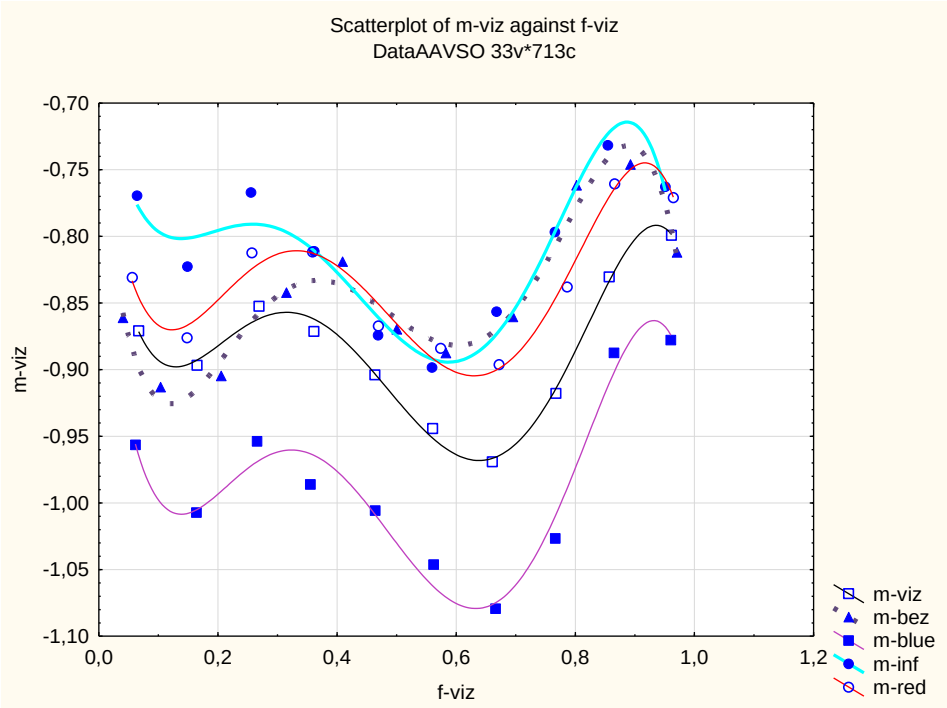

Figure 5: The light curves of the UZ Equulei in individual colors.

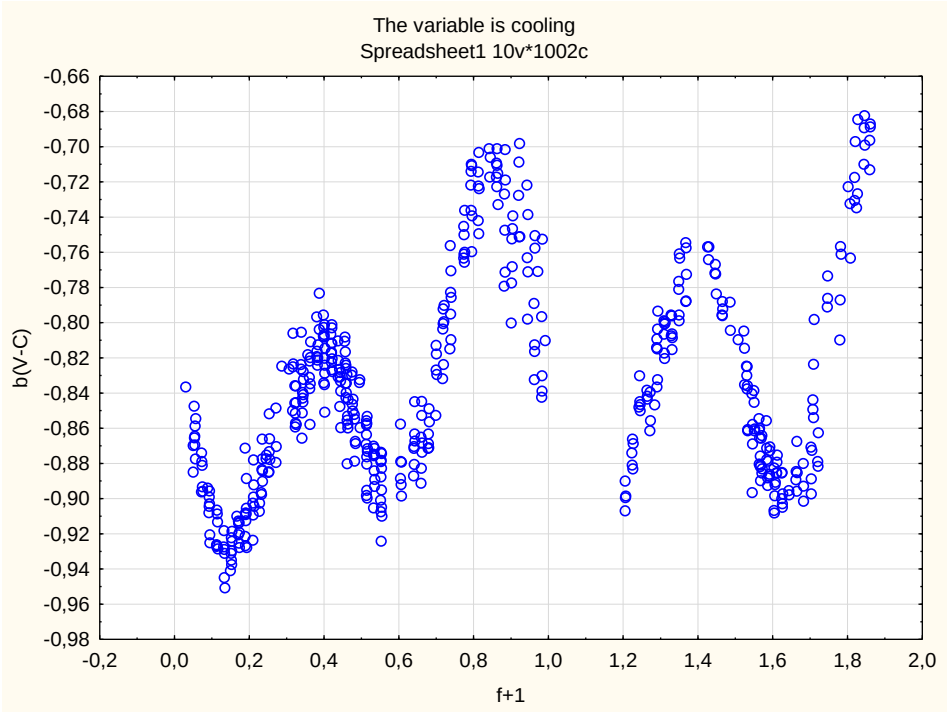

Figure 6: Two consecutive light curves of the UZ Equulei.

Conclusions

As we have mention in the introduction there is happenstance that we have selected this system as the probe for our CCD camera. Now we see that this object is worthwhile to be observed in the future seasons for us.

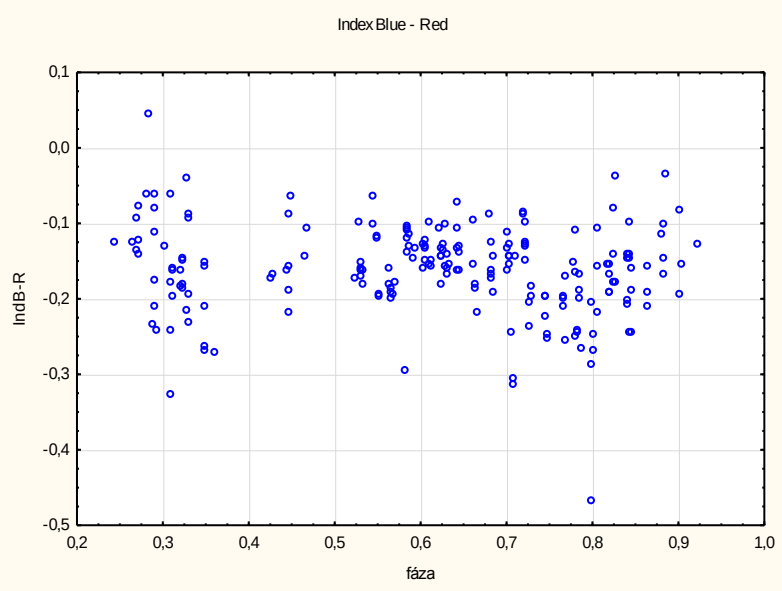

Figure 7: Color index B–R data.

Especially very interesting are the color indexes which according to our observations show no period dependence. Of course this is true in the frame of our measurement accuracy.

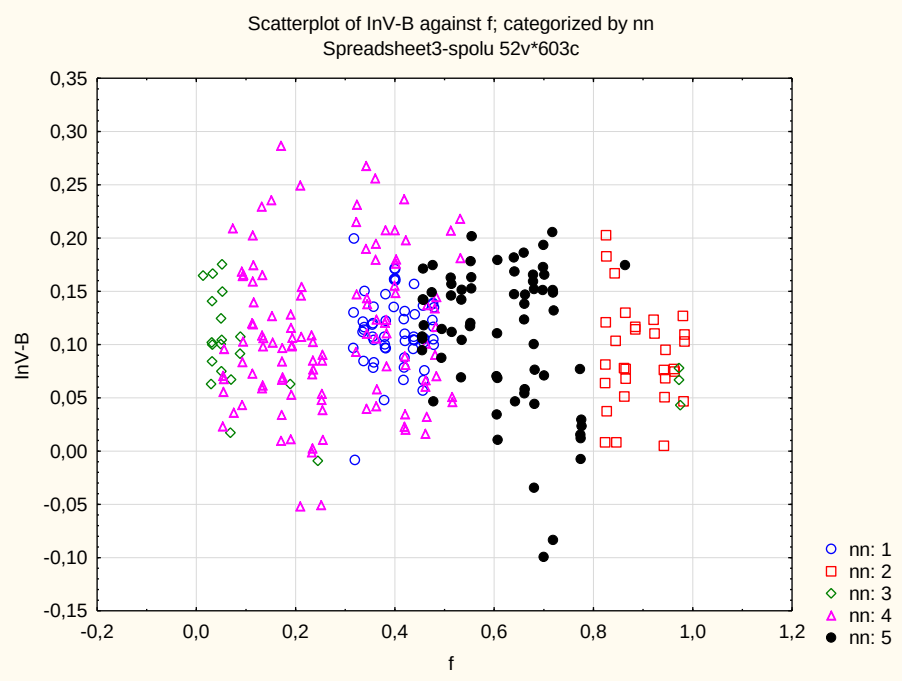

Figure 8: Color index V–B data.

We have tried to check if in the color indexes determination is not a systematic error. But from the results given on the Fig. 8 where there are the data given with respect to the observation day we conclude that our results or measurements are correct even if with rather higher scattering.

We are looking forward for the future larger and more precise observations from which we hope to obtain deeper insight into the UZ Equulei system.

Acknowledgement

We highly appreciated the support which we have obtained from the Czech Astronomical Society (ČAS) and from the Slovak Union of Astronomers (SZA).

References

Dubovsky Pavol, data on UZ Equulei, var2.astro.cz web page

AAVSO Web page

Variable Stars in the Field of V729 Aql

P. CAGAŠ [1]

(1) BSObservatory, Modrá 587, 760 01 Zlín, Czech Republic, pc@bsobservatory.org

Abstract: Wide field instruments can be used to acquire light curves of tens or even hundreds of variable stars per night, which increases the probability of new discoveries of interesting variable stars and generally increases the efficiency of observations. At the same time, wide field instruments produce a large amount of data, which must be processed using advanced software. The traditional approach, typically used by amateur astronomers, requires an unacceptable amount of time needed to process each data set. New functionality, built into SIPS software package, can shorten the time needed to obtain light curves by several orders of magnitude. Also, newly introduced SILICUPS software is intended for post-processing of stored light curves. It can be used to visualize observations from many nights, to find variable star periods, evaluate types of variability, etc. This work provides an overview of tools used to process data from the large field of view around the variable star V729 Aql and demonstrates the results.

Abstrakt: Širokoúhlé přístroje mohou být použity k získání světelných křivek desítek nebo dokonce několika set proměnných hvězd za noc, což zvyšuje pravděpodobnost nových objevů zajímavých proměnných hvězd a obecně zvyšuje efektivitu pozorování. Zároveň ale širokoúhlé přístroje produkuji velké objemy dat, které je nezbytné zpracovávat pokročilými programy. Tradiční přístup, používaný převážně amatérskými astronomy, vede na neakceptovatelně velké množství času potřebné ke zpracování pozorování. Nové funkce zabudované do programu SIPS mohou zkrátit čas potřebný k získání světelných křivek až o několik řádů. Také nově uvedený nástroj SILICUPS je určený k následnému zpracování již uložených světelných křivek. Může být použit k zobrazení pozorování z řady nocí, k hledání period proměnných hvězd, k vyhodnocování typů proměnnosti atd. Tato práce ilustruje použití nástrojů při zpracování širokoúhlého pole v okolí proměnné hvězdy V729 Aql a ukazuje výsledky, kterých může být dosaženo.

Introduction

The field of V729 Aql variable star was first observed at the BSObservatory[1] on September 29th, 2011. As a coincidence, this observing night was the first one, during which a new wide-field telescope/camera setup was used, allowing for 70'×70' field of view with approx. 1.4"/pixel sampling. Besides the V729 Aql, more than 30 previously unknown variable stars within the field of view were discovered during the year 2011.

The same field was subsequently observed during 43 nights, with the last observation dated September 30th, 2016. Beginning in June 2015, new TCMT (Thirty Centi-Meter Telescope) instrument set was used, providing a field of view 90'×90' and approx. 1.3"/pixel sampling. More than 160 variable stars were discovered within the field of view of which only three variable stars (V1058 Aql, V1065 Aql and already mentioned V729 Aql) were previously known.

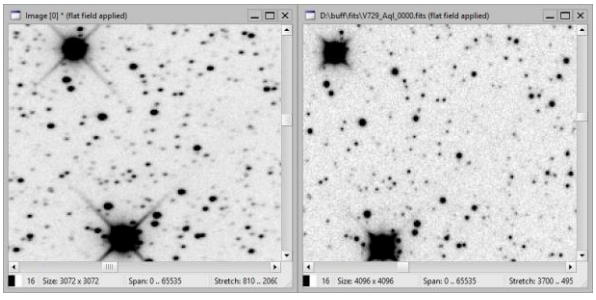

Figure 1: Comparison of image quality from original BSO wide-field instrument (left) and new TCMT (right). Although the left image was acquired with two-times longer exposure time, the right one offers better S/N of photometry.

The new instrument brought not only greater field of view and slightly better sampling but also significantly better tracking and bigger aperture (30 cm primary mirror is used instead of 25 cm). What is more, the field of view, despite 65% greater, is better corrected and suffers less from vignetting. The result is higher S/N of

[1] http://www.bsobservatory.org/

measured stars and a possibility to measure dimmer star, and thus it is possible to measure light curves of more stars at once.

The SIPS Photometry tool

The amount of data generated every night by TCMT is considerable. Single image size exceeds 32 MB, and there are between ~50 and ~250 images acquired every night. Single night data production can reach up to ~7.5 GB.

A number of stars detected in each image can reach several thousands when the target field is out of the Milky Way regions, but even more than 100 000 if the telescope points to Milky Way, which is the case of the field around V729 Aql. A total number of stars, which should be detected and for which photometry must be calculated on all images acquired during one night can reach approx. 25 million. Despite all optimizations of the SIPS[2] software, demands on computer resources (CPU speed, number of CPU cores, amount of memory, …) are high.

Of course, the number of stars practically useable for photometric measurements is much lower than the number of all detected stars – only between 20 000 and 30 000, depending on star minimum depth, Moon phase or light pollution, atmosphere transparency, etc. In the case of TCMT telescope of the BSObservatory, the limiting magnitude is around 18 Mag after 80 to 120 seconds of exposure time.

SIPS Photometry tool field description

Manual marking of more than a hundred of measured variable stars, corresponding comparison stars and possibly check stars on images with 4k×4k pixels resolution is no longer possible within a reasonable amount of time. SIPS software allows defining a description of stars within the field of view. Storing of light curves of all variable stars, defined in the description file, is a matter of minutes or tens of minutes, compared to hours or days necessary in the case of manual star marking.

Field description can be created either interactively using the SIPS GUI or programmatically, as the description is a simple text file.

```
[Description]
version = 1
catalog = UCAC4
[Stars]
CzeV278 = 5.214202445E+0; 2.416943678E-1; 520-116786; 5.214201737E+0; 2.416945087E-1
CzeV277 = 5.213997768E+0; 2.416949445E-1; 520-116759; 5.21399635E+0; 2.416958225E-1
CzeV276 = 5.211927943E+0; 2.291749071E-1; 516-118485; 5.211928455E+0; 2.29174239E-1
CzeV274 = 5.217900065E+0; 2.386507444E-1; 519-115804; 5.217901258E+0; 2.386517938E-1
CzeV273 = 5.217856905E+0; 2.306025753E-1; 517-114737; 5.217855933E+0; 2.306040272E-1
CzeV272 = 5.213611888E+0; 2.316463544E-1; 517-114241; 5.213612257E+0; 2.316458191E-1
...
[Variables]
CzeV272 = c060; ; ; ; ; ; ; ; ;
CzeV273 = c110; ; ; ; ; ; ; ; ;
CzeV274 = c060; ; ; ; ; ; ; ; ;
CzeV276 = c069; ; ; ; ; ; ; ; ;
CzeV277 = c060; ; ; ; ; ; ; ; ;
CzeV278 = c026; ; ; ; ; ; ; ; ;
...
```

Figure 2: Simple example of the SIPS Field Description file. The … indicate deleted portions of the file.

Prerequisite for work with Field Description is a complete astrometric solution of all images in the observing set because the description relies on equatorial coordinates of individual stars. SIPS Photometry tool supports advanced features like modeling of the field curvature, necessary to achieve robust astrometry solution of images acquired with wide-field instruments, often influenced by significant deviation from the ideal tangential projection of the celestial sphere. A detailed description of how to use SIPS for a photometric reduction in general and how to compensate field curvature, in particular, is out of the scope of this document. However, everything is thoroughly described in the SIPS User's Manual.

After the [Description] section, currently stating file format version and the used astrometry catalog, the [Stars] section follows in the description file. Each star occupies a single line in this section. The line begins with

[2] http://www.tcmt.org/software.html

assigned star name, followed with an equal sign and two or five semicolons delimited parameters. First two parameters are obligatory, and they define equatorial coordinates of the star determined by the SIPS astrometry (note the coordinates are expressed as floating point numbers, angles are in radians). If the star is matched with the corresponding star in the astrometry catalog, three more parameters follow – catalog identification and equatorial coordinates defined in the catalog. When the field description is used for processing, the catalog name and catalog coordinates have precedence to coordinates determined by SIPS. Only if the catalog matching star is missing, the coordinates determined by SIPS are used.

Only stars defined in the [Description] section may be used in the subsequent [Variables] section. Every line describes one Variable-Comparison-Check star relation. Variable star name is the first identifier, followed by the equal sign. Names of the used comparison stars follow (up to 10 comparison star can be defined) and possible check star can be stated as the last identifier on each line. Comparison and check star names are delimited by a semicolon.

When the observing set is processed in SIPS and field description is loaded, just selection of any line in the field description sheet selects a variable star, one or up to ten comparison stars and possibly also a check star. The light curve is immediately plotted and can be saved together with a corresponding selected image.

Finding new variable stars

Searching for new variable stars within dense star fields is not an easy task. Methods based on finding stars, which brightness deviation through the time of observation is higher than average, are almost useless because of a big number of false positives. A number of stars, whose brightness deviation through the observing time is very high for various reasons, can reach many thousands. This is an order of magnitude greater number than the number of actual variable stars in the field of view.

False detection of variable stars may be caused by a number of effects:

- Atmospheric extinction.
- Vicinity of a nearby star, affecting pixels within the photometric aperture of the measured star.
- Wrongly matched stars.
- “Disappearance” (dimming below the detection threshold) of a star during observation.

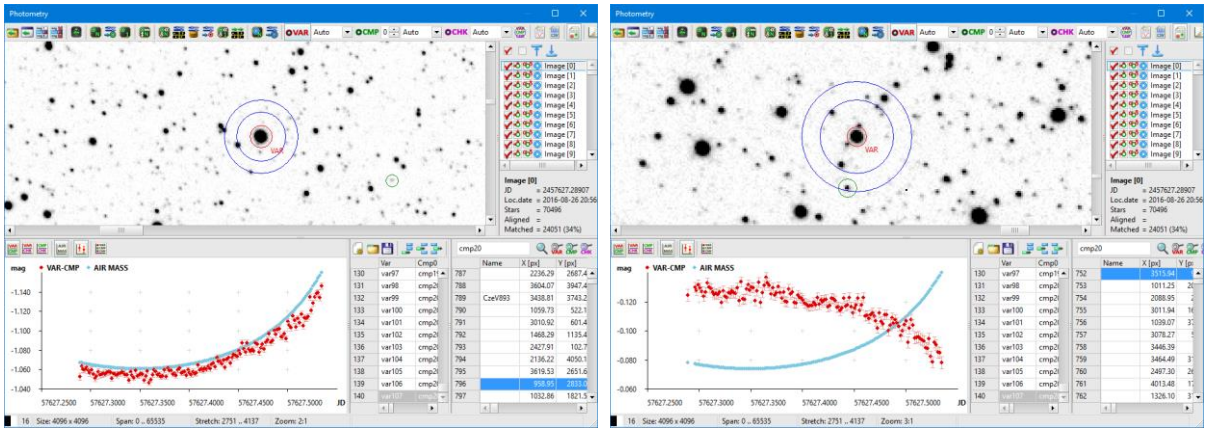

Figure 3: Example of false positive variable stars, which brightness change is caused by different colors. Relation to air-mass curve (displayed in light blue) indicates the brightness changes depend purely on air mass.

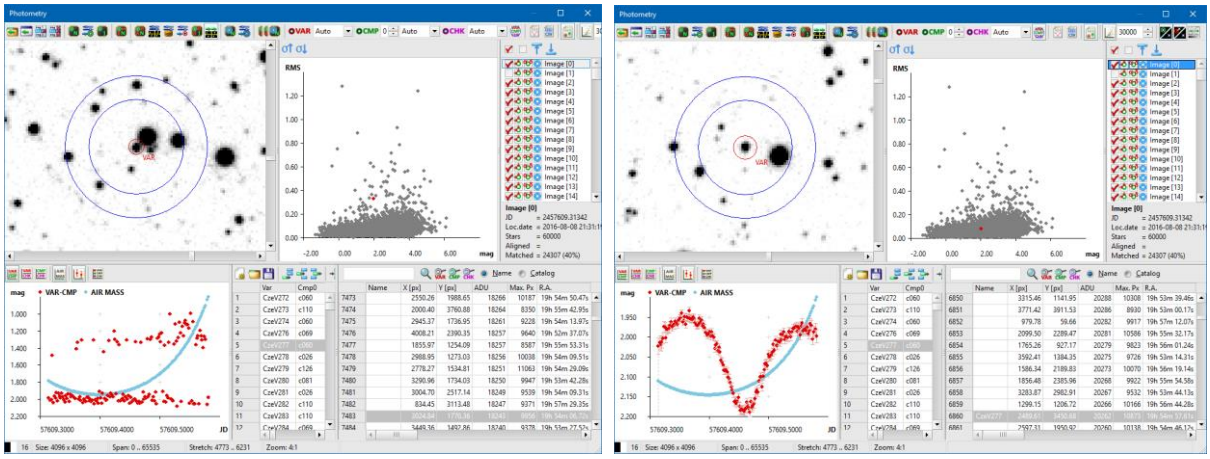

Figure 4: Example of a false positive star (left), which measured brightness is affected by the nearby bright star. The star is well above average in the chart showing the relation between instrumental magnitude and standard deviation. As opposite regular variable star with relatively low minimum depth (right) is within the standard deviation average on the same chart.

Obviously, many undiscovered variable stars may stay hidden in data. New reliable methods of automated searching for typical patterns of variable stars or exoplanets should be developed to discover them.

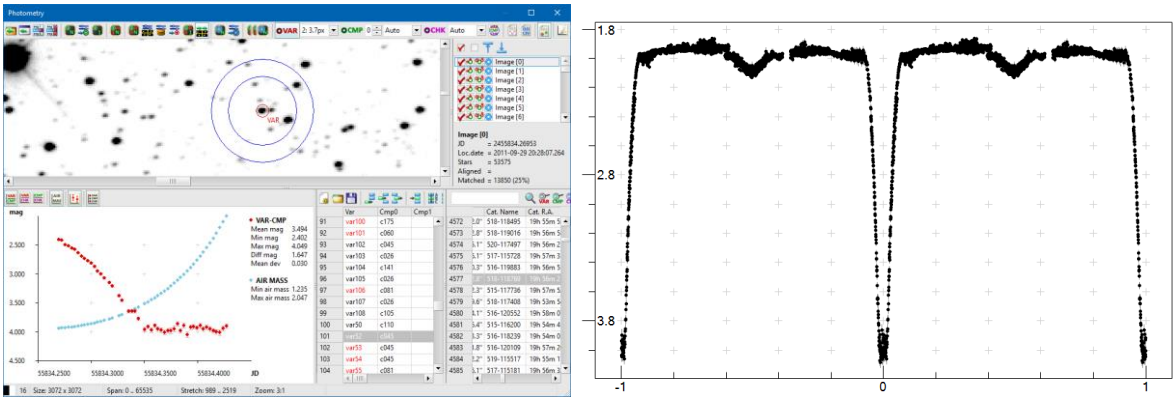

Figure 5: Example of the variable star CzeV978, discovered only in August 2016, despite the very deep minimum was recorded but overlooked during processing the very first night the V729 Aql field was observed on September 29th, 2011 (left). Phased light curve of the CzeV978 (right).

Choosing of comparison stars

As illustrated in the previous sub-chapter, the difference in color between variable and comparison star may cause significant artifacts in light curves due to atmospheric extinction. This is especially important when the observation is performed without a color filter, as is the case of wide-field observations at BSObservatory. Filters significantly limit throughput and thus also lowers the number of stars, which can be effectively measured.

Influence of extinction can be eliminated (or at last significantly reduced) by choosing the comparison star with color as close as possible to the variable star. However, there are also other requirements for the comparison stars – they should be as bright as possible to achieve best possible S/N of light curves. At the same time, comparison stars should not be too bright, because they must not saturate. Saturation of either of variable or comparison star invalidates any measurement.

Saturation of a star depends on many variables. Obviously, it depends on star brightness, telescope diameter, camera sensitivity and exposure time. However, many subtle effects influence saturation significantly, for instance, quality of optics, focusing, seeing, atmosphere transparency, etc. This means that a star with brightest pixels well within the camera dynamic range on exposures acquired during an average night may reach saturation level on exposures taken during an excellent night. Therefore, it is desirable to choose comparison stars on perfectly focused, high-quality images.

Either way, finding good comparison star, which fits all above-mentioned criteria, is not easy. To make it easier, SIPS software offers all information, which must be considered, in one table. At the same time, SIPS Photometry tool centers the image of selected star in another pane, so it is possible to judge other aspects, which influence star suitability as comparison star, for instance, close proximity to another star, etc.

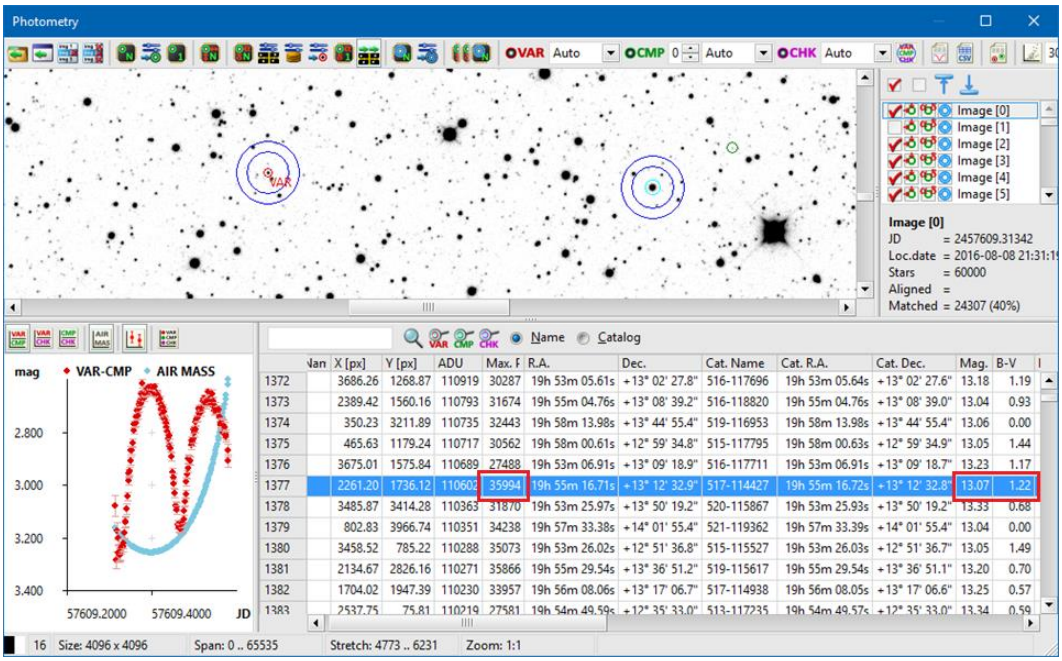

Figure 6: SIPS Photometry tool shows ADU value of the brightest pixel for every star, and if the star is matched with a catalog, also the catalog brightness and color (B-V) values are displayed.

Table 1. An example of a set of comparison stars selected for approx. 160 variable stars measured in the field of V729 Aql.

Number	Name	B-V	Mag.	UCAC4
1	c026	0.26	12.87	515-116712
2	c023	0.32	12.83	514-114194
3	c038	0.38	12.76	516-119237
4	c045	0.45	13.04	518-117617
5	c047	0.47	12.68	520-117125
6	c051	0.51	12.74	520-118042
7	c060	0.60	12.93	520-117983
8	c069	0.69	13.05	517-114219
9	c081	0.81	12.74	516-118841
10	c088	0.88	13.13	517-114489
11	c096	0.96	12.35	519-115141
12	c105	1.05	12.37	516-120170
13	c110	1.10	12.77	515-116705
14	c126	1.26	12.83	517-115203
15	c132	1.32	12.60	518-118500
16	c141	1.41	12.74	519-116383
17	c154	1.54	12.99	517-114363
18	c165	1.65	13.20	518-119279
19	c175	1.75	13.24	517-114841

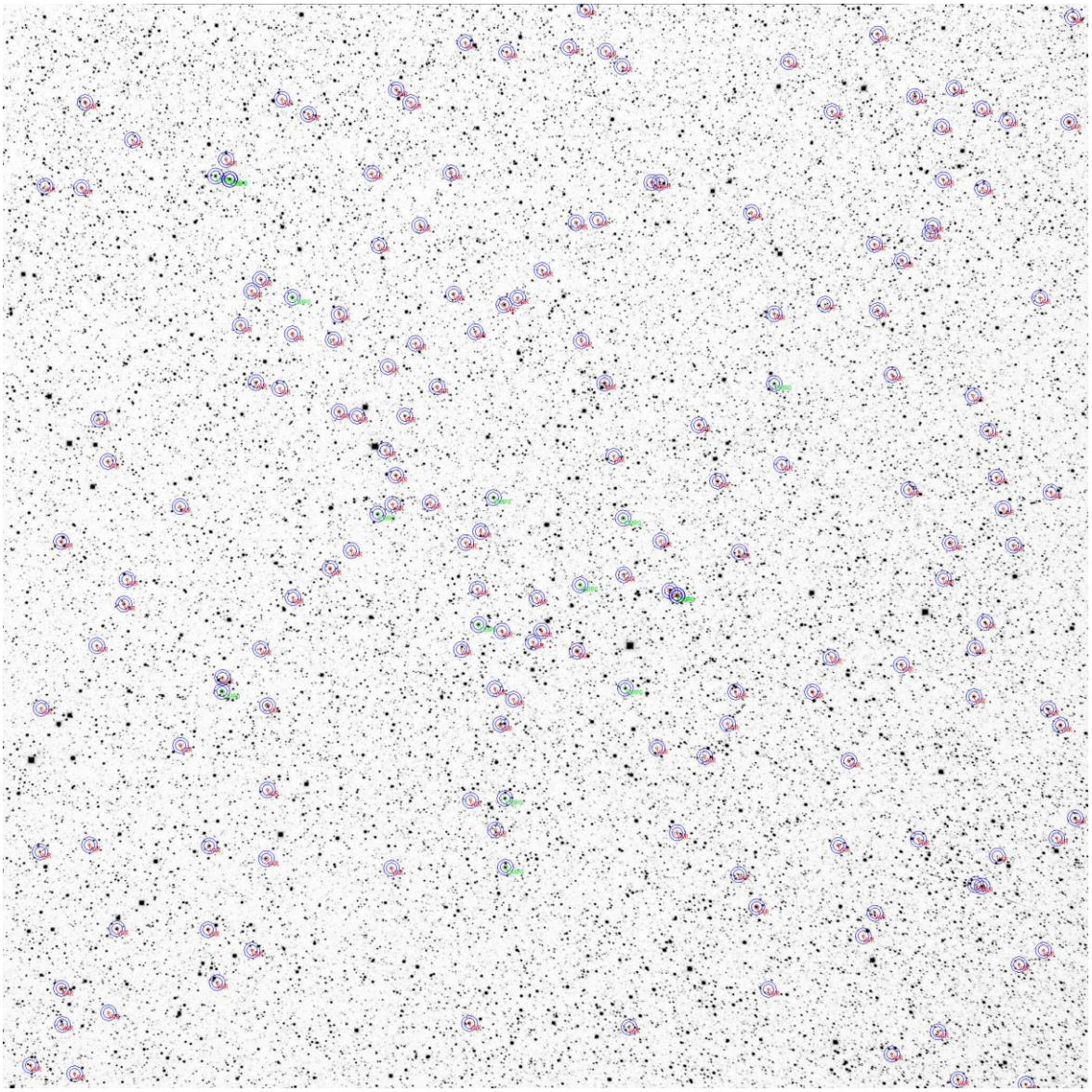

Figure 7: File around V729 Aql with all measured variable (red) and comparison (green) stars highlighted.

Subsequent processing of photometry data

Processing of every observing set generates a lot of light-curve data files. To make the data available to other researchers, the most common way of sharing them is uploading them to some web-based repository. However, using WWW-based forms to upload tens or even more than a hundred of light curves one by one needs much time.

It is quite common the measurement should be done again under different circumstances and already uploaded data must be edited. For instance, the B-V index stated in the catalog is not accurate or the particular variable star is so dim that its color is not included in the used catalog or the star is missing from the catalog at all. The absence of color information makes a selection of proper comparison star difficult. Unfortunately, light curve trends, caused by atmospheric extinction, may be obvious only after several nights, when the period of the star can be determined. In such cases, it is desirable to choose a different comparison star, which color better matches the variable star. All already saved light cure files must be overwritten with new ones. Keeping all data current using the WWW based forms, requiring every single observation to be manually reloaded, needs even more time.

All the problems mentioned above were the motivation for Václav Přibík to create new software tool called SILICUPS (SImple LIght CUrve Processing System)[3].

SILICUPS allows observers not just to "upload and forget" their observations, but to understand the stars they observe. This means to collect all saved observations of chosen star and to visualize the light curve, either in time-series or phased. Especially amateur astronomers then should be able to judge their observations, to determine the types of variability, to find periods, etc. By other words to be able to understand the stars they observe and to recognize if there is something interesting, which deserves continued study, publication, etc.

SILICUPS do not duplicate the magnitude data, created by the photometry software. Instead, it keeps the track where individual data files for each object are located. When any data file is changed, SILICUPS automatically reflect these changes without the necessity of performing any actions on the user's side.

Multiple objects are handled together as single "solution." Typically, one solution is created for every target field.

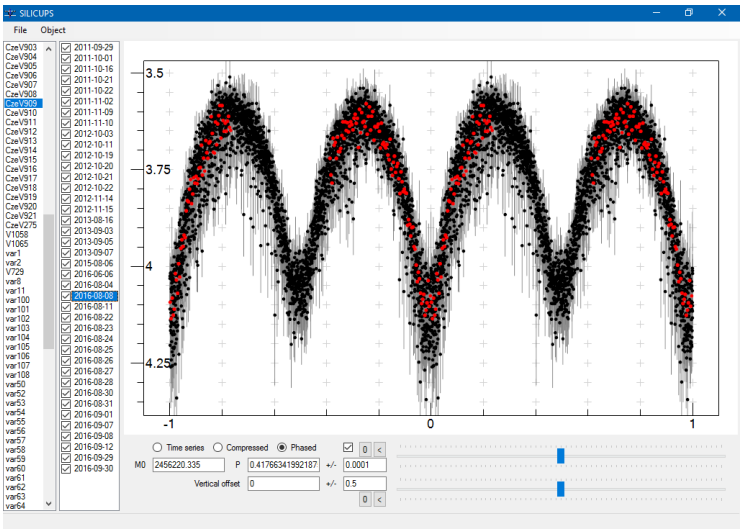

Figure 8: Example of SILICUPS user interface

Currently, SILICUPS provides basic functionality for light curve processing. However, it also provides room for future enhancements and developments. Planned new features include minima fitting, period search, O-C chart plotting, etc.

[3] https://github.com/HinataSoft/Silicups/blob/master/Silicups.exe

FrameSmooth software - new tool for the calibration of astronomical images

P. A. DUBOVSKÝ[1], O. B. BRIUKHOVETSKYI[2], S. V. KHLAMOV[3],I. KUDZEJ[1], Š. PARIMUCHA[4], A. V. POHORELOV[3], V. E. SAVANEVYCH[2], V. P. VLASENKO[2]

(1) Vihorlat Observatory, Mierová 4, 066 01 Humenné, Slovakia, var@kozmos.sk

(2) Western Radio Technical Surveillance Center, National Space Agency of Ukraine

(3) Kharkiv National University of Radioelectronics, Kharkiv, Ukraine

(4) Institute of Physics, Šafárik University, Košice, Slovakia

Abstract: The traditional procedure of image calibration in differential photometry is based on correction for dark-frame and flat-field. This approach don't remove big scale non-uniformities in the detector illumination caused by Moonlight or other scattered light. This can be corrected by mathematical methods. Ukranian developers of CoLiTec software use inverse median filter for astrometric tasks. We have tested the possibility to use it for photometry also. The answer is generally positive. There is a chance to skip the flat-field calibration in some cases. We present the FrameSmooth software which performs different image calibration procedures and also able to operate in fully automatic mode.

Abstrakt: Klasický postup pri redukcii astronomických snímkov určených na diferenciálnu fotometriu spočíva v korekcii na darkframe a flatfield. Tento prístup neodstráni veľkošálové nerovnomerosti v osvetlení čipu spôsobené napríklad Mesiacom, alebo iným parazitným svetlom. To sa dá odstrániť matematickými metódami. Skupina ukrajinských tvorcov programu CoLiTec používa pri riešení astrometrických úloh inverzný mediánny filter. Testovali sme, či sa takto upravené obrázky dajú použiť aj na fotometriu. Odpoveď je v zásade áno. Dokonca v niektorých prípadoch je možné vynechať redukciu na flatfield. Predstavujeme softvérový balík FrameSmooth, ktorý umožňuje kalibráciu obrázkov rôznymi spôsobmi a to aj v plne automatickom režime už počas pozorovania.

Introduction

Traditionally, equalization of astronomical frame background is made by hardware calibration. The calibration of astronomical images is reduced to pixel by pixel subtraction of Master-dark frame and dividing by Master-flat frame (McLean 2008, Howel 2006). Methods for calibration frame formation are fully described in the specialized literature (McLean 2008, Howel 2006, Berry & Burnell 2005, Warner 2006). The most time-consuming and inconvenient hardware calibration operation is advance (before night observation) preparation of the flat frame. Many astronomers want to abandon this due to a number of reasons. This leads to decreasing the quality of observational data. Hardware calibration of astronomical frames does not allow eliminate background from temporary parasitic illumination.

Andruk et al. (2002) proposes astronomical frame processing method within the MIDAS package (Buccheri et al. 1992) that does not use flat frames. The method is based on the separation of coarse-grained component of flat field from the frame using median filter. The disadvantage of this technical solution is using of third-party software. Also there is no analysis of quality indicators of proposed method of brightness equalization in this paper.

For brightness equalization of image background the low-pass filtering may also be used (Berry & Burnell 2005, Gonzales & Woods 2002, Solomon & Breckon 2011, O'Gorman et al. 2008, Martinez & Klotz 1998). The disadvantage of high-pass filtering is the necessity of representation an integer image in a floating point format in order to perform Fourier transformation. This tightens requirements for memory size. The presence of "ring"-type artefacts around bright objects on the equalized images (Gonzales et al. 2009) also limits usage of high-pass filtering for image equalization.

Substantiation of the inverse median filtering method usage for brightness equalization of astronomical images

Astronomical digital images may be divided into coarse-grained and fine-grained components. Each of these components has its own physical nature. Coarse-grained components correspond to the illumination of the image during astronomical observations at full moon or at sunrise/sunset and cover large part of frame. Fine-grained components correspond to the images of stars, asteroids and comets. The size of fine-grained components usually takes 5 ÷ 10 pixels and no more than 50 ÷ 60 pixels.

Difference between the images of interest (stars, asteroids, comets) and image background (coarse-grained components of astronomical images) makes it possible to use image frequency filtering for increasing the signal-to-noise ratio or decreasing the dynamic range of the image background. To remove coarse-grained components from the image it is advisable to use a high-pass filter that both attenuates low-frequency harmonics of the image spectrum and passes high-frequency harmonics. It is known that median filter with a certain window size may also perform functions of low pass filter. In this case high-pass filtering can be obtained by simple subtraction of the result of median filtering of the frame from initial frame.

In other words, difference between the sizes of images of objects of interest (stars, asteroids, comets) and image background (coarse-grained components of astronomical images) allows using image median filtering for coarse-grained components extraction. In this regard, described method has been called “inverse median filtering”.

Median filtering is non-linear image processing method. The median filter is implemented as a local processing procedure with sliding window of specified sizes (d_x , d_y) which includes an odd number of source image pixels A_{in} . Average count in this ordered set (median) is replaced by the central pixel of the filtered image window A_{med} (Fig. 1).

Gaussian values $G_k(\text{m},\text{n})$ are defined as:

$$G_k(\text{m},\text{n}) = \text{a}_k \exp\left\{-\frac{(m-m_k)^2+(n-n_k)^2}{2\sigma_k^2}\right\} \tag{1}$$

where k is the gaussian number;

a_k is the amplitude of the k gaussian;

m_k, n_k – the center coordinates of the k gaussian;

σ_k – the gaussian shape parameters.

Gaussians with shape parameters of $\sigma_2 = 1$, $\sigma_2 = 2$, $\sigma_3 = 3$ have respectively of 28, 113, 254 pixels which have brightness more than $0.01\,a_k$.

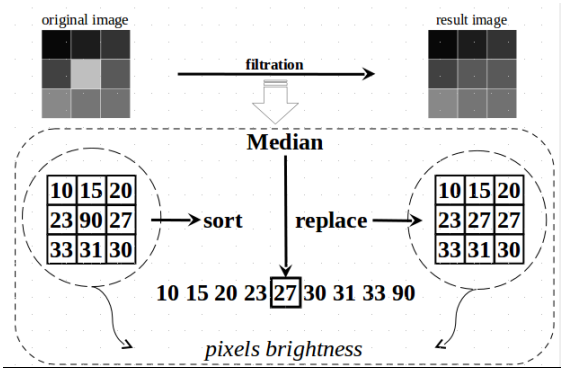

Figure 1: Median filtration

Using Calibration frames in Frame Smooth software

Proposed method of brightness equalization of frames has been implemented in the Frame Smooth software (Savanevych et al. 2016). This software may use calibration frames. It is especially important to use a master-dark frame. All master-frames are formed pixel by pixel. 10% of the largest and 10% of the smallest values of brightness of the each pixel is tentatively discarded. For the remaining K_1 values the pixel (m, n) brightness $A_k(\mathrm{m},\mathrm{n})$ related to used calibration frames the mean value is calculated:

$$\Delta_{K_1}(\mathrm{m},\mathrm{n}) = \frac{1}{K_1}\sum_{\mathrm{k}=1}^{K_1} A_k(\mathrm{m},\mathrm{n}). \quad (2)$$

and RMS:

$$\sigma_{K_1}(m,n) = \sqrt{\sum_{k=1}^{K_1}(A_k(m,n)-\Delta_{K_1}(m,n))^2/(K_1-1)}. \quad (3)$$

Brightness of the master-dark frame pixel is considered equal to the mean value of the pixel brightness only for K_2 ($K_2 \le K_1$) pixels that do not differ from the mean $\Delta_{K_1}(\mathrm{m},\mathrm{n})$ (2) by more than three sigma $\sigma_{K_1}(\mathrm{m},\mathrm{n})$ (3):

$$\sqrt{(A_k(m,n)-\Delta_{K_1}(m,n))^2}\ 3\cdot\sigma_{K_1}(m,n). \quad (4)$$

1. Preparation of the calibration frames.

1.1. The master-bias frame is formed on the basis of the bias frames according to the expressions (2) ÷ (3).

1.2. The master-dark frame is formed on the basis of the dark frames according to the expressions (2) ÷ (3). If there is a master-bias frame then before the formation of the master-dark frame the master-bias frame is subtracted from each of the original dark frame.

1.3. The master-flat preparation. If dark flat frames and/or master-bias frame exist, then the master-dark flat is tentatively formed similar to section 1.2. Then, the master-bias and the master-darkflat frames are subtracted from flat frames. After this operation, the flat frames are reduced to the same level of mean brightness of pixels per frame. This level is defined as the brightness level of the first frame. Normalization is performed by multiplying each pixel of the flat frame (except the first) on the normalization factor. This factor is equal to a ratio of the sum of all pixels brightness of the first frame to the sum of all the pixels brightness of the analyzed frame. Then, from the transformed flat frames the master-flat frame is formed using operations similar to section.1.1.

2. Brightness equalization of CCD-frames. Brightness equalization of image is performed as operation of pixel by pixel subtraction of master-flat from CCD frame. Obtained result is divided by the master-flat frame and filtered with use of inverse median filter. The use of the master-flat frame during inverse median filtration is optional and does not significantly affect the obtained results.

Testing on real images

Every mathematical method should be tested on real data. We have performed testing using images acquired on several telescopes of Astronomical Observatory on Kolonica Saddle (Kudzej et al. 2007) during regular observing sessions. Generally the test consisted in comparison of traditional way of calibration with the new one proposed in this paper. Traditional way means the reduction of the images as usually was done in the observatory: calibration by master-dark (subtraction) and master-flat (division). Master-dark is usually constructed as median of 20 dark frames taken in the same temperature and with the same exposure time as raw images. Master-flat is the average of sky flats subtracted by corresponding master-dark. The new way means the calibration using the inverse median filter. There are several ways how to include the inverse median filtration into the calibration process. Here we present results of the most logical and most simple configuration: master-dark subtraction, master-flat division and than inverse median filtration.

The first step of testing was the visual inspection of the calibrated images. Actually, the images deteriorated by strong scattered light were flattened after the application of inverse median filter. The application only of the master-flat was not able to remove the large background structures on the images. One example is presented in Fig. 2.

Figure 2: Images from VNT telescope affected by scattered light. From left to right: raw image; image calibrated using classical procedure [master-dark + master-flat]; image calibrated with FrameSmooth software [master-dark + master-flat + inverse median filter]; image calibrated with FrameSmooth software [master-dark + inverse median filter without master-flat]

The second step of our testing was comparison of the values of standard stars obtained by differential photometry on the images calibrated by traditional way and the images calibrated by proposed approach. For this test we have chosen images without scattered light, without big background structures, already well flattened by master-flat. In these conditions one has to expect the same result independent on the way of image calibration. Moreover, any unwanted impact of the inverse median filter application should be visible. Here we present results from four time series runs on C14 telescope (Celestron Edge HD CGE Pro 1400 equipped with Moravian Instruments G2-1600 camera). After the calibration the reduction process was the same for all images. The photometry was performed using the C-Munipack software (Motl 2009). Then the method of artificial comparison star was applied as implemented in the MCV software (Kim et al. 2004). This method use the concept of the main comparison star which brightness should be entered arbitrary. As we were not interested in absolute values of the photometry, we used the value 0 for the main comparison star. To avoid the influence of some trends caused by extinction we have selected only short segments (~ 30 minutes) of the time series. The mean values of measured stars were compared for classical calibration process (C) and the calibration with inverse median filter (F). The results are shown in the Figure 3 and Table 1. It is evident that two methods are equivalent in this situation.

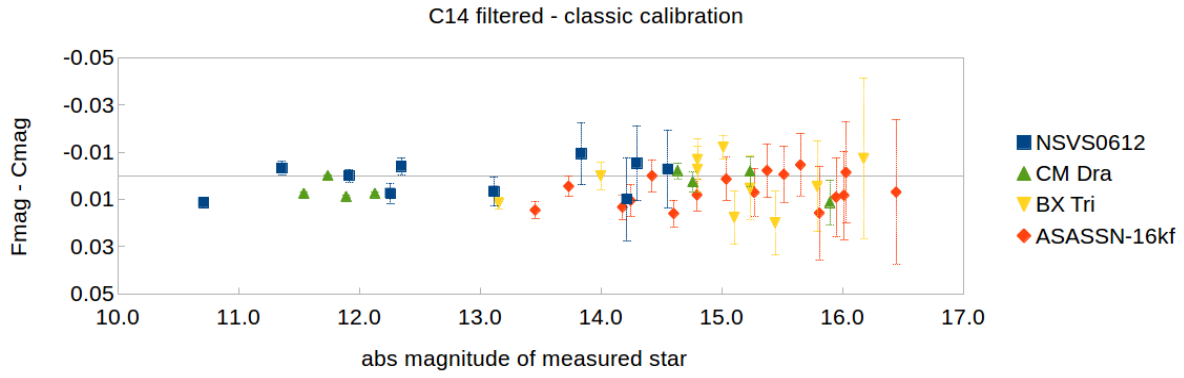

Figure 3: Differences between photometry on images calibrated in classical way (Cmag) and images calibrated by inverse median filter (Fmag). Results for 4 different time series runs on C14 telescope are shown. Only images well calibrated by classical master-flat were selected.

Table 1. Differences between photometry on images calibrated by inverse median filter (F) and classical calibration using C-Munipack software (C).

Time series run on target:	Filter	Number of measured stars	Average error of determination of mean magnitudes of measured stars [mag]	Mean value of F-C [mag]	RMS (F-C) [mag]
NSVS0612 2016-08-30	Rc	11	0.011	0.001±0.007	0.007
ASASSN-16kf 2016-09-09	Clear	17	0.012	0.006±0.006	0.009
CM Dra 2016-09-09	V	10	0.012	0.003±0.011	0.011
BX Tri 2016-09-12	Rc	8	0.003	0.004±0.005	0.007

The third step of testing consists in the repetition of the second step but on the images with severe impact of scattered light. We chose the observation of VNT telescope (Kudzej & Dubovsky 2010) during moonlight. Figure 2 came from this time serie. Now the difference between the traditional and the new method of calibration becomes visible. In the Figure 4 we present comparison of classical result with filtered one without using master-flat. The values obtained by the second way are much morecloser to the values of Henden's photometry (Henden 2005). It is clearly visible that the discrepancies depend on the value of the master-flat image around the position of the given star. So the problem is caused by wrong master-flat. One can say that this is only happy coincidence and the "correct" values are those obtained by classical procedure. There are several ways how to reveal wrong data. For example, the r-R values should have some dependency on colour index of standard stars. In the Figure 5 we present these plots. The filtered points are usable for determination of the transformation coefficient. The classical values do not show significant dependency.

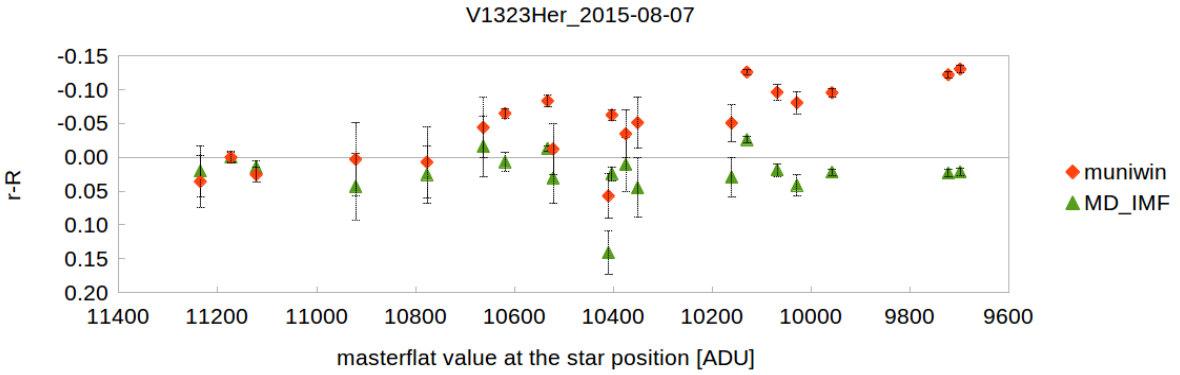

Figure 4: Measurements of standard stars in the field of V1323 Her. R - standard values from Henden's photometry, r – measured values on our images, 'muniwin' stands for classical procedure, 'MD_IMF' means result of FrameSmooth software using master-dark and inverse median filter without application of master-flat. In order to show the influence of wrong master-flat we use the value of the corresponding master-flat at the position of the measured star as the abscissa value.

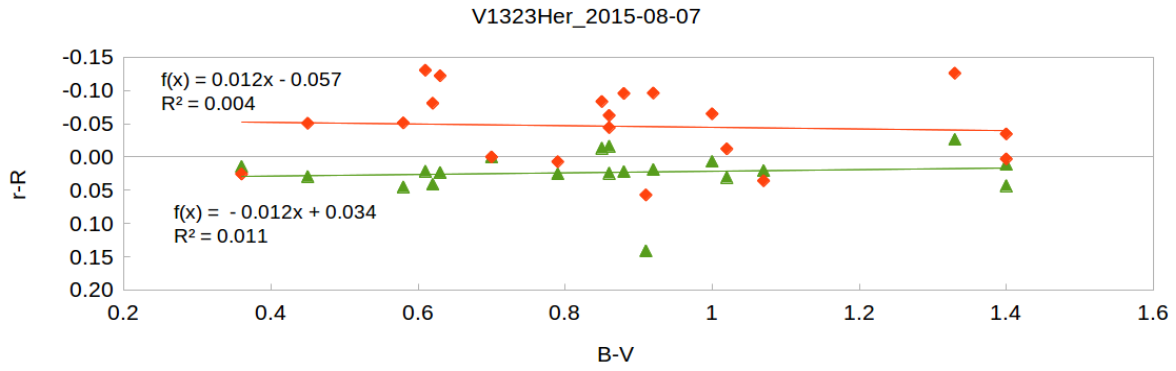

Figure 5: The same values as in Figure 4 plotted against color index B-V of standard stars. Linear fits are also shown.

Another proof of correctness is comparison of differential photometry on the frames with significant shift in physical position of stars on the detector. Actually, this is the principle of the method of stellar calibration of CCD flat fielding proposed by Manfroid (1995). In real life the meridian flip on german equatorial mount can be used without loss of observing time. Unfortunately, VNT telescope has fork mount so we have had to wait to accidental failure of autoguiding system to obtain frames with stars gradually drifting on the detector. The result of photometry in such conditions is depicted in the Figure 6. Although the background was well flattened by sky master-flat, there are severe trends present on the photometry of constant stars. No trends are present on the frames calibrated by FrameSmooth software using the inverse median filter.

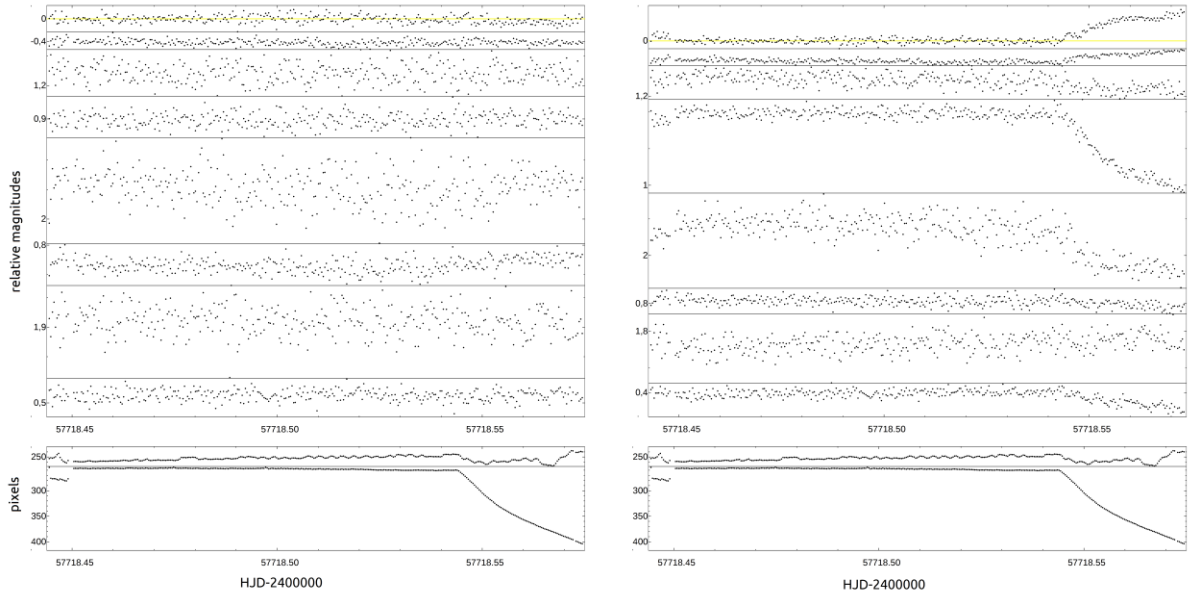

Figure 6: The light curves of comparison stars in the field of the variable GJ3236 restored using the "multi-comparison star" method implemented in "MCV" software (Kim 2004). Left: frames calibrated with inverse median filter. Right: Frames calibrated by conventional master-flat. Bottom: Tracking errors in RA and Dec respectively.

Conclusions

This article describes the computational method of brightness equalization of astronomical images based on the inverse median filtration and implementation of proposed method for large images. As indicators of the background equalization quality we introduced estimation of the mean values and standard deviation of the background pixels brightness both on the original and equalized frame's segments. The analysis of quality indicators of equalization of the astronomical images background have been carried out. Results demonstrated that the range of mean values of background pixels brightness was reduced in two times by the 5% level of the maximum histogram value. This decrease is greater the larger the size of the window is being used.

Furthermore, utilization of equalized images leads to increasing of astrometry accuracy indicators and stars photometry quality as well as the quality indicators of asteroids and comets detection.

Proposed computational method increases the signal-to-noise ratio and reduces the dynamic range of astronomical images background. Method was implemented and successfully used as part of CoLiTec (Savanevych et al. 2015a, Savanevych et al. 2015b, Pohorelov et al. 2016) software of automatic discovering of asteroids and comets on a series of digital frames This method has also been implemented in the Frame Smooth free software (Savanevych et al. 2016).

The proposed method of inverse median filter application can be used for calibration of astronomical images without negative influence on the results of the photometry. It can replace the master-flat application if there are no structures on the images background with size similar to the sizes of the stars. It is usually enough when the aim is relative photometry at 0.01 mag level. When absolute photometry with high accuracy is required, one has to be aware that even excellent uniformity of the background doesn't mean correct calibration for stellar sources. See Tobin (1993) for details.

Acknowledgement

This work was supported by the by the project APVV-15-0458 "Interacting binaries - Key for the Understanding of the Universe".

References

Andruk, V. N., Ivaschenko Yu. N., Butenko G. Z., 2002, Обработка ПЗС-изображений звездных полей в пакете MIDAS/ROMAFOT. Abstr. Int. Conf. ASTROECO- 2002 "Current status and prospects of international research in observational astronomy, ecology and extreme physiology in the Elbrus region", 71-74

Berry, R., Burnell, J., 2005, The Handbook of Astronomical Image Processing (Second English Edition), Willmann-Bell, 684

Buccheri, R., Crane, P., di Gesù, V., et al., 1992, Data Analysis in Astronomy IV. Ettore Majorana International Science Series, Springer Science & Business Media New York, 59.

McLean, I. S., 2008, Electronic Imaging in Astronomy. Detectors and Instrumentation (Second Edition), Springer, 552

Howell, S. B., 2006, Handbook of CCD Astronomy (Second Edition), Cambridge University Press, 208

Gonzales R., Woods, R., 2002, Digital Image Processing, Prentice Hall

Gonzales R., Woods, R., Eddins, S., 2009, Digital Image Processing using MATLAB 2nd ed., Prentice Hall

Henden, A. 2005, ftp://ftp.aavso.org/public/calib/j1803.dat

Kim, Y., Andronov, I.L., Jeon, Y. B., 2004, J. Astron. Space Sci., 21, 191-200

Kudzej, I., Dubovsky, P. A., 2010, Odessa Astronomical Publications, 23, 70

Kudzej, I., Karetnikov, V. G., Dubovsky, P. A., et al. 2007, Odessa Astronomical Publications, 20, 100

Manfroid. J.; 1995, Astron. Astrophys. Suppl. Ser., 113, 587-591

Martinez, P., Klotz, A., 1998, A practical guide to CCD astronomy, Cambridge University Press

Motl, D. 2009, C-Munipack, http://c-munipack.sourceforge.net/

O'Gorman, L., Sammon, M. J., Seul, M., 2008, Practical algorithms for image analysis: description, examples, and code, Cambridge University Press

Pohorelov, A.V., Khlamov, S.V., Savanevych, et al., 2016, Odessa Astronomical Publications, 29, 136–140.

Savanevych, V. E. et al., 2016, FrameSmooth, http://www.neoastrosoft.com/filter_en/

Savanevych, V. E., Briukhovetskyi, O. B., Ivashchenko, Yu. N., et al., 2015, Kinematics and Physics of Celestial Bodies, 31, 302–313.

Savanevych, V. E., Briukhovetskyi, O. B., Sokovikova, N.S., 2015, MNRAS, 451, 3287–3298.

Solomon, Ch., Breckon, T., 2011, Fundamentals of Digital Image Processing. A Practical Approach with Examples in Matlab, Willey-Blackwell

Tobin, W., 1993, in Stellar photometry – Current techniques and future developments, IAU Coll. 136, (Cambridge University Press) 304.

Warner, B. D., 2006, A Practical Guide to Lightcurve Photometry and Analysis, Springer

Outburst activity of the symbiotic binary AG Dra

R. GÁLIS[1], J. MERC[1] & L. LEEDJÄRV[2]

(1) Department of Theoretical Physics and Astrophysics, Institute of Physics, Faculty of Science, P. J. Šafárik University, Park Angelinum 9, 040 01 Košice, Slovakia, rudolf.galis@upjs.sk

(2) Tartu Observatory, Observatooriumi 1, Tõravere, 61602 Tartumaa, Estonia, laurits.leedjarv@to.ee

Abstract: AG Dra regularly undergoes quiescent and active stages which consist of a series of individual outbursts repeating at about a one-year interval. After seven years of flat quiescence following the 2006–08 major outbursts, in the late spring of 2015, AG Dra begun rising again in brightness toward what appeared to be a new minor outburst. The recent outburst activity of AG Dra was definitely confirmed by a more prominent outburst in April 2016. The photometric and spectroscopic observations suggest that these outbursts are of the hot type. Such behaviour is quite unusual, because the major outbursts in the beginning of active stages are usually cool. Can we expect the major cool or minor hot outburst during the spring of 2017? AG Dra demonstrates the importance of long-term monitoring of symbiotic stars in order to disentangle the nature and mechanisms of their active stages and outbursts.

Abstrakt: Symbiotický systém AG Dra charakterizuje pravidelné striedanie sa období pokoja a období búrlivej aktivity, pozostávajúcich zo sérií jednotlivých vzplanutí. Po siedmych rokoch pokojného obdobia, ktoré nasledovalo po dvojici hlavných vzplanutí v rokoch 2006–2008, jasnosť AG Dra začala na sklonku jari 2015 znovu stúpať. Ako sa ukázalo, išlo o menej jasné, vedľajšie vzplanutie. Nové aktívne obdobie AG Dra bolo definitívne potvrdené ďalším, jasnejším vzplanutím v apríli 2016. Fotometrické a spektroskopické pozorovania potvrdili, že ide o vzplanutia horúceho typu. Takéto správanie je však značne netypické, keďže hlavné vzplanutia na začiatku aktívnych období sú zvyčajne chladného typu. Čo môžeme očakávať počas jari 2017: hlavné chladné alebo vedľajšie horúce vzplanutie? AG Dra jasne demonštruje, že iba dlhodobé monitorovanie symbiotických hviezd môže pomôcť pri odhalení povahy fyzikálnych mechanizmov zodpovedných za aktivitu týchto interagujúcich dvojhviezd.

Introduction

AG Dra belongs to the subclass of so-called yellow symbiotic stars. Its cool component is of early K spectral class instead of M as in most other symbiotic stars. The hot component is a white dwarf (WD) with an effective temperature of 10^5 K and a luminosity of $\sim 10^3$ $L_\odot$ (Mikołajewska et al. 1995) obtained from the *International Ultraviolet Explorer* (*IUE*) data. However, Sion et al. (2012) have derived T_{eff} = 80 000 K from the FUSE far-ultraviolet spectrum.

AG Dra is an open (detached) binary with an orbital period of 550 days (Meinunger et al. 1979; Gális et al. 1999). The accretion most likely takes place from the stellar wind of the cool giant. Both components are in a circumbinary nebula, partially ionized by the white dwarf. A shorter period around 350 – 380 d has also been detected in photometric and spectroscopic variability of AG Dra (Bastian 1998; Gális et al. 1999; Friedjung et al. 2003; Hric et al. 2014). Gális et al. (1999) ascribed this period to the pulsations of the K giant.

The light curve (LC) of AG Dra, available since 1890 (Robinson 1969), manifests characteristic symbiotic activity with alternating quiescent and active stages. The latter ones consist of several outbursts repeating at about a one-year interval with a brightening of about 1 – 1.4 mag in the V/visual band and up to 2.3 and 3.6 mag in the B and U bands, respectively. Active stages occur in intervals of 9 – 15 yr (in 1936, 1951, 1966, 1980, 1994, 2006 and 2015).

On the basis of the analysis of all IUE observations González-Riestra et al. (1999) showed that there are two types of outbursts: cool and hot. Major outbursts at the beginning of active stages (e.g. 1981–83, 1994–96 and 2006–08) are usually cool, during which the expanding pseudo-atmosphere of the WD cools down and the He II Zanstra temperature drops. In smaller scale hot outbursts, the He II Zanstra temperature increases or it remains unchanged. Leedjärv et al. (2016) showed that cool and hot outbursts of AG Dra can be clearly distinguished by the behaviour of the emission lines in the optical spectrum of this symbiotic system.

One of the promising explanations of at least some individual outbursts of AG Dra might be the combination nova model proposed for Z And by Sokoloski et al. (2006). In this model, when accretion rate onto the white dwarf exceeds some critical value, thermonuclear reactions are ignited and luminosity of the hot component

increases significantly. One of the subsequent tasks would be to study whether the recent outbursts of AG Dra will fit into such a picture.

Observations

We use all photometric observations of AG Dra that had already been analysed and discussed in our previous study (Hric et al. 2014). New photometric data were obtained from AAVSO International Database (Kafka, 2016) and from Martin Vrašťák (2016).

High-resolution spectra were obtained at *Canada–France–Hawaii Telescope* (3.58 m) with Echelle Spectro-Polarimetric Device for the Observation of Stars (R = 68 000) and *Nordic Optical Telescope* (2.56 m) with Fibre-fed Echelle Spectrograph (R = 46 000) at JD 2 456 906.72 (September 6th, 2014) and JD 2 457 176.51 (June 3rd, 2015), respectively.

Intermediate-dispersion spectroscopy of AG Dra was carried out at the Tartu Observatory in Estonia. Altogether, 515 spectra obtained during almost 14 yr (from JD 2 450 703.3 to JD 2 455 651.5) on the 1.5-metre telescope (R ≈ 6 000, 7 000 and 20 000), were analysed in our paper (Leedjärv et al. 2016). We focused on the strongest emission lines in the wavelength regions under study: the hydrogen Balmer lines Hα (λ6563) and Hβ (λ4861), the neutral helium He I line at λ6678, the ionized helium He II line at λ4686 and the Raman scattered O VI line at λ6825. Equivalent widths (EWs), fluxes in lines, peak intensities relative to the continuum and the positions of these lines were measured. In present paper we used these measurements to compare spectroscopic behaviour of AG Dra during the outbursts in 2015–16 with previous activity of this interacting binary.

New spectroscopic observations were obtained from *Astronomical Ring for Access to Spectroscopy* database. Despite the fact that the spectra were obtained with small telescopes (25 – 35 cm, R ≈ 1 800 – 11 000), they provided us valuable information about recent activity of AG Dra.

Photometric behaviour of AG Dra

The LC of AG Dra, which manifests 127 yr of the photometric history of this symbiotic system is depicted in Fig. 1. The LC over the period 1889–1966 was constructed using the compilation of photographic observations by Robinson (1969). The first photoelectric photometry of AG Dra was obtained by Belyakina (1969). Since 1974, the system has been observed systematically, mainly photoelectrically in *UBV*. The historical LC of AG Dra over the period 1966–2016 was constructed using our compilation of photoelectric and CCD observations in *U*, *B* and *V* filters (Fig. 2).

AG Dra regularly undergoes quiescent and active stages which consist of the series of individual outbursts repeating at about a one-year interval. During the period (1890–2016), the AG Dra system underwent six (or seven?) phases of activity: *A* (1932–1939), *B* (1949–1955), *C* (1963–1966), *D* (1980–1986), *E+F* (1993–2008) and *G* (2015–). In total, we recognized 34 outbursts in this period.

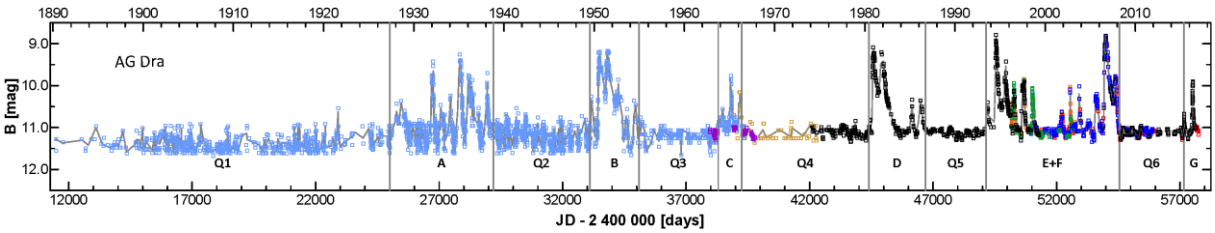

Figure 1: The historical LC of AG Dra over the period 1889–2012, constructed on the basis of photographic and *B* band observations. The LC is divided into active (A – G) and quiescence (Q1 – Q6) stages by vertical lines. The thin curves show spline fits to the data points.

We carried out the complex and detailed period analysis of all photometric data of AG Dra covered a time interval of 124 yr (Hric et al. 2014). The results of period analysis of these data are two real periods present in this symbiotic system: 550 and 350 d, related to the orbital motion and postulated pulsation of the cool component, respectively.

The orbital period is mainly manifested during the quiescent stages at shorter wavelengths (*U* band), while the pulsation period is present during quiescent as well as active stages at longer wavelengths (*B* and *V* bands). The period analysis of active stages confirmed the presence of a period of around

365 d, which is the median of the time interval between outbursts. It is worth noting that these time intervals vary from 300–400 d without an apparent long-term trend.

After seven years of flat quiescence following the 2006–08 major outbursts, in May 2015, the brightness of the symbiotic system AG Dra begun rising again. Around JD 2 457 166, the maximal brightness (10.7 and 9.6 mag in *B* and *V* band, respectively) was achieved and this brightening appeared to be a new minor outburst (G0). In April 2016, the recent outburst activity of AG Dra was definitely confirmed by a more prominent outburst (G1) around JD 2 457 517. The maximal brightness of 9.9 and 9.1 mag in *B* and *V* band, respectively, ranks this brightening to the minor outbursts of symbiotic binary AG Dra.

Such photometric behaviour of the active stage is very unusual in the historical LC of AG Dra. More often, the activity of AG Dra starts with major outburst, during which the brightness can reach the 8.8 and 8.4 mag in *B* and *V* band, respectively. These major outbursts were preceded by the pre-outbursts with brightness around 10.4 and 9.4 mag in *B* and *V* band, respectively, in the case of the active stages B, E and probably C. The minor outburst at the beginning of activity probably occurred only in the case of very weak active stage C, which is, however, covered only by (not completely reliable) photographic measurements.

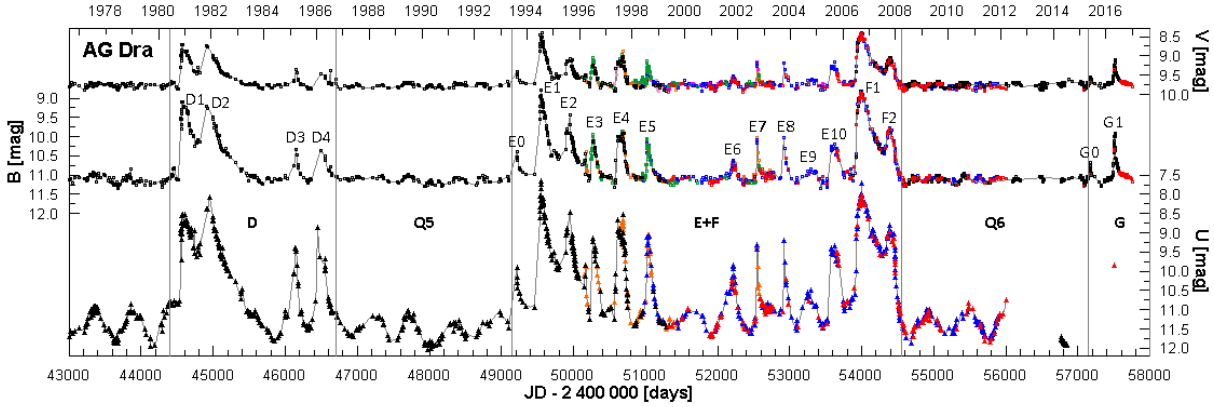

Figure 2: *UBV* LCs from the period 1977–2016 with marked active stages (D, E + F and G) and quiescent ones (Q4, Q5 and Q6). Particular outbursts are assigned as D1 – D5, E0 – E10, F1, F2 and G0, G1. The thin curves show spline fits to the data points.

Spectroscopic behaviour of AG Dra

We analysed behaviour of emission lines in the optical spectrum of AG Dra during almost 14 years (1997 September to 2011 April) using own intermediate-dispersion spectroscopic observations (Leedjärv et al. 2016). It is worth noting that these emission lines originate in the circumbinary nebula, which is generated by the stellar wind of the cool giant. Moreover, the nebula is partially ionized by short-wave radiation of the white dwarf, resulting in its complex structure and variability.

We studied the variability of EWs of the selected emission lines: Hα (λ6563), Hβ (λ4861), He I (λ6678), He II (λ4686) and the Raman scattered O VI line at λ6825. One of the most interesting features of this variability is the significant increase of the EWs of all the five emission lines considered, but in particular that of Hα and O VI (λ6825), during the minor outburst E10.

The major (cool) outburst F1 of AG Dra that started after JD 2 453 900 (July 2006) is not specifically distinct in the fluxes of hydrogen and helium lines, but the weakening of the Raman scattered O VI (λ6825) line is very well seen. A simple interpretation of this behaviour could be that during the cool outburst, the temperature of the hot component decreased considerably, so that the high excitation O VI (λ6825) line faded significantly and almost disappeared[4], however leaving the lower excitation lines mainly unaffected.

Direct comparison of the high-resolution spectra of AG Dra obtained during the quiescence stage Q6 (JD 2 456 906) and recent active stage G (JD 2 457 176) reveals significant increase of EWs of all studied emission lines during the pre-outburst G0 (Fig. 3). Such spectroscopic behaviour is typical for the hot outbursts of AG Dra. Moreover, the absorption component observed in the profiles of the emission lines He I (λ6678), Hα (λ6563) and

4 The formation of the Raman scattered O VI (λ6825) emission line requires specific physical conditions – the simultaneous presence of a hot radiation source, capable of ionizing oxygen atoms five times, and enough neutral hydrogen atoms that scatter the photons of the O VI resonance line.

Hβ (λ4861) completely disappeared during this outburst. According to both photometric and spectroscopic behaviour, the minor brightening G0 is the hot type of outbursts of symbiotic binary AG Dra.

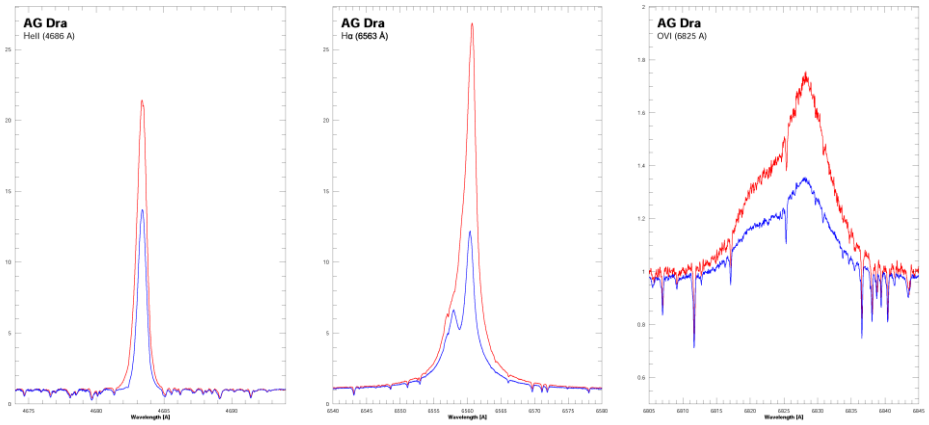

Figure 3: The profiles of the emission lines He II 4686 Å (left panel), Hα 6563 Å (middle panel) and the Raman scattered O VI line 6825 Å (right panel) of AG Dra obtained during the quiescence stage Q6 (JD 2 456 906) and recent active stage G (JD 2 457 176).

The EWs of emission lines Hα (λ6563), Hβ (λ4861), He I (λ6678), He II (λ4686) manifest an even more prominent increase during the next minor outburst G1 (Fig. 4). Such behaviour would suggest that this brightening belongs to the hot outbursts of AG Dra as well as. On the other hand, the EWs of the Raman scattered O VI line at λ6825 dropped to deep minimum during this outburst, which was observed only during the major cool outbursts of AG Dra in 2006.

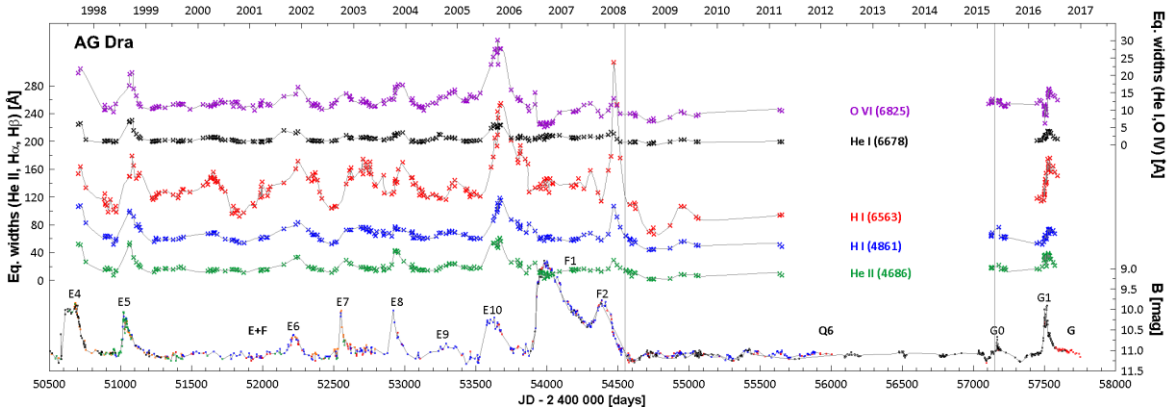

Figure 4: The curves of EWs for particular spectral lines together with the LC of AG Dra in B filter. The scales on the left and right axes are valid for EWs of He I (6678 Å) and He II (4686 Å), respectively. Particular outbursts are assigned as E4 – E10, F1, F2 and G0, G1. The active (E+F, G) and quiescent (Q6) stages are distinguished by the vertical lines. The thin curves show spline fits to the data points.

Discussion and Conclusion

Periodical outbursts and their relation to periodicities in the symbiotic system AG Dra have been a matter of long-term debate. As mentioned in the introduction, González-Riestra et al. (1999) have distinguished between cool and hot outbursts of AG Dra according the spectroscopic behaviour of this interacting binary observed in the far ultraviolet. In our previous study (Leedjärv et al. 2016) we showed that cool and hot outbursts of AG Dra can be clearly distinguished by the behaviour of the emission lines in the optical spectrum of this symbiotic system.

The Raman scattered O VI line λ6825 almost disappeared during the cool outburst of AG Dra in 2006, confirming a drop in the hot component's temperature, as was also found from the variations of other emission lines. Emission lines of hydrogen and neutral helium did not change significantly during the cool outbursts of AG Dra. They are correlated with the orbital motion of this interacting binary in quiescence and become stronger in hot outbursts.

The recent activity stage of AG Dra began with the weak pre-outburst in 2015 followed by the more prominent outburst in 2016. According to photometric behaviour, both brightenings belong to the minor outbursts of AG Dra. Such photometric behaviour of the active stage is very untypical, because more often, the activity of AG Dra starts with the major outburst. The only exception was probably the weak active stage during period 1963–66. The spectroscopic observations suggest that the minor outburst of AG Dra in April 2016 demonstrates the behaviour of both hot and cool outbursts. Is it a new type of outburst or some kind of transition between (or combination of) the hot and cool outbursts?

Another interesting question is the next evolution of activity of the symbiotic binary AG Dra. According to our detailed period analysis of photometric and spectroscopic observations we know that the median of the time interval between outbursts is around 365 days. It is worth noting that these time intervals vary from 300–400 d without an apparent long-term trend. Nevertheless, can we expect the major cool or minor hot outburst during the late spring of 2017? Or maybe none of them and AG Dra will return to quiescence as we have already detected such behaviour during the weak activity stage 1963–66. In any case, AG Dra clearly demonstrates the importance of long-term monitoring of symbiotic stars in order to disentangle the nature and mechanisms of their active stages and outbursts.

Acknowledgement

We acknowledge with thanks the variable star observations from the *AAVSO International Database* and *ARAS Database* contributed by observers worldwide and used in this research. This research was supported by the Slovak Research and Development Agency project APVV 15-0458.

References

Bastian U., 1998, A&A, 329, L61

Belyakina T. S., 1969, Izv. Krymskoj Astrofiz. Obs., 40, 39

Friedjung M., Gális R., Hric L., Petrík K., 2003, A&A, 400, 595

Gális R., Hric L., Friedjung M., Petrík K., 1999, A&A, 348, 533

González-Riestra R., Viotti R., Iijima T., Greiner J., 1999, A&A, 347, 478

Hric L., Gális R., Leedjärv L., Burmeister M., Kundra E., 2014, MNRAS, 443, 1103

Kafka, S., 2016, Observations from the AAVSO International Database, https://www.aavso.org

Leedjärv, L., Gális, R., Hric, L., Merc, J., Burmeister, M., 2016, MNRAS, 456, 2558

Meinunger L., 1979, IBVS, 1611

Mikołajewska J., Kenyon S. J., Mikołajewski M., Garcia M. R., Polidan R. S., 1995, AJ, 109, 1289

Robinson L., 1969, Peremennye Zvezdy, 16, 507

Sion E. M., Moreno J., Godon P., Sabra B., Mikołajewska J., 2012, AJ, 144, 171

Sokoloski, J. L., Kenyon, S. J., Espey, B. R., 2006, ApJ, 636, 1002

Vrašťák, M., 2016, private communication

Disentangling of spectra of variable stars

P. HADRAVA[1]

(1) Astronomical Institute, Academy of Sciences, Boční II 1401, 141 31 Praha 4, Czech Republic, had@asu.cas.cz

Abstract: Variability of spectra of binaries or pulsating stars, together with their photometric and other changes, enables us to determine many important physical parameters of the observed systems. In this contribution a brief introduction is presented into the method of the so called 'disentangling of spectra' which enables to process efficiently the spectroscopic observations and to extract from them information about the motion and the intrinsic radiation of the components of the system.

Abstrakt: Proměnnost spekter dvojhvězd nebo pulzujících hvězd spolu s jejich fotometrickými a dalšími změnami umožňuje určit řadu důležitých fyzikálních parametrů pozorovaných soustav. V tomto příspěvku je podán stručný úvod do metody tzv. 'rozmotávání spekter', která umožňuje efektivně zpracovat spektroskopická pozorování a získat z nich informace o pohybech a vlastním záření složek soustavy.

Introduction

Time variability of stars enables us to get observationally more information about their properties than in the case of non-variable stars. For both intrinsic and extrinsic variables, the time series of observations yield an evidence about the stellar parameters or even about the internal structure of the stars and their atmospheres. Different methods of observations – photometry, spectroscopy, interferometry etc. – constrain the unknown parameters in different degree. It is thus preferable for the interpretation to have at disposal complementary observations of different kinds, in different wavelength bands and different epochs.

A classical example of complementarity of the observational methods is the photometry of eclipsing binaries from which the orbital period (and its possible changes) and inclination can be well determined, and a constraint can also be imposed on the eccentricity and periastron longitude. In addition to these orbital parameters also the ratios of the component radii to the orbital semimajor axis, ratios of components luminosities and some other physical parameters of the components can be determined. The eccentricity and periastron longitude can better be determined from the radial-velocity curve, the semiamplitude of which determines the absolute dimension of the orbit up to the multiplicative factor given by the inclination. Consequently, the dimension of the binary can be found if both photometry and spectroscopy are available. If the components temperatures are estimated either from the spectra or colour photometry, absolute magnitudes and photometric distance of the system can also be found. If the interferometry is also available then the geometric distance can be calculated (cf., e.g., Zwahlen et al., 2004).

While relatively small and cheep telescopes are sufficient for the photometric observations, the necessary high-resolution spectroscopy requires more light and hence longer exposures at larger telescopes what makes the spectroscopy more expensive. It is thus advantageous to exploit the photometry as much as possible. The photometry is thus a good opportunity for amateur astronomical observations. Time series of spectra of different variable stars are becoming publicly available in some data archives and a photometric follow up can increase their value. It may thus be useful for photometric observers to master not only processing of their own data but also the methods of interpretation of spectroscopic and other observations.

One of the methods for interpretation of spectroscopic observations is the so called disentangling of spectra. It was originally designed to solve for orbital parameters of a multiple stellar system and simultaneously to separate the spectra of its components which are superimposed in each exposure with a different Doppler shift. Generalizations of the method which take into account line-profile variations can be applied also to spectra of some intrinsic variables like the pulsating stars. An explanation which could enable to handle the method exceeds the possibilities of this contribution. Its aim is thus to outline its basic idea only and to refer to the literature where more details can be found.

Disentangling of spectra – its principle and use

An interpretation of observational data is mostly performed by comparison of the data with some theoretical model from which the observable quantities can be predicted. The model usually has some free parameters which can be fitted to achieve a better agreement of the model with the observed data. The optimal values of the parameters are taken as the solution of the data (e.g. the component radii etc. obtained from light curves of

eclipsing binaries). However, there is no guarantee that the chosen model is correct and substantially different models can agree with the same data (e.g. a small sinusoidal variation of luminosity can be caused either by pulsation, ellipticity or brightness non-uniformity of a binary component). A better agreement with model may indicate a preferable explanation, however, it is still limited by the observational noise. Additional free parameters may decrease the residual noise, but it does not prove the assumptions of the chosen model and usually only some different kind of observations may distinguish between the alternative models. A greater sophistication of a model, even if it is based on reliable physical principles, does not necessarilly mean an advantage because there are always used some simplifying assumptions which may be improper for a particular application (e.g. the Roche model assumes the hydrostatic equilibrium violated in real binaries, especially in the interacting ones, etc.).

In the particular case of stellar spectroscopy we can compare the observed spectra with synthetic spectra computed from models of stellar atmospheres constructed for a chosen temperature, gravity acceleration, chemical composition of the atmosphere etc. These models may differ in their sophistication (e.g. in taking into account non-LTE effects, turbulence), but they mostly assume stationarity, homogeneity and a simple plane-parallel or spherical symmetry, which are violated in variable stars. Moreover, in the case of multiple stars we can only see the superposition of spectra of all component stars (and possibly also the circumstellar matter). Fortunately, the component spectra often move in wavelength due to the Doppler shift, what enables to distinguish the spectral lines of different components and at the same time it carries the important information about the orbital parameters. To measure this Doppler shift we need to distinguish the lines of individual components, which are often blended with the others. There is a possibility to separate the component spectra numerically provided we have a sufficient number of exposures (at least equal to the number of components) obtained at different known Doppler shifts. The information about the spectra of individual components and about the radial velocities given by the orbital parameters is thus entangled in the set observed spectra. To separate the spectra and to find the orbital parameters is thus the problem of disentangling. It should be noted that, provided we can assume the Doppler shift to be due to the orbital motion, it is more efficient to solve directly for the orbital parameters instead of for the radial velocities in the individual exposures because this physical assumption of Keplerian orbit constrains partly the errors caused by the observational noise.

The separation of component spectra is a linear problem and it can be performed by several numerical techniques. Because of its high dimension given by the number of pixels of the observed spectra, it is efficient to use the Fourier transform which enables to solve independently each Fourier mode. This is a linear problem of dimension equal to the number of components only (Hadrava, 1995). The solution of orbital parameters is a non-linear problem, which can be performed using some optimization technique (e.g. the simplex method). The complete task of the disentangling is then done iteratively in successive steps of the separation and optimization of the orbital parameters. The Fourier analysis is one of the so called spectral methods in mathematics. Some users use the term 'spectral disentangling' instead of 'disentangling of spectra'. This is, however, somewhat misleading because there is not as much important which mathematical method we use but it is rather more substantial that we disentangle the observed spectra and the information contained in them.

In practice, the author's code KOREL can be used to disentangle the spectra. Manual for its use can be found on web (Hadrava, 2009b) and the code itself is available as a Virtual-Observatory service on the address https://stelweb.asu.cas.cz/vo-korel (cf. Škoda et al., 2010, 2012). Some older versions of the source-file of the KOREL-code circulate between its earlier users, however, these are unreliable copies due to unprofessional modifications and they are lacking later improvements (e.g. the sub-pixel resolution, cf. Hadrava, 2009a). It is thus recommended to use the VO-Korel which always provides the latest version of the code.

As an example, disentangled spectra of the chemically peculiar binary star *o* Leo are shown in Fig. 1. The observed spectra normalized to the continuum, which are the input for the disentangling, are depicted with a constant offset by blue lines in the upper part of the panel. The spectra of the primary and the secondary component separated using the KOREL code are shown in the bottom part of the figure. The superposition of these components each one Doppler-shifted according to its radial velocity in each exposure is then overplotted by the red lines over the blue input spectra. A good coincidence of the red and blue lines indicates a good fit of the input data. Usually the blue colour is not perfectly hidden by the red one because of the random observational noise of the input data, which is supressed by the averaging in the disentangled spectra. In the case shown in Fig. 1 we can see that the blue colour appears mainly at the edges of the spectral region. This is due to the fact that for a perfect reconstruction of the component spectra close to the edges we would need the information about the observed spectra outside the chosen wavelength interval in some exposures when a line is shifted behind its edges. For this reason, it is preferable to choose the edges of the wavelength regions in continuum where there are no prominent features. This is possible to satisfy in early-type stars but not in the later

spectral types like are the components of *o* Leo. However, these discrepancies are quickly damped from the edges inwards the spectral region on a wavelength scale given by the amplitude of radial velocities.

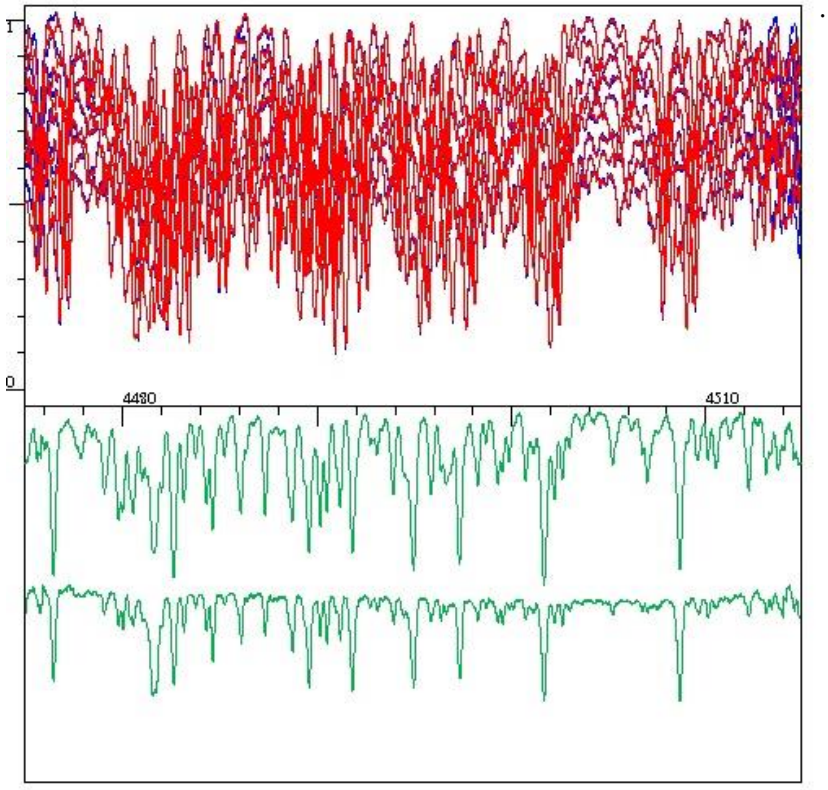

Figure 1: Disentangled spectra of *o* Leo (cf. Gebran et al. 2015)

The observed blue lines are actually overplotted first by green lines which are a reconstruction using the radial velocities, which correspond to the disentangled orbital parameters. Each exposure is then fitted separately by a superposition of the disentangled component spectra with radial velocities converged as free parameters. This superposition is plotted in red and in our case it practically coincides with the green lines. The radial velocities obtained in this way are typed as one of outputs from KOREL and they enable to check the consistency of the results and also to combine them with radial velocities published in the literature (e.g. using the code FOTEL for simultaneous solution of light- and radial-velocity curves, cf. Hadrava, 2004). This additional step is similar to the older method of cross-correlation (cf., e.g., Simkin, 1974), however, the template spectra are not *ad hoc* chosen but obtained from the whole set of exposures. It should be pointed out that the directly disentangled orbital parameters are more reliable than a solution of radial-velocity curve obtained by this additional step (unless the data are substantially enriched from another source).

Generalized disentangling

The method of disentangling works well if its assumptions are satisfied. The most critical is the assumption that the intrinsic spectra of the components are constant and only Doppler-shifted in all exposures. This is, however, often violated. For instance, during the eclipses the light-ratio varies and consequently also the strength of the observed lines, or there may be a change of line-profiles due to the rotational effect. Similar changes can take place also in non-eclipsing systems with a pronounced reflection efect, i.e. a reprocessing of the radiation from the companion star. Moreover, there may be a real change of the radiation of each of the component stars, e.g. due to spots on its surface or due to its pulsations.

In the case of violation of the assumptions there are two possibilities how to proceed. The simpler one is to neglect the complications and to hope that the disentangling will find some mean shape of the component spectra and approximate values of the orbital and other parameters. The variations of the spectra, e.g. pulsational line-profile variations, can then be investigated as O–C, i.e. deviations of each exposure from the reconstruction which corresponds to the mean disentangled spectra.

A better but more difficult way is to generalize the method and to include the variations into the model. For instance, the line-strength variations can be solved as an additional linear problem but they enrich significantly the applicability of the method; it improves the disentangling of otherwise often omitted exposures taken during the eclipses and provides a kind of photometry made from spectra, enables to separate the telluric lines etc. (Hadrava, 1997). There can also be directly modelled the line-profile variations caused by pulsations. The line-profile changes caused by radial pulsations can be approximated analytically and used for disentangling the spectra of Cepheids (cf. Hadrava et al., 2009). Different physical processes, which violate the simplifying assumptions, require different changes of the code and generalizations of the method of disentangling which challenges its further development.

Errors of disentangled parameters

An estimate of errors of the solution obtained by disentangling is of great importance. The observed spectra suffer mainly from the photon noise which propagates to the disentangled component spectra. This noise is decreasing with the square root of number of the input spectra owing to the fact that the separation of the spectra is a linear problem. Weighting of the exposures may be useful if they differ in their signal-to-noise ratio. Another problem may be caused by unprecise normalization of the input spectra which can increase due to the instability of low Fourier modes. Filtering of these modes enabled by KOREL is often useful in such cases or the disentangled spectra can be constrained by a template.

More tricky is the problem of errors of the disentangled parameters because their solution is a non-linear task. A simple possibility to estimate these errors is to treat the scatter of results obtained independently from different spectral regions. Another possibility is to use the methods of bootstrap or jackknife (cf. Ilijić, 2003, Zwahlen et al., 2004). However, the problem is more complicated because the optimization in the space of the free parameters does not necessarily lead to a single solution. This can be illustrated by the search for the epoch of periastron passage (or minima in the case of eclipsing binaries) which has an infinite number of equivalent solutions. The uncertainty of the values of parameters cannot be expressed by simple 'plus-or-minus errors' (and corresponding correlations in a multidimensional space) but it needs to be mapped as a probability distribution of the solution in the space of the parameters. This distribution can be found using the Bayesian statistics. Its application to the spectroscopy is described by Hadrava (2016). The KOREL-code enables such a mapping in an arbitrary two-dimensional cross-section of the parameter space. The residual noise can be approximation by the standard quadratic form in a small vicinity around the local minimum, but it can be asymmetric in larger distances.

Conclusions

The method of disentangling of spectra is more precise and at the same time less laborious than the classical methods of measurement of radial velocities and subsequent solution of radial-velocity curves. Owing to its efficiency, it opens a possibility for further generalizations and combinations with treatment of other observational data like the photometry. Such data yield valuable complementary information which may significantly improve the results obtainable from the spectroscopy.

Acknowledgement

This work has been supported by the project GAČR 14-37086G.

References

Gebran, M., Hadrava, P. et al. 2015, Astrophys. Sp. Sc., 357, 137

Hadrava, P. 1995, A&AS, 114, 393

Hadrava, P. 2004, Publ. Astron. Inst. ASCR 92, 1

Hadrava, P. 2009a, A&A 494, 399

Hadrava, P. 2009b, arXiv0909.0172

Hadrava, P. 2016, Disentangling of stellar spectra, in: H.M.J. Boffin et al. (eds.), Astronomy at High Angular Resolution, Springer, Switzerland, pp. 113-135

Hadrava, P., Šlechta, M., Škoda, P. 2009, A&A, 507, 397

Hensberge, H., Ilijić, S., Torres, K. B. V. 2008, A&A 482, 1031

Ilijić, S. 2003, Master thesis, University of Zagreb

Simkin, S. M. 1974, A&A, 31, 129

Škoda, P., Hadrava, P. 2010, ASP Conference Series, Vol. 435, p. 71

Škoda, P., Hadrava, P., Fuchs, J. 2012, IAU Symp. 282, p. 403

Zwahlen, N., North, P. et al. 2004, A&A, 425, L45

Astronomical satellite Gaia: First results

P. KOUBSKÝ[1]

(1) Stellar department, Astronomical Institute, Academy of Sciences of the Czech Republic, Fričova 298, 251 65 Ondřejov, Czech Republic, koubsky@asu.cas.cz

Abstract: The ESA Gaia satellite was launched by the end of 2013, routine observations started in summer 2014. The double telescope of the satellite, which is continuously scanning the sky, is able to detect more than one billion objects both in close (solar system objects) and distant universe (stars, galaxies and quasars). The instruments in the common focus of both telescopes provide very accurate astrometry and photometry for all objects between 2.0 and 20.7 magnitude. In mid September 2016, the first data release was made public. The data represents 14 months of satellite observations. This way, a new huge sky survey, which should continue at least till 2021, started. An interesting project – Gaia Science Working Group – has been initiated. It calls for a broad ground based support of Gaia transient sources observations.

Abstrakt: Družice ESA Gaia byla vypuštěna koncem roku 2013, rutinní pozorování zahájila v létě 2014. Dvojitý palubní dalekohled, který průběžně sleduje celou oblohu, je schopen zachytit více než jednu miliardu objektů v blízkém (sluneční soustava) i vzdáleném vesmíru (hvězdy, galaxie a kvasary). Přístroje ve společném ohnisku obou dalekohledů dovolují určit velmi přesnou astrometrii a fotometrii pro všechny objekty mezi 2,0 a 20,7 magnitudou. Polovině září 2016 byla veřejnosti zpřístupněna první část dat, která družice získala za 14 měsíců pozorování. Vzniká nová mohutná přehlídka oblohy, která bude pokračovat minimálně do roku 2021. Podpora pozorování družice, kterou organizuje skupina Gaia Science Alerts Working Group je velmi zajímavý program pro nejrůznější pozemské dalekohledy.

Introduction

Gaia is an ambitious mission to chart a three-dimensional map of our Galaxy, the Milky Way, in the process revealing the composition, formation and evolution of the Galaxy. Gaia will provide unprecedented positional and radial velocity measurements with the accuracies needed to produce a stereoscopic and kinematic census of more than one billion stars in our Galaxy and throughout the Local Group. This amounts to about 1 per cent of the Galactic stellar population. In addition, Gaia will be able to detect and study some extragalactical objects, too.

Gaia's mission is scheduled to last for five years (nominal active livetime). During that time, it will log the position, brightness and colour of every visible celestial object that falls within its field of view. By repeating these observations throughout its mission, astronomers will be able to calculate the distance, speed and direction of motion of each of the celestial objects, chart variations in their brightness, and determine whether they have nearby companions.

This kind of data is the lifeblood of astronomy, and Gaia will gather it with unprecedented accuracy. It will allow astronomers to painstakingly piece together the history of our Galaxy, since each celestial object preserves something of the era during which it was born.

The Gaia satellite

Gaia was launched by Arianespece, using a Soyuz ST-B rocket with a Fregat-MT upper stage, from the Ensemble de Lancement Soyuz at Kourou in French Guiana on 19 December 2013 at 09:12 UTC (06:12 local time). The satellite separated from the rocket's upper stage 43 minutes after launch at 09:54 UTC. The craft headed towards the Sun–Earth Lagrange point L2 located approximately 1.5 million kilometres from Earth, arriving there 8 January 2014.The L2 point provides the spacecraft with a very stable gravitational and thermal environment. There it uses a Lissajous orbit that avoids blockage of the Sun by the Earth, which would limit the amount of solar energy the satellite could produce through its solar panels, as well as disturb the spacecraft's thermal equilibrium. After launch, a 10-metre diameter sunshade was deployed. The sunshade always faces the Sun, thus keeping all telescope components cool and powering Gaia using solar panels on its surface.

The on-board telescope

Similar to its predecessor Hipparcos, but with a precision one hundred times better, Gaia consists of two telescopes providing two observing directions with a fixed, wide angle of 106.5° between them. The spacecraft rotates continuously around an axis perpendicular to the two telescopes' lines of sight. The spin axis in turn has a slight precession across the sky, while maintaining the same angle to the Sun. By precisely measuring the relative positions of objects from both observing directions, a rigid system of reference is obtained. The size of the primary mirror (M1) for each telescope is 1.45 × 0.5 m, while the resulting focal length is 35 m. Each telescope comprises four identical sets of mirrors (M1 to M4). Two additional mirrors (M5 and 6) are used by both telescopes to direct the light into the same focal plane. All of the mirrors were fabricated from blanks made of sintered silicon carbide (SiC).

The light from both telescopes is projected on 1.0x0.5 m focal plane array, which in turn consists of 106 CCDs of 4500 × 1966 pixels each, for a total of 937.8 megapixels (commonly depicted as a gigapixel-class imaging device).

Each celestial object will be observed on average about 70 times during the mission, which is expected to last five years. These measurements will help determine the astrometric parameters of stars.

Scientific instruments

The astrometry instrument (**Astro**) precisely determines the positions of stars of magnitude 5.7 to 20.7 by measuring their angular position. By combining the measurements of any given star over the five-year mission, it will be possible to determine its parallax, and therefore its distance, and its proper motion--the velocity of the star projected on the plane of the sky. Astro will also provide broad-band photometry for all objects in the range of 2 – 20.7 magnitude (G band).

The photometric instrument (**BP/RP**) allows the acquisition of luminosity measurements of stars over the 320–1000 nm spectral band. The blue and red photometers (BP/RP) are used to determine stellar properties such as temperature, mass, age and elemental composition. Multi-colour photometry is provided by two low-resolution fused-silica prisms dispersing all the light entering the field of view in the along-scan direction prior to detection. The Blue Photometer (BP) operates in the wavelength range 330–680 nm; the Red Photometer (RP) covers the wavelength range 640–1050 nm.

The Radial-Velocity Spectrometer **(RVS)** is used to determine the velocity of celestial objects along the line of sight by acquiring high-resolution spectra in the spectral band 847–874 nm (field lines of calcium ion) for objects up to magnitude 17. Radial velocities are measured with a precision between 1 km/s (V=11.5) and 30 km/s (V=17.5). The measurements of radial velocities are important to correct for perspective acceleration which is induced by the motion along the line of sight. The RVS reveals the velocity of the star along the line of sight of *Gaia* by measuring the Doppler shift of absorption lines in a high-resolution spectrum.

The spacecraft subsystems are mounted on a rigid silicon carbide frame, which provides a stable structure that will not expand or contract due to heat. Attitude control is provided by small cold gas thrusters that can output 1.5 micrograms of nitrogen per second.

The telemetric link with the satellite is about 3 Mbits/s on average, while the total content of the focal plane represents several Gbit/s. Therefore, only a few dozen pixels around each object can be downlinked.

Mission progress

The testing and calibration phase, which started while Gaia was en route to L2 point, continued until the end of July 2014, three months behind schedule due to unforeseen issues with ice deposits and stray light entering the detector. After the six-month commissioning period, the satellite started its nominal five-year period of scientific operations on 25 July 2014 using a special scanning mode that intensively scanned the region near the ecliptic poles; on 21 August 2014 Gaia began using its normal scanning mode which provides more uniform coverage. Although it was originally planned to limit Gaia's observations to stars fainter than magnitude 5.7, tests carried out during the commissioning phase indicated that Gaia could autonomously identify stars as bright as magnitude 3 (or even 2). When Gaia entered regular scientific operations in July 2014, it was configured to routinely process stars in the magnitude range 2 – 20.7.

On 12 September 2014, *Gaia* discovered its first supernova in another galaxy. On 3 July 2015, a map of the Milky Way by star density was released, based on data from the spacecraft. As of August 2016, more than 50 billion focal plane transits, 110 billion photometric observations and 9.4 billion spectroscopic observations have been successfully processed.

Data releases

The Gaia catalogue will be released in stages; it is expected that the early releases will be incomplete, especially for fainter stars located in dense star fields. The first data release, Gaia DR1, based on 14 months of observations made through September 2015, took place on 13 September 2016. The data release includes "positions and … magnitudes for 1.1 billion stars using only Gaia data; positions, parallaxes and proper motions for more than 2 million stars" based on a combination of Gaia and Tycho-2 (Hipparcos observations) data for those objects in both catalogues; "light curves and characteristics for about 3000 variable stars; and positions and magnitudes for more than 2000 … extragalactic sources used to define the celestial reference frame". Data from this DR1 release can be accessed at the Gaia archive[5], as well as through astronomical data centers such as CDS.

The second data release, scheduled for the fourth quarter of 2017, will include positions, parallaxes and proper motions, red and blue photometric data, and radial velocity measurements for many simple cases. The third data release, tentatively scheduled for 2018, will include orbital solutions for many binary stars and classifications for spectroscopically "well behaved" objects. The fourth data release, tentatively scheduled for 2019, will include variable star classifications, solar system results, and non single-star catalogues. The complete final Gaia catalogue is tentatively scheduled to be released in 2022, but the data release schedule would have to be altered in case the mission is extended beyond its nominal 5 years.

The Gaia Science Alerts Working Group

Gaia has been operating already for two and a half years. Hundreds of billions of observations have been collected and with the first Gaia Data Release in September 2016, Gaia is initiating a revolution in astronomy in general and in our understanding of the Milky Way in particular. In the mean time a group of ground based observers – Gaia Science Alerts Working Group[6], has been organized to provide follow-up observations of variable sources like supernovae, microlensing events, exploding and eruptive stars detected by the instruments of Gaia. More than 1000 alerts have been issued by the Gaia Science Alerts group so far. Gaia is now the second largest provider of transients in the world! Many of the alerts has been intensively followed-up by multiple observatories, with interesting discoveries of rare types of supernovae, cataclysmic variables, microlensing events and other exotic transients.

[5] http://gea.esac.esa.int/archive

[6] https://www.ast.cam.ac.uk/ioa/wikis/gsawgwiki/index.php/Main_Page

Binary systems with an RR Lyrae component – progress in 2016

J. LIŠKA[1,2,3], M. SKARKA[4], Á. SÓDOR[4], ZS. BOGNÁR[4]

(1) Department of Theoretical Physics and Astrophysics, Faculty of Science, Masaryk University, Kotlářská 2, CZ-611 37 Brno, Czech Republic, jiriliska@post.cz

(2) Department of Physics, Technical University of Liberec, Studentská 2, CZ-461 17 Liberec, Czech Republic

(3) CEITEC BUT, Purkyňova 656/123, CZ-612 00 Brno, Czech Republic

(4) Konkoly Observatory, Research Centre for Astronomy and Earth Sciences, Hungarian Academy of Sciences, Konkoly Thege Miklós út. 15-17, H-1121 Budapest, Hungary, marek.skarka@csfk.mta.hu, sodor@konkoly.hu, bognar@konkoly.hu

Abstract: In this contribution, we summarize the progress made in the investigation of binary candidates with an RR Lyrae component in 2016. We also discuss the actual status of the RRLyrBinCan database.

Abstrakt: V tomto příspěvku shrnujeme pokrok, který byl proveden ve výzkumu kandidátů na dvojhvězdy s RR Lyrae složkou za rok 2016. Diskutujeme také aktuální stav RRLyrBinCan databáze.

Introduction

Till the end of 2016 about 100 000 pulsating stars of RR Lyrae type have been identified in the Galactic field and bulge, globular clusters, SMC, and LMC. Despite that several dozen candidates for RR Lyrae stars in binary systems are known, none of them has been unambiguously confirmed. This is in clear contrast to other types of stars where binarity is very common.

More than a half of the candidates were discovered between 2014 and 2016 (e.g. Li & Qian, 2014; Hajdu et al., 2015; Liška et al., 2016a). In addition, the best candidate TU UMa was thoroughly re-analysed in Liška et al. (2016b). The reasons for the low number of known candidates were discussed e.g. in Liška et al. (2016a) and Skarka et al. (2016). In this short note we discuss candidates that appeared in literature in the second half of 2016 (were not presented in 47th Conference on Variable Stars Research), namely TU Com, KIC 2831097, RW Ari, and eclipsing systems in the LMC. We also update the status of the RRLyrBinCan database, the only up-to-date list of this kind of objects currently available.

TU Com

TU Com is an RR Lyrae pulsator (RRab type) showing Blazhko effect. De Ponthière et al. (2016) obtained new observations with five-year time span which disproved 75-days long Blazhko period published in the General Catalogue of Variable Stars. They identified two Blazhko periods of 43.6 and 45.5 days based on maxima timings and frequency analysis. In addition, 1676-days long cycle is apparent in their and SuperWASP data which can be explained with light-travel time effect caused by orbital motion of a binary system.

KIC 2831097

KIC 2831097 is a first-overtone RR Lyrae pulsator discovered by our team in original Kepler field (Sódor et al., 2017). We analysed stability of its pulsation period and found out that the star shows large phase variation with amplitude of 0.1 d. It can be interpreted as combination of a linear decrease of pulsation period (probably evolutionary effect) and cyclic variation explainable as light travel-time effect caused by orbital motion in a binary system. The characteristics of both processes found in KIC 2831097 are unusual. The rate of the pulsation period decrease is extreme among known RR Lyrae stars. In addition, the assumed orbital period of approximately 2 years is the shortest among the non-eclipsing RR Lyrae binary candidates. The possible companion of RR Lyrae component is a candidate for black hole due to its high mass (at least 8.4 M_{Sun}) and evolutionary status. In addition, the star shows numerous additional non-radial pulsation frequencies and an ~ 47-d Blazhko-like irregular light-curve modulation.

RW Ari

RW Ari (RRc type) belongs among candidates for eclipsing systems with an RR Lyrae component for 45 years. Wiśniewski (1971) detected the eclipses in photoelectric data and found eclipsing period of 3.1754 d. After that, many authors tried to verify the eclipses, but the number of papers which confirm binarity is similar as the number of papers discarding it (see Table 1). The summary of the history of RW Ari investigation is presented e.g. in Liška et al. (2016c) or Odell & Sreedhar (2016). The last mentioned paper is also the last study focusing on binarity of RW Ari. They obtained and analysed new and archival photometric data, but they found normal brightness variation (no eclipses were detected) which is accompanied by significant changes in pulsation period. They noted at least three abrupt changes in period (one of them in 2012). Variation in radial velocity (RV) curve constructed from their data looks also normally. Probably nobody can exclude the strange features in the light curve observed by Wiśniewski (1971), but recently RW Ari behaves as a normal RRc star and not as an eclipsing binary.

Table 1. References confirming (YES) or disproving (NO) binarity of RW Ari.

YES	NO
Wiśniewski (1971) – photometry	
Abt & Wiśniewski (1972) – RV	
Woodward (1972) – literature photometry	Penston (1972) – photometry
Sidorov (1978) – literature photometry	Edwards (1978) – photometry
	Goranskij & Shugarov (1979) – photometry
Dahm (1992) – literature photometry	
	Jeffery et al. (2007) – RV
	Liška et al. (2016c) – photometry
	Odell & Sreedhar (2016) – photometry, RV
5:6	

Eclipsing RR Lyrae systems in LMC

Soszyński et al. (2016) presented five eclipsing candidates in LMC and OGLE IV database. Four of them are known from their former research (Soszyński et al., 2003, 2009), only OGLE-LMC-RRLYR-30844 is newly identified system with eclipsing period of approximately 1.48 d. All of the LMC eclipsing systems have relatively short orbital periods (from 1.48 to 16.23 d) which almost exclude the possibility that a classical RR Lyrae pulsator is present in the system. Binary evolution pulsators (Pietrzyński et al., 2012) or optical blends consisting of RR Lyr star and eclipsing binary are the best explanations for observed variations.

RRLyrBinCan database – the updates

A new database containing candidates for RR Lyrae stars in binary systems, RRLyrBinCan database, was introduced in our former papers (Liška et al., 2016a; Liška & Skarka, 2016). The list contains candidates with their basic parameters and references. CDS version from May 2016 contains 64 candidates. An updated version of the database that is available online[7] contains 109 records for 78 stars (November 12, 2016). Sixteen of the listed stars show the Blazhko effect and six other stars are candidate Blazhko stars. Catalogized objects are mostly of RRab type (73) and the rest of them are of RRc type (5). A new utility implemented into the webpage showed us that the database is visited from the whole world.

Conclusions

We present a short summary of the progress in research focusing on detection and confirmation of binary systems among RR Lyrae stars in 2016. The topic is still very actual and interesting. Our team contributed with the identification and analysis of several candidates and managing the RRLyrBinCan database.

Acknowledgement

This research has made use of NASA's Astrophysics Data System and of the International Variable Star Index (VSX) database, operated at AAVSO, Cambridge, Massachusetts, USA. The financial support of NKFIH K-

[7] http://rrlyrbincan.physics.muni.cz

115709 and K-113117 are acknowledged. MS acknowledges the support of the postdoctoral fellowship programme of the Hungarian Academy of Sciences at the Konkoly Observatory as a host institution. ÁS was supported by the János Bolyai Research Scholarship of the Hungarian Academy of Sciences. This research was carried out under the project CEITEC 2020 (LQ1601) with financial support from the Ministry of Education, Youth and Sports of the Czech Republic under the National Sustainability Programme II. This work was supported by the Brno Observatory and Planetarium.

References

Abt, H. A., & Wiśniewski, W. Z., 1972, Information Bulletin on Variable Stars, 697, 1

Dahm, M., 1992, BAV Rundbrief, 41, 62

de Ponthière, P., Hambsch, F.-J., Menzies, K., & Sabo, R., 2016, Journal of the American Association of Variable Star Observers (JAAVSO), 44, 18

Edwards, D. A., 1978, A photometric investigation of the variable RW Arietis, master thesis, University of Texas, Austin, USA

Goranskij, V. P., & Shugarov, S. Y., 1979, Peremennye Zvezdy, 21, 211

Hajdu, G., Catelan, M., Jurcsik, J., et al., 2015, MNRAS, 449, L113

Jeffery, E. J., Barnes, T. G., III, Skillen, I., & Montemayor, T. J., 2007, ApJS, 171, 512

Li, L.-J., & Qian, S.-B., 2014, MNRAS, 444, 600

Liška, J., Skarka, M., Zejda, M., Mikulášek, Z., & de Villiers, S. N., 2016a, MNRAS, 459, 4360

Liška, J., Skarka, M., Mikulášek, Z., Zejda, M., & Chrastina, M., 2016b, A&A, 589, A94

Liška, J., Skarka, M., Hájková, P., & Auer, R. F., 2016c, in Proceedings of the 47th Conference on Variable Stars Research, Open European Journal on Variable Stars, 176, 4

Liška, J. & Skarka, M., 2016, in Proceedings of High-Precision Studies of RR Lyrae Stars, Communications of the Konkoly Observatory Hungary, 105, 209

Odell, A. P., & Sreedhar, Y. H., 2016, Information Bulletin on Variable Stars, 6180, 1

Penston, M. J., 1972, MNRAS, 156, 103

Sidorov, K. A., 1978, Peremennye Zvezdy, 20, 557

Skarka, M., Liška, J., Zejda, M., & Mikulášek, Z., 2016, in Proceedings of High-Precision Studies of RR Lyrae Stars, Communications of the Konkoly Observatory Hungary, 105, 141

Sódor, Á., Skarka, M., Liška, J., & Bognár, Zs., 2017, MNRAS, 465, L1

Soszyński, I., Udalski, A., Szymanski, M., et al., 2003, Acta Astronomica, 53, 93

Soszyński, I., Udalski, A., Szymański, M. K., et al., 2009, Acta Astronomica, 59, 1

Soszyński, I., Udalski, A., Szymański, M. K., et al., 2016, Acta Astronomica, 66, 131

Wiśniewski, W. Z., 1971, Acta Astronomica, 21, 307

Woodward, E. J., 1972, Journal of the American Association of Variable Star Observers (JAAVSO), 1, 68

Phenomenological modelling of light curves of non-eclipsing double stars

Z. MIKULÁŠEK[1], T. PRIBULLA[2], M. ZEJDA[1], M. VAŇKO[2]

(1) Department of Theoretical Physics and Astrophysics, Faculty of Science, Masaryk University, Kotlářská 2, 611 37 Brno, Czech Republic, mikulas@physics.muni.cz, zejda@physics.muni.cz,

(2) Astronomical Institute of Slovak Academy of Science, 059 62 Tatranská Lomnica, Slovak Republic, pribula@ta3.sk, vanko@ta3.sk

Abstract: The brightness of close non-eclipsing binary systems and eclipsing binaries besides eclipses themselves is changing due to proximity effects which are the result of the mutual interaction between components. Although the shape of resulting light curves or their segments is smooth and rather simple, the physics of proximity effects, including the deformation of components caused by tides and mutual warming and illumination, is considerably complex and untransparent. It represents one of the chief reasons that the solution of close binary star light curve modelling is a tedious process. That is why we are aiming at the building of the pertinent phenomenological light curve models that are much swifter and more flexible than the physical ones. Using our new phenomenological model we are now able to fit light curves of non-eclipsing binary simulated by the most advanced physical binary model software as a Roche or Phoebe with the accuracy of 0.0003 mag. The phenomenological model can be applied for binaries with both the circular and the elliptical orbits. The model enables to determine the eccentricity and the orientation of the elliptical orbit of the binary; as well it is apt also for the analysis of the possible apsidal motion in such systems. Obtained phenomenological model of elliptical variables provides an effective instrument for distinguishing of their light curves from double-wave ones of magnetic chemical peculiar stars. The full paper will be published elsewhere soon.

Abstrakt: Jasnost těsných nezákrytových dvojhvězd nebo zákrytových dvojhvězd mimo samotné zákryty se mění v důsledku efektů blízkosti, jež jsou výsledkem vzájemné interakce mezi složkami. Ačkoli je tvar výsledných světelných křivek a jejich úseků hladký a dosti jednoduchý, sama fyzika efektů blízkosti, zahrnující deformaci složek v důsledku slapů a vzájemného ohřívání a osvětlování, je nanejvýš složitá a neprůhledá. Je to i jeden z hlavních důvodů, proč je modelování světelných křivek těsných dvojhvězd tak zdlouhavým procesem. Proto jsme se zaměřili na sestavení vhodných fenomenologických modelů, které jsou mnohem rychlejší a flexibilnější než modely fyzické. Použitím našeho nového fenomenologického modelu jsme nyni schopni proložit světelné křivky simulované těmi nejpokročilejšími fyzickými modely v programech jako jsou Roche nebo Phoebe, s přesností 0,0003 mag. Fenomenologický model můžeme aplikovat na soustavy s kruhovými i eliptickými drahami. Model lze s výhodou využít pro určení výstřednosti a orientace eliptické dráhy dvojhvězdy, stejně jako pro analýzu případného apsidálního pohybu v soustavě. Současně jsme ve fenomenologickém modelu těchto eliptických proměnných získali účinný nástroj pro rozlišení jejich světelných křivek of dvouvlnných křivek chemicky pekuliárních hvězd. Celá práce již brzy bude publikována.

Note: This contributions contains only abstract. The authors are currently preparing a more extensive article for the prestigious A&A journal.

The Keplerian revolution of variable stars

L. MOLNÁR[1]

(1) Konkoly Observatory, Research Centre for Astronomy and Earth Sciences, Hungarian Academy of Sciences, H-1121 Budapest, Konkoly Thege Miklós út. 15-17, Hungary, molnar.laszlo@csfk.mta.hu

Abstract: The Kepler space telescope was conceived as an exoplanet statistics mission, but it turned out to be so much more. It has revolutionized many aspects of stellar astrophysics, ranging from pulsating stars to binaries and cataclysmic variables. Moreover, it has matured the field of asteroseismology, and, to quote Arthur Eddington from a century ago, finally allowed us to "obtain certain knowledge of that which is hidden beneath substantial barriers:" the insides of stars. In this short review, I present a few examples of the ways we achieved these breakthroughs.

Introduction

Almost a century ago, the great astronomer, Arthur Stanley Eddington, started his book, "The Internal Constitution of Stars", by addressing the scale of the problem in understanding stars:

"At first sight it would seem that the deep interior of the Sun and stars is less accessible to scientific investigation than any other region of the Universe. Our telescopes may probe farther and farther into the depths of space; but how can we ever obtain certain knowledge of that which is hidden beneath substantial barriers? What appliance can pierce through the outer layers of a star and test the conditions within?" (Eddington, 1926)

Although the quote suggests that the problem seemed impenetrable by him at the time, it should be noted that Eddington then went on to explain that two things do escape the interior of stars, namely, gravity and light. However, these two messengers still carry only very limited information.

Therefore, we can assume that Eddington would be very pleased with the advances of stellar astronomy since his time: with the advent of helio- and asteroseismology, we found a third messenger from the insides of stars, namely, stellar oscillations (see, e.g., Deubner & Gough 1984). (A fourth one would be neutrinos, of course, but observations are currently limited to the Sun itself, see, e.g., Suzuki (2000), and references therein.) And with the advent of space-based, high-precision observations, especially with the *Kepler* space telescope, asteroseismology itself matured to a diverse and prolific field within astronomy.

A brief history of Kepler

A photometric space mission called *FRESIP* (FRequency of Earth-Sized Inner Planets) was envisaged in the early 1990's by Bill Borucki and his colleagues, based on their pioneering scientific and engineering work in the late 1980's. The mission, later renamed to *Kepler*, would search for transiting exoplanets by monitoring, initially tens of, in later proposals, hundreds of thousands of stars, continuously. The same observations would then be used for asteroseismology to characterise the planet hosts. The mission proposal was rejected by NASA four times, before finally accepting it as a Discovery mission in 2000. The telescope was launched in 2009, and went on to observe the original *Kepler* field-of-view for four years. A detailed summary of the development history, characteristics, and first results of the mission was written by Borucki (2016).

But in 2013, disaster struck: a second reaction wheel of the spacecraft failed, making stable pointing of the telescope impossible. Not all was lost, however, and after some frantic work, a new, ingenious mission was proposed. In the K2 mission, the telescope would point parallel to the Ecliptic plane, instead of perpendicular to it, to distribute the incoming sunlight as evenly as possible for extended periods of time, to minimize the unbalanced torque exerted by the radiation pressure of the Sun. The mission would also change fields-of-views about every 80 days to keep the Sun to the side of the telescope. Initial testing commenced in early 2014, and soon the K2 mission officially started (Howell et al. 2014). In hindsight, it is fair to say that what seemed as a tragedy at first, might have been the best thing that could possibly happen to the mission, as the new K2 fields opened up many new ways to do science with the space telescope (the sky coverage of the missions is shown in Fig. 1). Just one important aspect is that whereas the original *Kepler* mission looked at exoplanet statistics of often faint and distant targets, K2 can search for planets around nearby stars more effectively. And these planets, such as K2-18b (Benneke et al. 2017) will very likely be among the first targets of the James Webb Space Telescope.

Figure 1: The sky, as observed by the *Kepler* and K2 missions. Blue dots represent the targets observed by K2 until

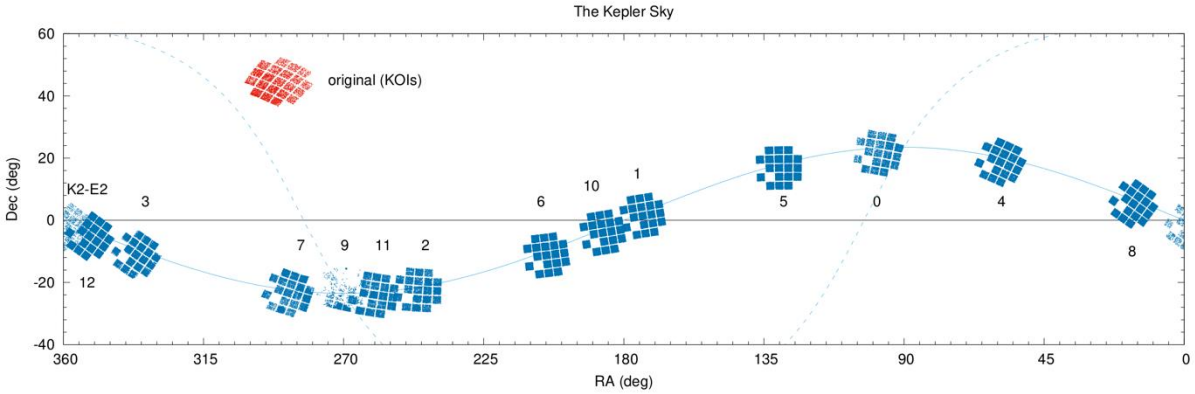

Campaign 12. In case of the original mission only the *Kepler* Objects of Interest (KOI) are shown. Updated version of the figure used by Molnár, Szabó & Plachy (2016).

The asteroseismic revolution

Solar-like oscillations (SLOs) are the low-level brightness and radial-velocity variations of stars that are not classical pulsating stars, e.g. the oscillations do not form coherent standing waves. They are caused by convective motions inside the star that continually excite these evanescent modes. Observing the SLOs can be crucial to understand these stars, as the parameters of the oscillation spectra can be much more sensitive to the properties of the star, such as age, mass, radius, than regular spectral line parameters. And these parameters are important not only for stellar astrophysics, but also for exoplanet science, as basically all planetary parameters and their respective uncertainties are derived from the properties of its star. Therefore, a better handle on the stellar radius, for example, translates into a more accurate estimation of the bulk density and composition of its exoplanets.

Detecting the oscillation spectra of stars and deducing their global parameters and inner structure remained largely a promise until the arrival of space photometric missions. Successful ground-based observations were limited to a handful of stars only, and the interpretation was hindered by the potential confusion between alias peaks (caused by gaps in the data) and avoided crossings of different modes (deviations from the expected separations between the frequency peaks). A summary of early results was provided by Bedding and Kjeldsen (2003).

The landscape fundamentally changed with the launch of the first asteroseismic space telescopes, especially the French-led CoRoT mission (Baglin et al. 2006). Still, these observations were mostly limited to red giant stars whose oscillation amplitudes are one two orders of magnitude larger than that of main-sequence stars (Kallinger et al. 2010, Mosser et al. 2011).

Main-sequence stars and planet hosts

While detecting thousands of exoplanet candidates down to sub-Earth sizes was a huge accomplishment in itself by the *Kepler* mission, many of those candidates benefitted strongly from the asteroseismic analyses of their host stars (see, e.g., Silva Aguirre et al. 2015). One excellent example for constraining stellar and planetary parameters is the Kepler-93 system, where the mass of the star was determined to an accuracy of 3.6%, and the radius of the single transiting planet to 1.3% (Ballard et al. 2014). The latter, based on the combination of optical and infrared data from the *Kepler* and *Spitzer* space telescopes, translates to an absolute uncertainty of only 120 km. Another great example is the Kepler-444 system that hosts five small, sub-Earth planets, and asteroseismology revealed that it is older than 11 billion years, e.g., it is 2.5 times older than the Sun and has seen most of the 13.8-billion-year long history of the Universe (Campante et al. 2015).

Another interesting aspect of the asteroseismic analysis is that the relative amplitudes of the oscillation modes depend on the inclination of the rotational axis star. Since the inclination of a transiting exoplanet is confined to a small range, such measurements can reveal spin-orbit misalignments between stars and their respective exoplanets (Campante et al. 2016).

But main-sequence stars can be of importance on their own right, not just as exoplanet hosts. A prime example is the nearby, bright visual binary star, 16 Cyg A and B. Both stars were observed during the prime mission of *Kepler*. Independent model fits to their asteroseismic data indicated that the two stars have the same age (7.0 ±

0.3 Gyr) and chemical composition (Metcalfe et al. 2012, 2015). This is the result we expect from a binary star that is assumed to born from the same molecular cloud, at the same time, but it is reassuring that the results actually confirm this theory. Since the two stars are bright and relatively close to the Sun, it was also possible to measure their radii directly, via optical interferometry. The results agreed with the asteroseismic radii, indicating that the asteroseismic models that are based on the Sun are valid for other main-sequence stars as well (White et al. 2013).

The K2 mission also brought about the first ever asteroseismic detections of main-sequence stars in open clusters: oscillations of two members of the Hyades were identified by Lund et al. (2016).

Red giants

While stellar oscillations revealed a wealth of information about main-sequence stars, the modes we can observe are limited to the stellar envelope, because the pressure modes observable at the surface only penetrate the star to a certain depth. Gravity modes propagate within the core, but they diminish before reaching the surface, and hide the information they might carry. The *p*- and *g*-modes are also separated by oscillation frequencies. However, as stars start to evolve away from the Main Sequence, their cores contract and their envelopes expand, raising and lowering the limiting frequencies for g- and p-modes, respectively. Soon the two frequency domains start to overlap, and so-called mixed modes start to appear: modes that propagate a predominantly *g*-modes in the core, but may penetrate into the envelope and continue with the same frequency but as predominantly *p*-mode oscillations. Therefore, mixed modes are able to carry information about the core right out to the stellar surface and thus to our instruments, finally allowing us to really peer behind Eddington's substantial barriers.

P- and *g*-modes can be distinguished in the oscillation spectra based on their separation: while *p*-modes of consecutive order are separated (more or less) by equal frequency spacings, *g*-modes are separated by equal period spacings. Given the required sensitivity, e.g., by *Kepler*, one only has to disentangle the two interlaced combs of peaks (Beck et al. 2011). This method was then applied to separate two kinds of red giants in the initial *Kepler* observations. Some red giant stars are burning hydrogen in their shells surrounding their contracting, but not yet burning core. Other ones are already burning the Helium in their cores. Now, these stars look remarkably similar from the outside, and are notoriously hard to separate via conventional spectroscopy, complicating the studies of stellar populations and mass loss, for example. Since their cores are different, their *g*-mode spacings are also different (~50 s versus 100-300 s), and with *Kepler*, we were able to actually separate them for the first time (Bedding et al. 2011).

What else can we uncover about the interiors of red giants? Quite a lot, it turns out. A long-standing problem of stellar evolution is the transport of angular momentum inside stars. Basic physics principles tell us that the contracting cores of red giants should speed up. But when we finally get to see those cores as white dwarfs, they rotate relatively slowly again, in the order of days, meaning that the must have lost much of their core angular momentum. *Kepler* confirmed that this is indeed the case: the cores and envelopes of larger, e.g. more evolved stars rotate faster and slower, respectively (Deheuvels et al. 2014). However, soon after, the core rotation rates start to decrease (Mosser et al. 2012). Clearly, *Kepler* showed that our general picture on the evolution of red giant and red clump stars are correct: we only have to pin down the exact mechanism(s) that could transport the angular momentum away at the right rate.

Blue giants

Data from *Kepler* provided many surprising discoveries over at the hot side of the Hertzsprung-Russell diagram as well. Massive O- and B-type stars possess numerous physical processes that complicate their understanding. Here not the envelopes, but the cores of stars are convective, and they can be able transport and mix in fresh fuel from the bottom of the envelope into the core. Therefore, without the understanding of processes like convective overshoot, effects of fast rotation, magnetic fields, mixing, etc., even simple questions such as the lifetimes of these stars remain hard to answer. The original *Kepler* field was more or less limited to B-type stars only, but with the start of the K2 mission, we are now able to study the variations of the rare O-type stars as well (Buysschaert et al. 2015).

We have known for a long time that many B-type stars pulsate. High-precision observations revealed that several stars are in fact hybrid pulsators: they exhibit both β Cephei- and SPB (Slowly Pulsating B)-tye variations that originate from *p*- and *g*-mode pulsations, respectively (Balona et al. 2011). Given enough observable pulsation components, their modelling is analogous to that of solar-like oscillations: precise *Kepler* data led to the detailed analysis of several B-type stars (see, e.g, Pápics et al. 2014). One very intriguing finding that I selected to highlight is the possible presence of counter-rotating envelopes. While the internal rotation of stars can be complicated, as we have seen in red giant stars, we at least assume that the whole rotates in one direction.

However, asteroseismic modelling indicated that B stars may experience counter-rotation between the core and the envelope, with layers that are essentially standstill within the star (Triana et al. 2015).

RR Lyrae and Cepheid stars

The first observations of *Kepler* revealed just how biased the gound-based observations can be. RR Lyrae stars pulsate with a characteristic timescale of half a day, which means that consecutive cycles are very hard to observe. As such, we had to wait until the arrival of continuous space-based photometry to discover the presence of period doubling in fundamental-mode RR Lyrae stars (Kolenberg et al. 2010, Szabó et al. 2011). The observations of the *Kepler* (and also, *CoRoT*) missions transformed our understanding of RR Lyrae stars. They are no longer seen as simple radial pulsators, but rather as stars with intricate dynamics between various modes that are further complicated by the presence of the Blazhko effect (see, e.g., Molnár et al., 2012, Benkő et al. 2014, Moskalik et al., 2015, Plachy et al., 2014, Szabó et al. 2014). However, despite the recent progress in the theoretical understanding of RR Lyae stars, and the emergence of new, promising proposal, such as the radial mode resonance hypothesis (Buchler & Kolláth 2011) an unambiguous explanation of the Blazhko effect is yet to emerge.

The field-of-view of the original mission included only a single, fundamental-mode Cepheid. Nevertheless, the analysis of the data set revealed many new details about this star. The *Kepler* observations of V1154 Cyg showed short-term variations in the pulsation and slower, low-amplitude modulation cycle. The data was precise enough to detect the granulation noise in the star, the first time for a Cepheid star. However, no signs of solar-like oscillations were found, suggesting that the pulsation inhibits or at least quenches other oscillation modes, even though granulation, an thus a convective layer is present in the envelope of the star (Derekas et al. 2012, 2017).

And across the HR diagram

It is impossible to account for all the discoveries *Kepler* made over the years in this short review, covering virtually all ranges of the HR diagram. It observed the rotational variations of brown dwarfs (Scholz et al. 2015) and M dwarfs (Davenport et al. 2015).

Observations of pulsating subdwarf and white dwarf stars also revealed surprising new findings. The differences between the *p*- and *g*-modes in the pulsating subdwarf B star KIC 3527751 indicate that the core of the star rotates almost three times slower than the outer envelope. This is the first indication of radial differential rotation in an sdB star (Foster et al. 2015). Some pulsating white dwarfs were found to show peculiar, repeating outbursts during which both the average brightness and the pulsation amplitude of the stars increase (Bell et al., 2015, Hermes et al. 2015). The duration of these outbursts is typically several hours, and thus they were easy to confuse with atmospheric extinction variations from the ground, and the lack of detection so far. The origin of these bursts is still a matter of debate.

Analysis of δ Scuti stars revealed convective motions can plausibly excite not only non-coherent, solar-like oscillations, but coherent pulsations as well (Antoci et al. 2014). With the K2 mission, of δ Scuti-type pulsations can be exploited even further. Stars may evolve through the instability strip not only as they leave the main sequence but as they evolve towards it. Pre-main sequence pulsators can be then used to examine the inner structure of very young stars via asteroseismic analysis (Ripepi et al. 2015, Zwintz et al. 2015).

The baseline of the original mission was also long enough to provide new insights into yellow and red supergiants. Analysis of the single RV Tau-type star displayed intricate changes in the pulsation amplitude and the order of low- and high-amplitude cycles (Bódi et al. 2016). A combined analysis of all M giants indicated that the transition from solar-like oscillations to pulsations occur at periods about 10 days, where the amplitudes start to grow faster than the scaling relation of the oscillation amplitudes (Bányai et al. 2015).

The extremes

The prosperity of the results delivered by the *Kepler* mission can also be illustrated by the extremes of the observations carried out. The faintest targets the mission has observed are in the *Kp* = 21-22 mag range, and include extragalactic RR Lyrae stars and supernovae (Molnár et al. 2015). The continuous temporal coverage of the mission was invaluable to detect the earliest stages of supernova explosions, including the shock breakout before a II-type event, and the non-detection of reflected light form a Ia-type supernova that suggested a merging white dwarf pair as progenitor (Garnavich et al. 2015, Olling et al. 2015).

Observations of very bright stars are hindered by the increasing saturation of the CCD modules. The saturation can be compensated by various means, such as collecting all saturated pixels, or using the smear data for science (Pope et al., 2016). And then, for stars in the *Kp* = 3-4 mag range, the reflection halo from the optical surfaces around the image of the stars can be exploited. This latter method was used to detect the variation of the O-type star HD 188029 that was located between the CCD modules during the original mission (Aerts et al., submitted). Halo photometry was also used to reconstruct the light variations of the brightest members (the seven sisters) in the cluster Pleiades (White et al., submitted). The difference between the faintest and brightest targets of *Kepler* is about 18 mag, a flux difference in excess of 10^7.

Conclusions

In this review, I presented a sample of discoveries from the *Kepler* and K2 missions to illustrate the rich and diverse accomplishments achieved with the space telescope so far. The mission has not only enriched the field of exoplanet research (Coughlin et al. 2016), but also provided an answer for the question Eddington proposed a century ago. Asteroseismology, employing high-precision time series photometry, has finally provided us with a tool to "obtain certain knowledge of that which is hidden beneath substantial barriers". And the work will be continued even after *Kepler* exhausts its fuel in 2018. The American TESS mission will provide us with data from the bright stars all around the sky. The first SONG telescope has finally, after a long wait, delivered the first results, collecting precise radial velocity measurements of bright stars from the ground (Grundahl et al. 2017). And in the next decade, the European PLATO mission will build on the legacy of *Kepler*, and expand the field of asteroseismology even further.

Acknowledgements

L.M. is grateful for the hospitality of the Czech Astronomical Society. This project has been supported by the Lendület LP2014-17 Program of the Hungarian Academy of Sciences, and by the PD-116175 grant of the Hungarian National Research, Development and Innovation Office. L.M. was supported by the János Bolyai Research Scholarship of the Hungarian Academy of Sciences. This research has made use of NASA's Astrophysics Data System.

References

Antoci, V., Cunha, M., Houdek G., et al., 2014, ApJ, 796, 118

Baglin, A., Auvergne, M., Barge, P., et al., 2006, Proceedings of "The CoRoT Mission Pre-Launch Status - Stellar Seismology and Planet Finding", ESA SP-1306, pp. 33.

Ballard, S., Chaplin W. J., Charbonneau, D., et al., 2014, ApJ, 790, 12

Balona, L. A., 2016, MNRAS, 457, 3724

Balona, L. A., Pigulski, A., De Cat, P., et al., 2011, MNRAS, 413, 2403

Beck, P. G., Bedding, T. R., Mosser, B., et al., 2011, Science, 332, 205

Bedding, T. R., Kjeldsen, H., 2003, Publ. Astr. Soc. Austr., 20, 203

Bedding, T. R., Mosser, B., Huber, D., et al., 2011, Nature, 471, 608

Bell, Keaton J., Hermes, J. J., Bischoff-Kim, A., et al., 2015, ApJ, 809, 14

Benkő, J. M., Plachy, E., Szabó, R., Molnár, L., Kolláth, Z., 2014, ApJS, 213, 31

Benneke, B., Werner, M., Petigura, E., et al., 2017, ApJ, 834, 187

Bódi, A., Szatmáry, K., Kiss, L. L., et al., 2016, A&A, 596, 24

Borucki, W. J., 2016, Rep. Prog. Phys., 79, 036901

Buchler, J. R., Kolláth, Z., 2011, ApJ, 731, 24

Buysschaert, B., Aerts, C., Bloemen, S., et al., 2015, MNRAS, 453, 89

Campante, T. L., Barlay, T., Swift, J. J., et al., 2015, ApJ, 799, 170

Campante, T. L., Lund, M. N., Kuszlewicz, J. S., et al., 2016, ApJ, 819, 85

Coughlin, J. L., Mullally, F., Thompson S. E., 2016, ApJS, 224, 12

Davenport, J. R. A., Hebb, L., Hawley, S. L., 2015, ApJ, 806, 212

Deheuvels, S., Doğan, G., Goupil, M. J., et al., 2014, A&A, 564A, 27

Derekas. A., Szabó, Gy. M., Berdnikov, L., et al., 2012, MNRAS, 425, 1312

Derekas, A., Plachy, E., Molnár, L., et al., 2017, MNRAS, 464, 1553

Deubner, F-L., Gough, D., 1984, Ann. Rev. Astr. and Astrophys., 22, 593

Eddington, A. S., 1926, The Internal Constitution of Stars, Cambridge University Press, Cambridge

Foster, H. M., Reed, M. D., Telting, J. H., Østensen, R. H., Baran, A. S., 2015, ApJ, 805, 94

Garnavich, P. M., Tucker, B. E., Rest, A., et al., 2015, ApJ, 820, 23

Grundahl, F., Fredslund Andersen, M., Christensen-Dalsgaard, J., 2017, ApJ, in press, arXiv:1701.03365

Hermes, J. J., Montgomery, M. H., Bell, K. J., et al., 2015, ApJ, 810, 5

Kallinger, T, Weiss, W., Barban, C., et al., 2010, A&A, 509, 77

Lund, M. N., Basu, S., Silva Aguirre, V., et al., 2016, MNRAS, 463, 2600

Metcalfe, T. S., Chaplin, W. J., Appourchaux, T., et al., 2012, ApJ, 748, 10

Metcalfe, T. S., Creevey, O. L., Davies, G. R., 2015, ApJL, 811, L37

Molnár, L., Kolláth, Z., Szabó, R., Bryson, S., Kolenberg, K., Mullally, F., Thompson, S. E., 2012, ApJL, 757, L13

Molnár, L., Pál, A., Plachy, E., et al., 2015, ApJ, 812, 2

Molnár, L., Szabó, R., Plachy, E., 2016, JAAVSO, 44, 168

Moskalik, P., Smolec, R., Kolenberg, K., et al., 2015, MNRAS, 447, 2348

Mosser, B., Barban, C., Montalbán, J., et al., 2011, A&A, 532, 86

Mosser, B., Goupil, M. J., Belkacem, K., et al., 2012, A&A, 548, 10

Olling, R. P., Mushotzky R., Shaya, E. J., et al., 2015, Nature, 521, 332

Pápics, P. I., Moravveji, E., Aerts, C., Tkachenko, A., Triana, S. A., Bloemen, S., Southworth, J., 2014, A&A, 570, 8

Plachy, E., Benkő, J. M., Kolláth, Z., Molnár, L., Szabó, R., 2014, MNRAS, 445, 2810

Pope, B. J. S., White, T. R., Huber, D., et al., 2016, MNRAS, 455, 36

Ripepi, V., Balona, L., Catanzaro, G., Marconi, M., Palla, F., Giarrusso, M., 2015, MNRAS, 454, 2606

Scholz, A., Kostov, V., Jayawardhana, R., Mužić, K., 2015, ApJ, 809, 29

Silva Aguirre, V., Davies, G. R., Basu, S., et al., 2015, MNRAS, 452, 2127

Suzuki, Y., 2000, Int. J. Mod. Phys. A, 15, 201

Szabó, R., Benkő, J. M., Paparó, M., et al., 2014, A&A, 570, 100

Triana, S. A., Moravveji, E., Pápics, P. I., Aerts, C., Kawaler, S. D., Christensen-Dalsgaard, J., 2015, ApJ, 810, 16

White, T. R., Huber, D., Maestro, V., et al., 2013, MNRAS, 433, 1262

Zwintz, K., Fossati, L., Ryabchikova, T., 2015, ASPC, Proceedings of the Physics and Evolution of Magnetic and Related Stars conference, eds. Yu. Yu. Balega, I. I. Romanyuk, and D. O. Kudryavtsev, vol. 494, pp. 157

Multiple variability in RR Lyrae stars

Z. PRUDIL[1,2]

(1) Department of Theoretical Physics and Astrophysics, Faculty of Science, Masaryk University, Kotlářská 2, 611 37 Brno, Czech Republic, prudilz@ari.uni-heidelberg.de

(2) Astronomisches Rechen-Institut, Zentrum fur Astronomie der Universität Heidelberg, Mönchhofstr. 12-14, 69120 Heidelberg, Germany

Abstract: RR Lyrae stars have always been considered as radial variables, pulsating either in the fundamental mode (RRab), first-overtone mode (RRc) or simultaneously in both modes (RRd). Recently, this idea had been expanded thanks to the OGLE ground base phometric survey and space telescopes *CoRoT* and *Kepler* the RR Lyraes with multiple periodicities had been discovered. This additional variability present a challenge for current models of stellar pulsation. The most numerous group consists of RRd and RRc type stars, exhibiting additional periodicity with a period ratio in range 0.61 ~ 0.64. Furthermore, another longer periodicity had been found among several stars in these two groups that has not been explained yet. A small fraction of RRab stars also exhibits additional periodicity but with different period ratio, than in the previous two groups. Extensive photometric missions is drastically changing our view of this class of variable stars and distort the idea of strictly radially pulsating RR Lyrae pulsators.

Abstrakt: Hvězdy typu RR Lyrae byly vždy považovány za radiální pulzátory, pulzující v základním módu (RRab), prvním harmonickém (RRc) a v obou módech zároveň (RRd). V posledních letech, ale tato představa doznává povážlivé trhliny. Díky přehlídce OGLE a vesmírným misím *CoRoT* a *Kepler* byli objeveny hvězdy typu RR Lyrae, které vykazují dodatečnou proměnnost a představují výzvu pro současné modely hvězdných pulzací. Dosud nejpočetnější skupinu hvězd, mající vícenásobnou periodicitu, tvoří hvězdy patřící do podskupin RRc a RRd. U hvězd těchto dvou podskupin se poměr period mezi hlavním pulzačním cyklem a dodatečným, nově objeveným, pohybuje v rozmezí od 0.61 do 0.64. Dále mezi hvězdami těchto dvou kategorií byla nalezena variabilita s delší periodou, která nebyla doposud vysvětlena. Zlomek hvězd patřících do podskupiny RRab rovněž vykazuje vícenásobnou proměnnost, avšak s rozdílným poměrem period, než u předchozích dvou podskupin. Rozsáhlé fotometrické mise tedy razantně mění pohled na tuto třídu proměnných hvězd a narušují naši představu o striktně radiálních pulzací u hvězd typu RR Lyrae.

Introduction

The RR Lyrae stars possess a large astronomical importance. They are mostly radially pulsating variables with periods from 0.25 ~ 1.0 day. The majority of RR Lyrae stars pulsate in the fundamental mode (RRab or RR0), first-overtone (RRc or RR1), and occasionally in both modes at the same time (RRd or RR01), for examples of light curves see Fig. 1. They can serve as standard candles to old stellar populations, and therefore helps study galactic structure and evolution. With the RR Lyrae stars is linked several open issues for example, the Oosterhoff dichotomy, the Blazhko effect quasi-periodic modulation of amplitude and/or phase (see Szabó, 2014) and recently detection of additional periodicities.

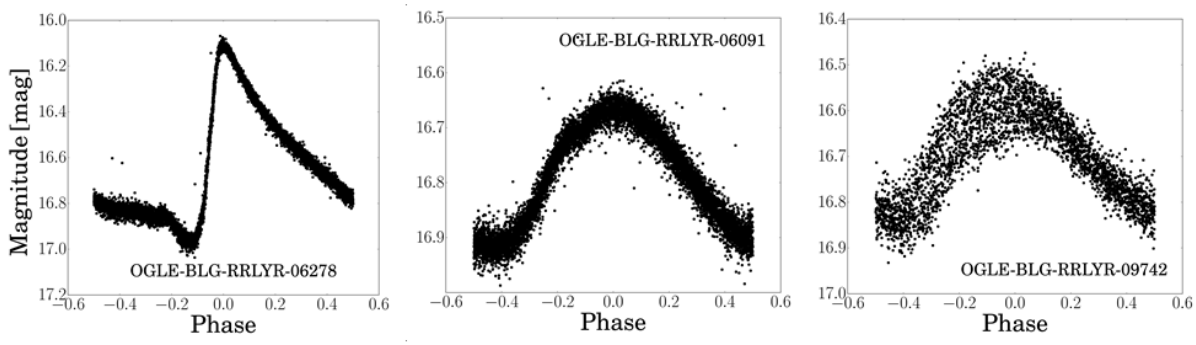

Figure 1: Three examples of phase curves for subtypes of RR Lyrae stars. From the left RRab, RRc, and RRd subtype. Data from OGLE-IV survey (Soszyński et al., 2014).

Additional periodicities in RR Lyrae stars

To study additional variability in RR Lyrae stars we can use the Petersen diagram (Petersen, 1973 see Fig. 2), where on horizontal axis we have a logarithm of the longer period versus period ratio on vertical. Its original purpose was to estimate metallicity and mass of double-mode Cepheids, today it is often used to identify various types of multiperiodic variables. Multi-mode pulsations occur commonly in RR Lyrae stars, RRd type variables pulsate in two modes at the same time. Period ratio P_{SHORT}/P_{LONG} of both modes is in a range 0.726 – 0.748 for the Galactic bulge RRd stars (red squares in Fig. 2, data from OGLE-IV survey, Soszyński et al., 2014).

First RR Lyrae star deviating from the general status quo was AQ Leo, an RRd star in which Gruberbauer et al. (2007) found in the MOST photometry additional shorter variability. In later years space telescopes *Kepler* and *CoRoT* (Szabó et al. 2014, Moskalik et al., 2015) and ground base photometric survey OGLE (Netzel et al., 2015a,c) revealed similar additional periodicity among other RRd and RRc stars. The period ratio between the additional and dominant periodicity is in the range 0.61 ~ 0.64 (blue dots in Fig. 2). The amplitude of the additional variability varies around few percent of the dominant mode. There are more than 300 known cases of this extra periodicity. Recently an explanation of this variability had been proposed by Dziembowski (2016). He suggests that nonradial f-modes trapped in the outer layers of the envelope are responsible for additional periodicity. The example of a star with this additional periodicity is in Fig. 3, top left panel.

Thanks to continues photometric missions *CoRoT* and *Kepler*, the second-overtone mode had been found among RRab type stars (yellow pentagons in Fig. 2, data from Moskalik (2013)). This additional mode occurs only in several stars exhibiting Blazhko phenomenon (an example is in the top middle panel of Fig. 3, data from Benkő et al., 2014). In addition, its low amplitude makes it difficult to detect in ground base observation.

Several first-overtone pulsators show additional longer periodicity. The period ratio between the dominant first-overtone mode and additional periodicity is around 0.686 (Netzel et al., (2015b), green triangles in the Fig. 2). This extra variability occurs sporadically and has a very low amplitude (around 4 percent of the dominant mode). The explanation for this longer, low amplitude periodicity is so far unknown. The example of a star with this extra variability is in the top right-hand panel of Fig. 3.

In OGLE-IV photometry for the Magellanic system Soszynski et al. (2016b) found 22 RR Lyraes that pulsates in the fundamental and first-overtone at the same time, but differ from RRd stars found in the Magellanic clouds (orange circles in Fig. 2). The period ratios are lower (around 0.725 – 0.738), than for classical double-mode pulsators in the Magellanic system. In the vast majority of these anomalous pulsators, the fundamental mode is dominant and the amplitude ratio between the first-overtone and fundamental mode varies from 18 up to 200 percent of the fundamental mode. A large number of these anomalous RRd type stars exhibit long-term amplitude modulation. Other examples of anomalous RRd type stars were found in the Galactic bulge (Smolec et al. 2015) and globular cluster M3 (Jurcsik et al. 2014, 2015). The example of a star with this additional periodicity is in the bottom left-hand panel of Fig. 3.

Furthermore, few fundamental mode pulsators in the OGLE-IV exhibit additional shorter periodicity (Smolec et al. (2016), purple dots in the Fig. 2). The period ratio falls in a similar range as for the RRd type pulsators, with exception of a one star which period ratio is almost exactly 0.7. The amplitude of the extra periodicity is quite low, in average 5 percent of the dominant fundamental mode (an example of a star with this extra variability is in the bottom middle panel of Fig. 3). If we assume, that the additional variability is interpreted as the first-overtone mode, then most of these variables are an extreme case of RRd type stars with high metallicity.

A recently discovered group of double-periodic stars originally identified as RR Lyrae stars was found in OGLE-IV photometry (Prudil et al. (2017), black stars in Fig. 2). This small group consists of 42 stars (mostly stars originally classified as RRab type variables). The period ratio of both periodicities varies in a range from 0.68 up to 0.72. The additional variability is always shorter than the dominant mode, but with a relatively large amplitude, approximately 25 percent of the dominant mode. The nature of the additional periodicity cannot be explained with stellar pulsation models and even classification of these objects as RR Lyrae stars is not clear. The example of a star with this additional periodicity is in the bottom right-hand panel of Fig. 3.

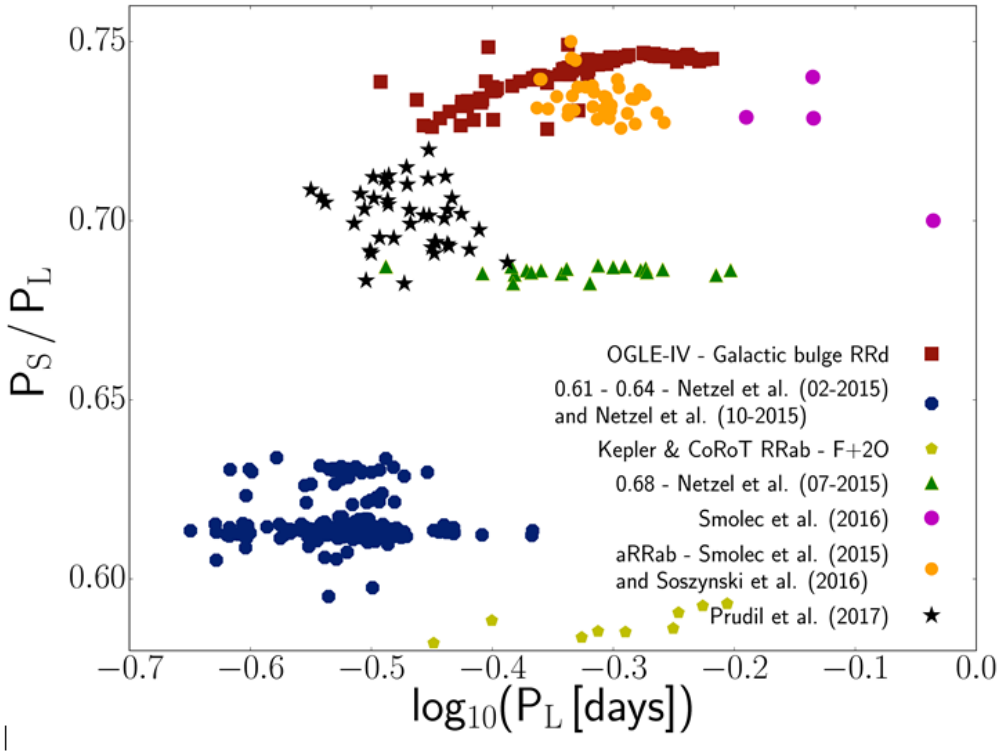

Figure 2: The Petersen diagram for the multiperiodic RR Lyrae stars. Dark red squares belong to RRd type stars (data from OGLE-IV survey, Soszyński et al. (2014)), blue circles, and green triangles represent stars found by Netzel et al. (2015a,c) and Netzel et al. (2015b). The yellow pentagons belong to modulated RRab type pulsators that exhibit the second-overtone mode (data from Moskalik (2013)). Orange circles represent anomalous RRd type variables found by Soszyński et al. (2016b). Magenta circles belong to stars found by Smolec et al. (2016) and black stars represents variables found by Prudil et al. (2017).

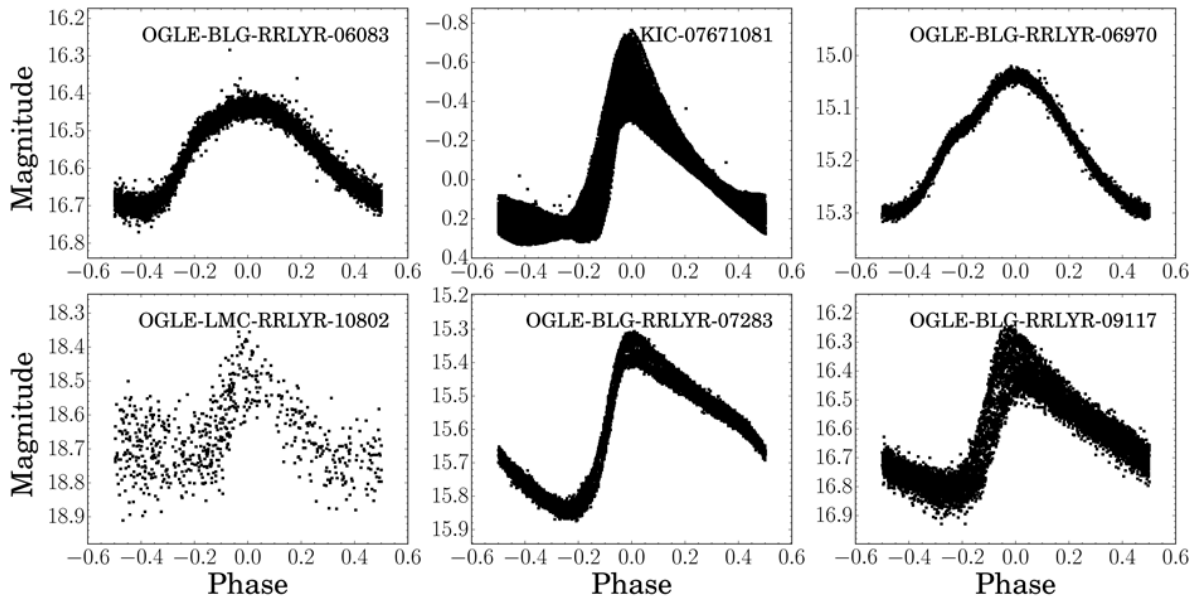

Figure 3: The examples of phase curves for RR Lyrae stars with multiple periodicities. Data from OGLE-IV survey Soszyński et al. (2014), Soszyński et al. (2016a) and *Kepler* (Benkő et al., 2014).

To summarize, our view of RR Lyrae variables, as simple radially pulsating stars is gradually changing. With more data from space photometric missions and ground base surveys, more instances of multiperiodic RR Lyrae stars might be within our reach.

References

Benkő J. M., Plachy E., Szabó R., Molnár L., Kolláth Z., 2014, ApJS, 213, 31

Dziembowski W., 2016, Comm. Konkoly Obs., vol. 105, 23

Gruberbauer M., Kolenberg K., Rowe J. et al., 2007, MNRAS, 379, 1498

Moskalik P., 2013, ASSP, 31, 103

Moskalik P., Smolec R., Kolenberg K. et al., 2015, MNRAS, 447, 2348

Netzel H., Smolec R., Moskalik P., 2015a, MNRAS, 447, 1173

Netzel H., Smolec R., Dziembowski W., 2015b, MNRAS, 451, L25

Netzel H., Smolec R., Moskalik P., 2015c, MNRAS, 453, 2022

Petersen, J. O. 1973, A&A, 27, 89

Prudil Z., Smolec R., Skarka M., Netzel H., 2017, MNRAS, 465, 4074

Smolec R., Prudil Z., Skarka M., Bakowska K., 2016, MNRAS, 461, 2934

Soszyński I. et al., 2014, Acta Astron., 64, 177

Soszyński I., et al., 2016a, Acta Astron., 66, 131

Soszyński I., et al., 2016b, MNRAS, 463, 1332

Szabó R., 2014, in Guzik J. A., Chaplin W. J., Handler G., Pigulski A., eds, Proc. IAU Symp. 301, Precision Asteroseismology. Cambridge Univ. Press, Cambridge, p. 241

Szabó R., Benkő J.M., Paparó M., 2014, A&A, 570, A100

Long-term activity of cataclysmic variables

VOJTĚCH ŠIMON[1,2]

(1) Astronomical Institute, The Czech Academy of Sciences, 25165 Ondřejov, Czech Republic, simon@asu.cas.cz

(2) Czech Technical University in Prague, Faculty of Electrical Engineering, Technická 2, 16627 Prague, Prague, Czech Republic

Abstract: Cataclysmic variables are objects in which matter transfers onto the white dwarf from a close companion (usually low-mass main sequence star). The orbital period of such systems is typically several hours. This mass transfer is the reason of the very large variability of these systems on many timescales. We show the examples when it is possible to observe this strong long-term activity like outbursts or transitions between the high and low states even with the commonly accessible instruments. We also show examples of the relation of this activity to the activity in X-rays.

Abstrakt: Kataklyzmické proměnné jsou objekty, v nichž proudí hmota na bílého trpaslíka z jejich těsného hvězdného průvodce s typickou orbitální periodou několika hodin. To je důvodem velké proměnnosti těchto systémů na mnoha časových škálách. Ukážeme příklady, kdy je možné pozorovat velice silnou optickou aktivitu i běžně dostupnými přístroji. Bude to především dlouhodobá aktivita, jako jsou vzplanutí nebo střídání vysokých a nízkých stavů jasnosti. Ukážeme také některé příklady toho, jak souvisí tato optická aktivita s tím, co pozorujeme u těchto objektů v rentgenovém oboru.

Introduction

Cataclysmic variables (CVs) are objects which often display very strong activity on various timescales, from seconds to more than a century. For the amateur astronomers, the photometric activity of these objects on the long timescales (e.g. months, years) is very important because the variations with the peak-to-peak amplitude of several magnitudes can occur. Moreover, this long-term activity is not always monitored sufficiently.

CVs are binary systems with the orbital period $P_{\rm orb}$ typically of hours. In CVs, matter transfers onto the white dwarf (WD) from a close companion (donor) (usually a low-mass main sequence star). This mass transfer is the reason for the very large variability of these systems on many timescales (see Warner 1995 for a review). In CV with the accretion disk, the dominant part of the optical emission which we observe is caused by thermal emission from the accretion disk which encircles the WD. CVs are also X-ray emitters. Most X-rays are radiated by bremsstrahlung mechanism from boundary layer (the boundary between the equator of the WD and the accretion disk encircling this object) or from the accretion columns onto the magnetic poles of the WD if this object possesses strong magnetic field. The X-ray emission of the cosmic objects including CVs is observable by the instruments onboard the satellites.

Variations of the mass transfer between the components (the donor and the WD) and/or the process called the thermal-viscous instability (e.g. Smak 1984; Hameury et al. 1998) which operates in the accretion disk play a large role in the observed activity of CVs (e.g. Warner 1995). The optical brightness can change by several magnitudes during the transitions between these states or in the outbursts.

The character of the activity often varies for the individual types of CVs.

Dwarf novae

Dwarf novae display strong outbursts that are interpreted as instabilities of the accretion disk which encircles the WD. This process is called a thermal-viscous instability of the accretion disk (e.g., Smak 1984; Hameury et al. 1998). In the optical band, thermal emission of the disk dominates during this outburst. The optical brightness of dwarf novae strongly rises during the outburst (typically by 2-4 mag), which is caused by the transitions of the disk from the cool state to the hot state and vice versa.

GK Per is a CV in which large variations of its activity were observed during the last more than a century. GK Per exploded as the classical nova in 1901 (Pickering 1901). This CV displays strong activity also after return to quiescence from this nova outburst. The type of activity of GK Per then changed from classical nova to novalike, and finally to dwarf nova during several tens of years after the nova explosion (Hudec 1981; Sabbadin & Bianchini 1983).

GK Per behaves as a dwarf nova in the last decades (Fig.1). These dwarf nova outbursts appeared several decades after the end of the classical nova explosion. The temperature of the surface of the WD (strongly heated by the classical nova explosion) already decreased sufficiently in this time, so this WD was not able to irradiate the accretion disk sufficiently to keep it sufficiently hot (and blocking thus the instability of the accretion disk, necessary for the occurrence of the outburtsts of dwarf nova).

The properties of the light curve of the dwarf nova outburst largely differ for the individual, even neighboring events. For example, the peak magnitude of the outburst differs for the individual events by more than 1 magnitude in Fig.1.

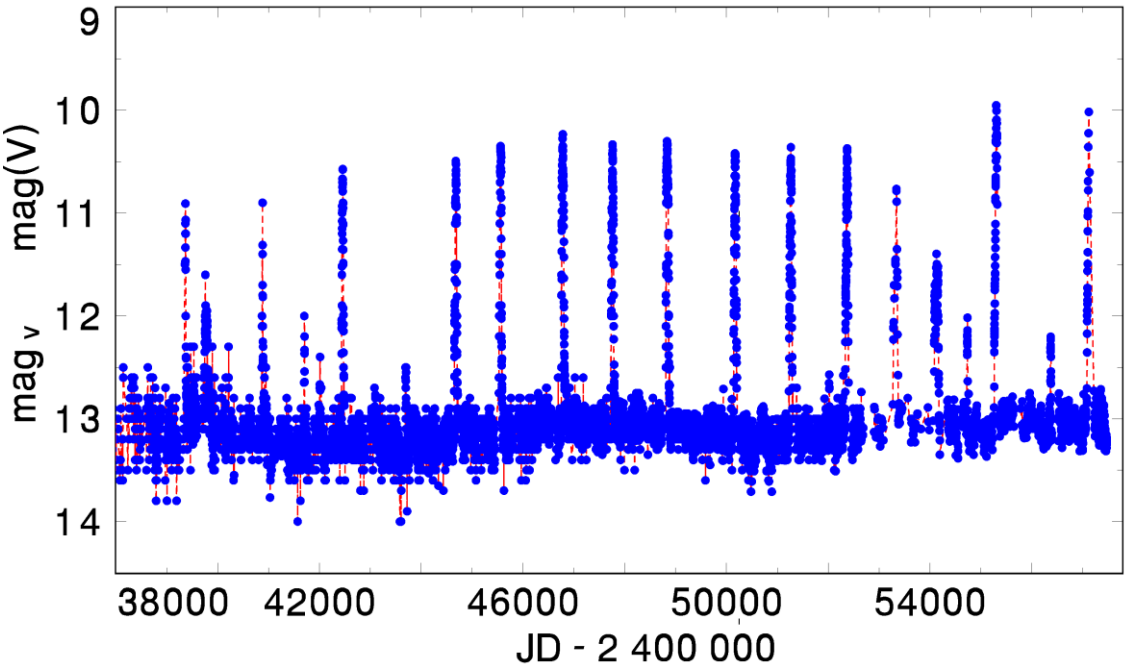

Figure 1: Long-term activity of GK Per. Only the current plase of activity in which GK Per displays dwarf nova outbursts is shown. The peak magnitude of the outburst can differ for the individual events by more than 1 magnitude. Both CCD measurements (mag (*V*)) and the one-day means of the visual data (mag_v) are used to secure the long-term light curve. Data source: AAVSO (Henden 2014; Kafka 2016).

The long dwarf nova outburst of GK Per, caused by the instability of the accretion disk (Fig.2), shows a large discrepancy between the profiles in the optical (thermal emission) and hard X-ray band (bremsstrahlung radiation). The times of the start and the end of the outburst are mutually the same for the optical and X-ray light curves, but the profiles of these light curves largely differ from each other near the time of the center of the outburst. Since the profile of the optical light curve differs from that in the X-ray band, this suggests the complexity in the mass flow through the disk and through the accretion regions on the WD. This emphasizes the necessity to examine an ensemble of outbursts in such systems.

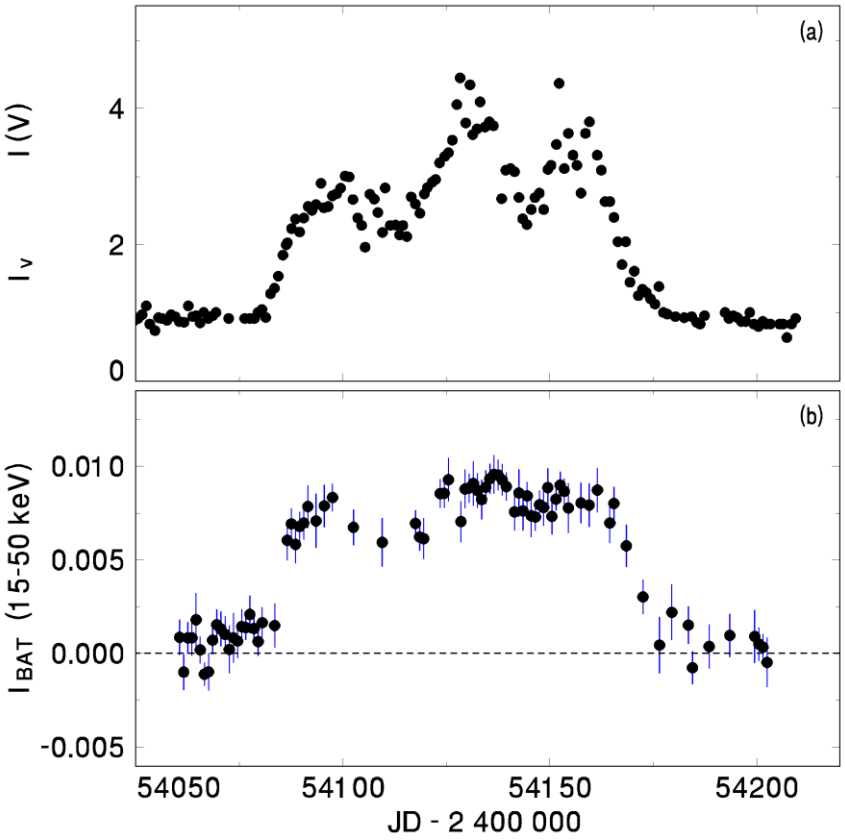

Figure 2: Dwarf nova outburst of GK Per in two bands. **(a)** The optical band (one-day means, intensity scale) (AAVSO data; Henden 2014). **(b)** One-day means of the very hard X-ray *Swift*/BAT (15-50 keV) observations (data source: Krimm et al. 2013). The error bars in panel **b** denote the uncertainties of intensity. Adapted from Šimon (2015) where more details are shown.

Novalikes

Episodes of the low states in the novalike type of CVs are a remarkable feature of activity of systems in which the instability of the accretion disk which gives rise to the dwarf nova outbursts (Hameury et al. 1998) does not operate. The brightness of novalikes can even decrease by about 4-5 mag during transition from the so-called high state to the so-called low state. These events were observed in the novalikes called VY Scl type (e.g. Warner 1995).

Novalikes are supposed to possess so high mass transfer rate into the disk in the high state that their accretion disks reside in the state which is similar to that of dwarf novae in outburst (e.g. Warner 1995). Transition into the low state is ascribed to a decrease of the mass transfer rate from the donor to the accretion disk. The depth of the individual episodes of the low state in a given novalike often appears to vary more than the brightness in the high state. This suggests that the amount by which the mass transfer rate is reduced varies for the individual episodes. Novalikes generally spend more time in the high state than in the low state.

Even small telescopes can provide important long-term light curves of variable objects. CCD *V*-band observations of the ASAS-3 project (http://archive.princeton.edu/~asas (Pojmanski 1997)) were obtained with a 200/2.8 camera (field of view 8.5º x 8.5º, exposure time of 180 s, one CCD image of the field obtained per night). Among other fields, they mapped the field of V1223 Sgr in a densely covered time segment during the years 2001-2009. Details of observing V1223 Sgr can be found in Šimon (2014).

A comparison of the activity in the *B*-band with the activity in the hard X-rays enables us to relate the intensities of the optical emission from the accretion disk and the hard X-ray emission (15-50 keV) from the accretion regions on the WD in V1223 Sgr (Fig.3). Even the relatively shallow optical low states (decreases by about 1 mag from the high state, much less than in the very deep low states discovered by Garnavich & Szkody 1988) are accompanied by significant decreases of the hard X-ray luminosity. This suggests the decreases of the mass inflow to the disk from the donor. Since the profile of the optical light curve sometimes differs from that in the X-ray band, this suggests the complexity of the mass flow through the accretion disk.

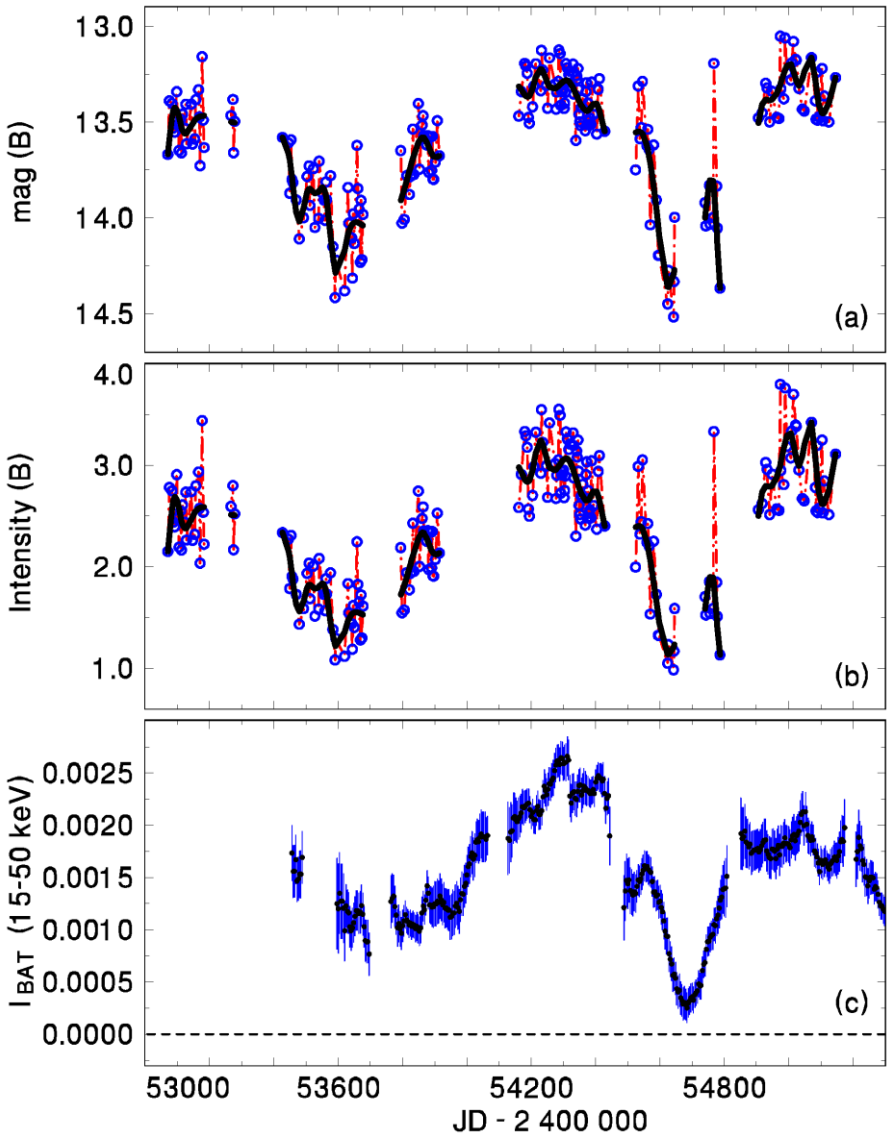

Figure 3: Relation of the light curve of V1223 Sgr in the *B*-band (ASAS data (Pojmanski 1997)) (magnitude scale in panel **a**, intensity scale in panel **b**) and in the very hard X-rays (15-50 keV) (panel **c**) (moving averages of *Swift*/BAT (Krimm et al. 2013) data). To guide the eye, the individual data points in the densely mapped seasons in panels **a** and **b** are connected by the lines. The thick lines in panels **a** and **b** represent the long-term evolution of brightness using the fits by the code HEC13.

Supersoft X-ray sources

Supersoft X-ray sources (SXBs) are a special type of cataclysmic variables with so large mass transfer rate between the components that the accreting matter causes the so-called steady-state hydrogen burning on the WD (van den Heuvel et al. 1992). In this context, the V Sge-type stars (VSs) are close binaries which display very similar properties in the optical band as the `classical' SXBs. The potential members, based mainly on the similarities in their optical spectra, were listed by Steiner & Diaz (1998).

V Sge with P_{orb} of 0.514195$ d (Herbig et al. 1965) is a transient supersoft X-ray source. The long-term optical activity of V Sge displays the active states (comprising the series of episodes of the high and low states), from time to time separated by the so-called flat segments when the brightness displays only small changes and remains between those of the high and low states (Šimon & Mattei 1999). The character of the optical activity of V Sge varies on the timescale of years. A segment of the complicated optical activity is shown in Fig.4.

V Sge also shows a very specific activity as regards its X-ray varations. Greiner & van Teeseling (1998) used X-ray data of V Sge from the satellite *ROSAT* and showed an anti-correlation of intensities of the optical and X-ray emission. This suggests that when V Sge is in the optical high state (so it is very bright), it is only a very faint X-ray source. On the other hand, when V Sge is in the optical low state (faint in the optical band), then it becomes a bright X-ray source. This is ascribed to a large sensitivity of the very soft X-ray emission to absorption intrinsic to V Sge (perhaps its accretion disk).

Fig. 4 shows a segment in the evolution of the long-term activity of V Sge using AAVSO data.

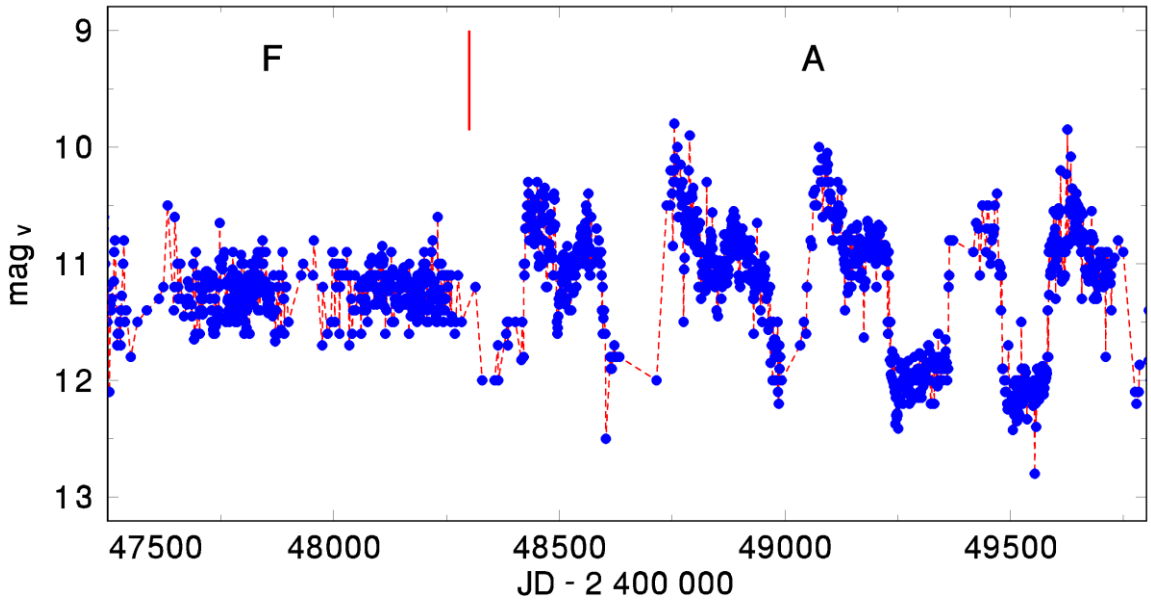

Figure 4: Segment of the long-term activity of V Sge using AAVSO data (one-day means). **A** denotes the so-called active segment in which a series of transitions between the high and low states occurs. **F** denotes the so-called flat segment in which no such transitions occur and the brightness remains between those of the high and low states. To guide the eye, the individual data points are connected by the lines. Data source: AAVSO (Mattei 1996). See Šimon & Mattei (1999) for details.

Polars

Polars (e.g. AM Her (Hudec & Meinunger 1976; Wu & Kiss 2008; Kafka & Hoard 2009)) are another type of CVs which are very active on long timescales. The dominant emission of polars which we observe comes from several processes (cyclotron in the optical band, bremsstrahlung in the hard X-rays) in small accretion region(s) on the WD (Kuulkers et al. 2006).

Polars are systems with large long-term variations which can be approximated by the episodes of the high and low states, roughly similar to those in novalikes. Polars contain so strongly magnetized WD that no accretion disk can form. The changes of the mass inflow onto the WD are thus rapidly reflected in the brightness variations. The levels of the high- and low-state brightnesses of a polar are typically separated by about 2 mag, and polars can spend a large fraction of time in the low states (Kafka & Honeycutt 2005).

Conclusions

Many CVs display strong activity on various timescales. Their long-term activity often has the amplitude of several magnitudes. This is easily observable even by the modest instruments (e.g. visual measurements, CCD detectors even without filters, digital cameras). The long-term activity of cataclysmics (specific for each type) is complex and non-periodic (at most cyclic). Unpredictable phenomena like outbursts or transitions between the states are the best observable events which are important for understanding the physical processes.

Acknowledgement

This study was supported by grant 13-39464J provided by the Grant Agency of the Czech Republic. This research has made use of public data from Swift/BAT transient monitor provided by the Swift/BAT team. This research has also made use of the observations from the ASAS project, AAVSO International database (USA) and the AFOEV database (France). I thank the variable star observers worldwide. I also thank Prof. Petr Harmanec for providing me with the code HEC13. The Fortran source version, compiled version and brief instructions on how to use the program can be obtained at this site: http:// astro.troja.mff.cuni.cz/ftp/hec/HEC13/

References

Greiner, J., van Teeseling, A., 1998, A&A, 339, L21

Garnavich, P., Szkody, P., 1988, PASP, 100, 1522

Hameury, J.-M., Menou, K., Dubus, G., et al., 1998, MNRAS, 298, 1048

Henden, A. A., 2014, Observations from the AAVSO International Database, http://www.aavso.org

Herbig, G. H., et al., 1965, ApJ, 141, 617

Hudec, R., Meinunger, L., 1976, IBVS, 1184, 1

Hudec, R., 1981, Bull. Astron. Inst. Czechosl., Vol. 32, 93

Kafka, S., 2016, Observations from the AAVSO International Database, http://www.aavso.org

Kafka, S., Honeycutt, R. K., 2005, AJ, 130, 742

Kafka, S., Hoard, D. W., 2009, PASP, 121, 1352

Krimm, H. A., Holland, S. T., Corbet, R. H. D., et al., 2013, ApJS, 209, article id. 14, 33 pp.

Kuulkers, E., et al., in Compact stellar X-ray sources. Ed. by Walter Lewin & Michiel van der Klis. Cambridge Astrophysics Series, No. 39, Cambridge University Press 2006.

Mattei, J. A., 1996, Observations from the AAVSO International Database, http://www.aavso.org

Pickering, E. C., 1901, ApJ, 13, 170

Pojmanski, G., 1997, AcA, 47, 467

Sabbadin, F., Bianchini, A., 1983, A&AS, 54, 393

Šimon, V., Mattei, J. A., 1999, Astronomy and Astrophysics Supplement, v.139, p.75-88

Šimon, V., 2014, New Astronomy, Volume 33, 44

Šimon, V., 2015, Astronomy & Astrophysics, Volume 575, id.A65, pp.

Smak, J., 1984, AcA, 34, 161

Steiner, J. E., Diaz, M. P., 1998, PASP, 110, 276

van den Heuvel, E. P. J., et al., 1992, A&A, 262, 97

Warner, B., 1995, Cataclysmic Variable Stars, Cambridge Univ. Press, Cambridge

Wu, K., Kiss, L. L., 2008, A&A, 481, 433

Eclipsing binaries – selection of targets

P. ZASCHE[1]

(3) Astronomical Institute, Faculty of Mathematics and Physics, Charles University in Prague, CZ-180 00 Praha 8, V Holešovičkách 2, Czech Republic, email: zasche@sirrah.troja.mff.cuni.cz

Abstract: Are the ground-based observations still needed in the era of robotic all-sky surveys? There were highlighted several fields in the eclipsing binary research, where also the amateur photometry would be very fruitful with also a few suitable systems where the monitoring is needed also using the smaller telescopes.

Abstrakt: Jsou v dnešní době robotických celooblohových přehlídek ještě potřeba pozemní amatérská pozorování? Bylo vypíchnuto několik možných podskupin zákrytových dvojhvězd, pro které i amatérská fotometrie s malými dalekohledy může být velice užitečná, včetně uvedení několika vhodných systémů.

Introduction

Having the access to various huge databases of photometric observations nowadays, it brings some aspects of the observational strategy and target selection. This especially applies for the eclipsing binaries. Large portions of the sky are periodically monitored photometrically and one has to ask whether some new observation is really needed and why. Is the short cadence of the data points the most crucial issue and substantiation of our ground-based observations? And what about some new discoveries of eclipsing binaries and their follow-up measurements? Is our effort well-justified?

In general

In general we can say that YES – it still can be interesting to observe some particular targets using our small ground-based instruments. However – the crucial point is the cadence of our data, target selection and also the time span of our observations. Concerning the target selection process, I divide the systems worth of study into three different groups:

1. Published systems

In the first group there will be those systems, which were already published and the papers with their analysis can be found. These typically are such systems, which were studied via spectroscopy and some additional bodies in such systems were found. However, the confirmation of these bodies via photometry or period variation was not done yet.

This is a typical situation – a detailed spectroscopic study is able to reveal some hidden component in a system (e.g. hierarchical system containing the eclipsing binary as the inner pair plus the distant component) and some estimation about its parameters as well as parameters of its orbit is given. But at this point the authors of the discovery paper usually stop collecting the data and moves to another interesting object. However, the confirmation about the third component via period changes in the O-C diagram is missing and here comes our contribution to the topic. We usually know what to expect – its period, some mass estimation, etc. So the detection of the period changes in the O-C diagram would be quite an easy task. But it is still needed, because it can set some constraints on the third-body orbit. Such systems are for instance *HD 86222* , *BD-22 5866*, *2MASS 13554346-0925058* , …

2. Dynamically interesting systems

Second group comprises such stars which are close enough that some additional effect can be detected there. It means that the inner eclipsing orbit and the outer third-body orbit have adequately low period ratio $P_1/P_2 < 30$ that the two orbits cannot be considered as isolated. A more sophisticated approach is needed for modelling of such systems and here also comes our contribution.

For the detailed analysis, one needs good data coverage – it means that such stars need to be observed more frequently and in more complex way. Not only small parts of the minima, but whole eclipses (the change of inclination can be detected, hence one needs complete eclipses for the amplitude derivation). Time time cadency is a crucial issue - to observe the target every week, month, year (depending on the periods). Typical examples of such dynamically interesting systems are for instance *Ksi Tau*, *Lam Tau*, …

Another possible selection criterion could be the shallowness of the minima. The more shallow the minima are, the more luminous the third component probably is. Of course, sometimes the depth of minima is due to the orientation of the orbit, but in many cases the crucial point is the presence of the third body in the system and its luminosity. Such systems with the high-mass third component are also very interesting from the theoretical as well as dynamical aspect. Typical examples are e.g. *Tau CMa*, *DI Lyn*, *KR Com*, *V819 Her*, …

3. Doubly eclipsing systems

And finally, which also deserves our attention are such systems, which show double eclipsing behaviour. It means where both eclipsing pairs were detected and their respective orbital periods are known. Such stars still represents very limited sample of stars. And more observations are very welcome because there can possibly be found the period changes of both pairs as they revolve on their mutual orbit. Only one such system where this effect was reliably proven is *V994 Her*. But also other double eclipsing systems are in the range of magnitudes for small telescopes (and their periods are not so long). However, it needs to be observed continuously over several years to compare the results over a longer time interval. Such systems are for example *CzeV343*, *1SWASP J093010.78+533859.5* , …

How to observe

There is a question about how to observe and what to observe in these interesting systems. As was already mentioned above, relatively easiest task is to observe only the eclipses. But to observe them means to observe the complete eclipses (both descending and ascending branches as well as the parts outside minima). The time cadency of the observations strongly depends on the periods of the stars. Sometimes it would be enough to observe the target once per year, but for some systems with rapid dynamical interaction some observations every week would be fine. The advantage is that there is no need for filtered photometry and observations in one filter would also be fine for some of these purposes.

New discovered systems

Concerning the new systems discovered by the observers, it would be suitable to observe these systems more frequently to find out the orbital period and then to observe the target time to time (a few observations after a month and another after a year). It would be suitable to focus more on such systems, which show some indication of presence of the third component – for example total eclipses together with shallow depth of these eclipses.

Target selection based on the O-C diagram

Sometimes the observers rely too much on the O-C diagram and choose the target according to its shape. However, for some systems the O-C diagrams look like a straight line but the systems are interesting dynamically interacting triple stars. For example again *Lambda Tau* or *Ksi Tau* are such examples due to the fact that the outer periods are too short and the usual time cadence is too poor. *EE Peg* is another example.

Conclusions

To conclude, the ground based observations still would be very fruitful and welcome for professional astronomers, however it is very important to choose a proper target and to observe it more frequently with the same reduction method.

Acknowledgement

This work was supported by the by Czech Science Foundation Grant No. GA15-02112S.

B[e] Stars - Penetrating the Mystery of the Circumstellar Matter

D. KORČÁKOVÁ[1], A. MIROSHNICHENKO[2], S.N. SHORE[3]

(1) Astronomical Institute, Charles University, V Holešovičkách 2, 180 00 Praha 8, Czech Republic, kor@sirrah.troja.mff.cuni.cz

(2) Department of Physics and Astronomy, University of North Carolina at Greensboro, Greensboro, NC 27402, USA, a_mirosh@uncg.edu

(3) Dipartimento di Fisica Enrico Fermi Universitá di Pisa, 56127 Pisa, Italy, steven.neil.shore@unipi.it

Abstract: We present a brief overview of the published analyses of the long-term variability of FS CMa stars, a subgroup of the B[e] stars. We stress the importance of persistence for the study of the various physical processes in these objects and the essential role to be played by amateur-professional observational campaigns.

Abstrakt: V příspěvku představujeme krátký přehled publikovaných analýz dlouhoperiodických proměnných hvězd typu FS CMa, podskupiny B[e] hvězd. Klademe důraz na dlouhodobé studium různých fyzikálních procesů u těchto objektů a klíčovou roli, kterou hrají společné observační kampaně profesionálních a amatérských pozorovatelů.

Introduction

The B[e] stars (IAUS 70, Conti 1976) are hot B-type[8] stars whose spectra contain emission lines from forbidden transitions (e.g. [Fe II], [O I]) along with strong Balmer emission and those of other permitted lines (e.g. Fe II, Na I), and strong (continuum) infrared emission (beyond a few microns) in excess of that expected from the stellar photosphere. In particular, the Hα line top intensity (Fig. 1) can reach flux levels 200 times that of the flanking continuum. The strong excess radiation detected from B[e] stars in the infrared region (Swings & Allen 1971) cannot be explained as thermal emission from the same gas responsible for the emission lines.

The B[e] phenomenon is found in stars of quite different types and at different evolutionary stages. Lamers et al. (1998) found it present in objects as different as compact planetary nebulae, pre-main-sequence Herbig stars, supergiants, and symbiotic stars, but they were not able to classify half of the stars known at that time. Miroshnichenko (2007) noticed that almost all unclassified stars have similar properties and introduced a new group called FS CMa objects after the prototype (HD 45677). The ensemble of spectral properties indicate the presence of extended circumstellar matter that includes hot dust. A rough picture, first suggested for supergiants (Zickgraf et al. 1985) and Herbig stars (e.g. Pudritz 1985), includes a wind emerging from higher stelar latitudes and a high density, equatorially concentrated (disk-like) dusty torus. Planetary nebulae and symbiotic stars can go through a B[e] phase as their envelope expands, but the FS CMa stars remain a mystery. The amount of circumstellar matter is too large to be produced during the evolution of a single star, especially since they do not seem to be either highly evolved (such as supergiants) or young stellar objects (such as Herbig Ae/Be stars). The likely explanation is binarity, but not many binaries have been found among FS CMa objects. A detailed discussion of this subject can be found Miroshnichenko (2007); Miroshnichenko et al. (2013), and Miroshnichenko & Zharikov (2015a). The visible hot star in FS CMa objects is significantly immersed in a circumstellar envelope. In extreme cases we do not even see photospheric lines in their spectra. However, distortion of the observed parameters by the circumstellar matter hampers using standard methods of analysis to obtain limits on their masses, luminosities, and surface gravities. In this situation, the study of temporal variability becomes important. It allows to determine basic physical processes that take place in the envelope and evaluate the central object properties.

[8] Note that the normal Be stars are so designated mainly based on the Balmer and He I emission lines, the "[]" indicates the presence of forbidden lines.

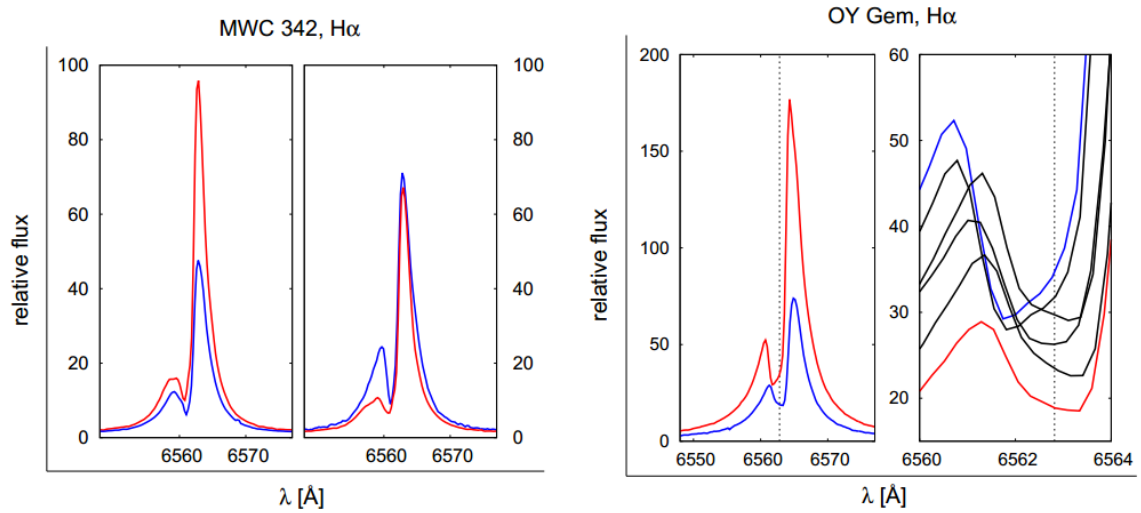

Figure 1: Spectral line variations of the FS CMa star MWC 342 and the post-AGB star OY Gem. *left panel:* Maximum (2007-09-13) and minimum (2010-10-09) intensity of the red peak and maximum (2009-08-29) and minimum (2007-04-16) intensity of the violet peak of MWC 342 between years 2004 and 2011. *right panel:* Maximum (2011-11-12) and minimum (2005-03-31) intensity of OY Gem between years 2005 and 2012. The vertical dashed lines show the laboratory wavelength of the Hα line. All the plotted spectra were obtained using the Ondrejov 2m telescope, Czech Republic.

Variability of FS CMa stars

The FS CMa stars display spectroscopic (line profile) variability on a vast range of timescales. Absorption lines show night-to-night variations (Fig. 2) and line profile changes in some objects have been observed within a few hours. Emission lines vary at the longer timescales, from days to decades. The spectral and photometric variations show multiperiodic behavior, to the extent that there are periodic changes, with the shortest periods being about 8 - 15 days with longer periods on the order of a months (20 - 60 days) to years (3 - 11 years). The amplitudes and "period" can change between different epochs and it is better to speak about a quasi-periodic behavior for these objects. A comprehensive description of such a behavior has been presented for MWC 342 (Kučerová et al. 2013, introduction - summary of photometric observations) and quasi-periodic variability is also spectroscopically detected for HD 50138 (Jeřábková et al. 2016).

Benefit of long-term observations of FS CMa stars

Given the lack of photospheric lines, usually attributed to extremely rapid rotation of the visible star, systematic spectroscopic observations are needed to reveal the **binary nature** of these objects. Binarity has been proposed to resolve the current paradox: evolutionary models of an isolated star are unable to produce such an amount of circumstellar matter. On the other hand, we do not *observe* evidence of binaries in a sufficient number of these stars (either multiple spectra or orbitally induced radial velocity variations). If their binarity of these stars is confirmed, long time series will allow the study the presumptive **mass transfer properties** in detail. The line profile variability can be due to several mechanisms, e.g., **rotating structures, pulsations, origin, dynamics, and the structure of the stellar wind**. The detection of the material **infall** is also possible. Moreover, we can see effects of the **expanding layers** or **excitation waves**. All these processes are associated with the several possible originating mechanisms for the FS CMa stars - binarity, (Miroshnichenko & Zharikov 2015b), single stellar evolution, or binary mergers (de la Fuente et al. 2015).

Spectroscopic observations are usually done in such a way that only continuum-normalised spectra are obtained. In this case, photometric observations are necessary to determine whether the changes of the intensity of spectral lines are caused by the change of continuum radiation or by the line formation. Line equivalent width and/or intensity variations do not sufffice. Photometric observations are not only complementary to the spectroscopy. They are very important for determination of the underlying physical processes, which reveal themselves by the presence of a regular period and/or multiperiodic or quasi-periodic behaviors.

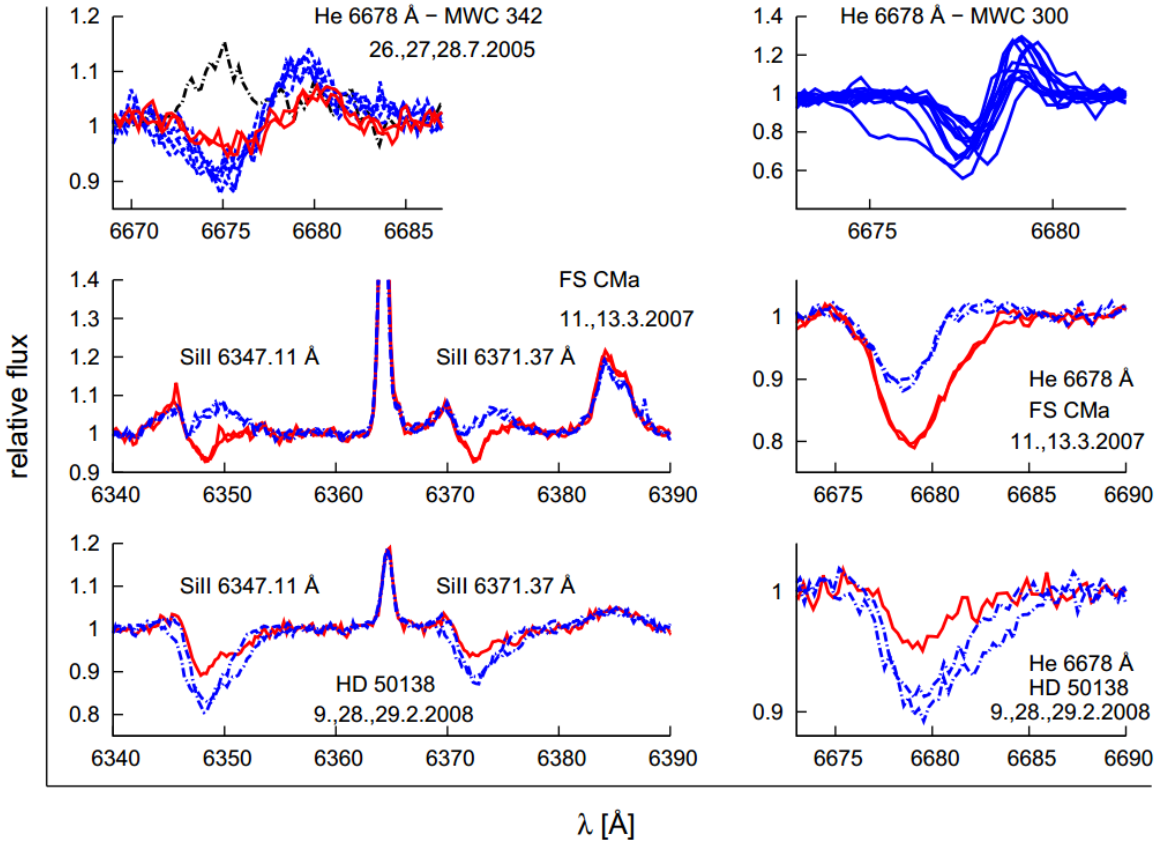

Figure 2: Night-to-night variability of some absorption lines.

Call for observations

Current stage

Despite the importance of long-term observations of FS CMa stars, there are very few time series to date. The first, and the last for a long time, long series was a ten-year spectroscopic campaign in the 20s of the last century by Merril (1931). Unfortunately, photographic plates were not sensitive in the red spectral region at that time, and only the observations around the Hβ line were possible (a problem that still plagues Be star studies). A new ten-year long campaign has been running since 2004 at the Ondřejov observatory in the Czech Republic. It suffers from the same problem: only the Hα region is usually observed (Polster et al. 2012; Kučerová et al. 2013; Jeřábková et al. 2016). Analysis of the data for MWC 728 (116 spectra, Miroshnichenko et al. 2015), and IRAS 00470+6429 (27 spectra, Miroshnichenko et al. 2009) have so far been published.

In the last decade, the size and price of small spectrographs dropped drastically, which allows small observatories and more observers to participate. Unfortunately, only FS CMa itself and HD 50138 (V743 Mon) are bright enough to follow at higher resolutions with small telescopes. Nevertheless, an extensive set of spectra has been obtained for these objects. Currently, the BeSS database[9] includes 304 spectra of HD 50138 from 2001 and 63 spectra of FS CMa obtained by amateur astronomers since 2009. The best temporal coverage is for the years 2013 and 2014, when 287 spectra of HD 50138 and 92 spectra of FS CMa were obtained.

The photometric variability of FS CMa stars is also not well covered in over long times. The longest interval is presented by Gottlieb & Liller (1978), who analysed the archival Harvard photographic plates and revealed variability of three FS CMa stars (MWC 645, MWC 819, and MWC 349) from ~ 1890 to ~ 1980. Note that these were unfiltered observations and are therefore a poorly calibrated mix of emission line and continuum contributions. Unfortunately, the data are too sparse, with an irregular cadence, to search for periodicity. The same problem exists for observations of Bergner et al. (1995), who obtained multicolor photometry of four FS CMa stars (MWC 342, MWC 349, MWC 623, and MWC 84) from April 1987 to August 1992. An extensive

[9] http://basebe.obspm.fr/basebe/MenuIntro.php

work, which allows determination of the periods of variations was done by Shevchenko et al. (1993). Power spectra are presented there for MWC 342 (Fig. 2 and 3) showing the most relevant period of about 14 days. They also studied MWC 137 but found no periodicity. Note here that if the variability is not on a stable timescale, such analyses may be misleading. Density of coverage is fundamental.

Table 1: Selected FS CMa stars

object	α(J2000) [h m s]	δ(J2000) [° ' "]	V [mag]
FS CMa	06 28 17.4	−13 03 11.1	8.5
HD 50138 (V743 Mon)	06 51 33.4	−06 57 59.5	6.7
HD 85567 (V596 Car)	09 50 28.5	−60 58 03.0	8.6
MWC 1055	22 08 25.4	+54 13 26.5	12.1
AS 386	20 10 54.2	+38 18 09.4	11.0
AS 446	20 50 55.9	+49 00 37.4	10.3
MWC 17 (V832 Cas)	01 47 38.5	+60 41 57.4	13.2
MWC 645 (V2211 Cyg)	21 53 27.5	+52 59 58.0	13.0
AS 78 (MO Cam)	03 58 59.4	+56 11 12.6	11.3
IRAS 00470+6429	00 50 06.0	+64 45 34.9	11.6
AS 116 (V791 Mon)	06 02 14.9	−10 00 59.6	10.4
IRAS 07080+0605	07 10 43.9	+06 00 07.8	12.8
IRAS 06341+0159	06 36 43.6	+01 57 04	12.4
V669 Cep	22 26 38.7	+61 13 31.6	12.5

Note: Photometric and spectroscopic observations of the brightest FS CMa stars: FS CMa itself, HD 50138, and HD 85567 are needed to complement the interferometric, polarimetric, radio, and UV observations of these objects. The other stars are selected from the FS CMa stellar list (Miroshnichenko 2017).

One of the FS CMa stars for which long-term photometric observations were obtained is GG Car. The results from January 1924 to June 1929 are presented in Kruytbosch (1930). Gaposchkin (1953) found the period about 62.086 days in data between 1938 and 1947. The same period was found Gosset et al. (1984) a few decades later, between 1978 and 1981. Old detailed studies are also available for MWC 349. The results of 14 years program are summarized in Jorgenson et al. (2000). They found a photometric period of about 9 years using red photographic plates taken between 1967 and 1981. Unfortunately, more recent observations are sparse and only cover shorter time intervals (22 observations between April 1987 and August 1992 Bergner et al. (1995), and 16 observations between October 1985 and August 1992 Yudin (1996)). Important information about MWC 342 could be found in Mel'Nikov (1997) and Miroshnichenko & Corporon (1999), where observations from 1986 - 1994 and 1995 -1998 are analyzed. The results from observing seasons of 1989 and 1993 are summarised in Chkhikvadze et al. (2002). Long-term variability is partially covered for MWC 84. Miroshnichenko (1995) found an 11.9 day period in data between 1989 and 1992. A three-year long program Barsukova et al. (2002b,a) indicates the presence of a longer period, 1100 ± 50 days. Additional photometry was obtained Goranskij & Barsukova (2009) in August 2005, 2006, and December 2006. A detailed study of the variability of IRAS 00470+6429 is presented in Miroshnichenko et al. (2009), where more than a thousand observations taken from June 1999 to December 2008 are analyzed. The temporal behavior of AS 78 and MWC 657 is described by Miroshnichenko et al. (2000).

Selected targets

An up-to-date list of FS CMa type stars is available on A. Miroshnichenko's website[10]. To encourage the community to obtain sufficient data for studies of the temporal variability, we highlight the most important targets (Table 1).

[10] contact him at amirosh@uncg.edu

FS CMa, HD 50138, and HD 8556

The brightness of these stars allows their observation with almost all available techniques - optical and infrared interferometry (VLTI, HD 50138 also with VEGA/CHARA), radio interferometry (ALMA), polarimetry, UV spectroscopy, and classical spectroscopy in the visible region.

MWC 1055, AS 386, and AS 446

Current data indicate a regular variability, possibly suggesting binarity.

MWC 17 and MWC 645

MWC 17 and MWC 645 show very strong emission-line spectra. Near-IR brightness variations have been detected, but to date their optical variability has not been studied.

AS 78, IRAS00470+6429, and AS 116

These stars have strong P Cygni profiles caused by the stellar wind. The hot star winds are known to be unstable, producing non-axisymmetric shocks and density inhomogeneities. If these objects are binaries, the presence of the secondary will affect the circumstellar matter leading to the large-scale structures. All this may be associated with photometric, as well as spectroscopic, variability. However, the optical variability of these stars has not been studied.

IRAS07080+0605

IRAS07080+0605 is one of the coldest FS CMa objects. A detailed study of this star could test whether the spectral anomalies among FS CMa type stars are caused only by the temperature difference.

IRAS06341+0159

IRAS06341+0159 is a poorly-studied star. Observations of this object are very much needed.

V669 Cep

V669 Cep shows two contributors to the spectrum - a hot, B-type, and a cold, K-type, similar to MWC 623. The most probable explanation is that the cool spectrum belongs to a binary companion but it could form in the circumstellar disk.

Observation strategy

Spectroscopy

A spectral resolving power better than 5000 is necessary for detailed analysis, and, given the weakness of the line wings and some of the absorption lines, the highest signal to noise ratio possible should be sought (at least 50). However, *any* high S/N ratio spectra are useful. It is best to try for coverage from 4750 Å (Hβ) to 8700 Å (OI 8446 Å, Paschen series). The necessary frequency (cadence) of measurements depends on the spectral region which is observed. Absorption lines show night-to-night variability. Spectral line changes are measurable during one night in some objects. The timescale of the variability of emission lines spans from weeks to years. Multiperiodic behaviour has been detected in a few well-studied stars. Moreover, periods of the variations can change after several epochs. In other words, the more the better.

Photometry

Multicolor photometry, at least UBV, is important. The FS CMa stars show photometric changes on different timescales: several days (8 - 15 days), about a month (20 - 60 days), and years (3 - 11 years). Moreover, the detected period in different seasons or epochs can change. An ideal observing strategy is taking two measurements nightly for several seasons with as few gaps as possible over a period of months. Such a hard work requires a broad community cooperation.

Conclusions

Determination of the scale of the changes and their regular, multiperioriodic, or quasi-periodic behavior point to the physical processes occurring in the circumstellar region and the photosphere of the visible star. Moreover,

the changes of the spectral line profiles can reveal the presence of rotating structures in the circumstellar matter, expanding envelopes, or the wind structure and dynamics.

Despite the small number of known FS CMa stars, comprising about 50 *bona fide* members, the study of these stars is very important, reaching beyond the B[e] stars alone. They are wonderful physical laboratories for testing hydrodynamic models of outflows and disks and their interactions as well as driving of flows through the collisional and radiative coupling of atomic and ionic levels. Such studies have a direct implication for understanding much more complex objects, such as η Car. Moreover, FS CMa stars and B[e] supergiants may be responsible for production of a few percent of galactic dust (Miroshnichenko 2007). As B[e] supergiants have also been found in low-metallicity galaxies, B[e] stars could be very important dust creators in the early universe.

Acknowledgement

The research of DK is supported by the grant 17-00871S of the Czech Science Foundation. We acknowledge the use of the electronic database from the CDS, Strasbourg and electronic bibliography maintained by the NASA/ADS system.

References

Barsukova, E. A., Borisov, N. V., Fabrika, S. N., Goranskij, V. P., & Metlova, N. V. 2002a, in Astronomical Society of the Pacific Conference Series, Vol. 261, The Physics of Cataclysmic Variables and Related Objects, ed. B. T. Gänsicke, K. Beuermann, & K. Reinsch, 463

Barsukova, E. A., Borisov, N. V., Goranskii, V. P., Lyutyi, V. M., & Metlova, N. V. 2002b, Astronomy Reports, 46, 275

Bergner, Y. K., Miroshnichenko, A. S., Yudin, R. V., et al. 1995, A&AS, 112, 221

Chkhikvadze, J. N., Kakhiani, V. O., & Djaniashvili, E. B. 2002, Astrophysics, 45, 8

de la Fuente, D., Najarro, F., Trombley, C., Davies, B., & Figer, D. F. 2015, A&A, 575, A10

Gaposchkin, S. 1953, Annals of Harvard College Observatory, 113, 67

Goranskij, V. P. & Barsukova, E. A. 2009, Astrophysical Bulletin, 64, 50

Gosset, E., Surdej, J., & Swings, J. P. 1984, A&AS, 55, 411

Gottlieb, E. W. & Liller, W. 1978, ApJ, 225, 488

IAUS 70, Conti, P. S. 1976, in IAU Symposium, Vol. 70, Be and Shell Stars, ed. A. Slettebak, 447

Jeřábková, T., Korčáková, D., Miroshnichenko, A., et al. 2016, A&A, 586, A116

Jorgenson, R. A., Kogan, L. R., & Strelnitski, V. 2000, AJ, 119, 3060

Kruytbosch, W. E. 1930, Bull. Astron. Inst. Netherlands, 6, 11

Kučerová, B., Korčáková, D., Polster, J., et al. 2013, A&A, 554, A143

Lamers, H. J. G. L. M., Zickgraf, F.-J., de Winter, D., Houziaux, L., & Zorec, J. 1998, A&A, 340, 117

Mel'Nikov, S. Y. 1997, Astronomy Letters, 23, 799

Merrill, P. W. 1931, ApJ, 73, 348

Miroshnichenko, A. & Corporon, P. 1999, A&A, 349, 126

Miroshnichenko, A. & Zharikov, S. 2015a, http://arxiv.org/abs/1508.06298; submitted in EAS Publication Series; Physics Of Evolved Star, June 8-12 2015, Nice, France

Miroshnichenko, A. S. 1995, Astronomical and Astrophysical Transactions, 6, 251

Miroshnichenko, A. S. 2007, ApJ, 667, 497

Miroshnichenko, A. S. 2017, in The B[e] Phenomenon: Forty Years of Studies, Astronomical Society of the Pacific Conference Series, in print

Miroshnichenko, A. S., Chentsov, E. L., Klochkova, V. G., et al. 2000, A&AS, 147, 5

Miroshnichenko, A. S., Chentsov, E. L., Klochkova, V. G., et al. 2009, ApJ, 700, 209

Miroshnichenko, A. S. & Zharikov, S. V. 2015b, in EAS Publications Series, Vol. 71, EAS Publications Series, 181 – 186

Miroshnichenko, A. S., Zharikov, S. V., Danford, S., et al. 2015, ApJ, 809, 129

Miroshnichenko, A. S., Zharikov, S. V., Manset, N., Rossi, C., & Polcaro, V. F. 2013, Central European Astrophysical Bulletin, 37, 57

Polster, J., Korčáková, D., Votruba, V., et al. 2012, A&A, 542, A57

Pudritz, R. E. 1985, ApJ, 293, 216

Shevchenko, V. S., Grankin, K. N., Ibragimov, M. A., Mel'Nikov, S. Y., & Yakubov, S. D. 1993, Ap&SS, 202, 121

Swings, J. P. & Allen, D. A. 1971, ApJ, 167, L41

Yudin, R. V. 1996, A&A, 312, 234

Zickgraf, F.-J., Wolf, B., Stahl, O., Leitherer, C., & Klare, G. 1985, A&A, 143, 421